

Analytic one-loop amplitudes for a Higgs boson plus four partons ^{*}

Lance J. Dixon and Yorgos Sofianatos

SLAC National Accelerator Laboratory, Stanford University, Stanford, CA 94309, USA

E-mail: lance@slac.stanford.edu, yorgos@slac.stanford.edu

ABSTRACT: We compute the one-loop QCD amplitudes for the processes $H\bar{q}q\bar{Q}Q$ and $H\bar{q}qgg$, the latter restricted to the case of opposite-helicity gluons. Analytic expressions are presented for the color- and helicity-decomposed amplitudes. The coupling of the Higgs boson to gluons is treated by an effective interaction in the limit of large top quark mass. The Higgs field is split into a complex field ϕ and its complex conjugate ϕ^\dagger . The split is useful because amplitudes involving ϕ have different analytic structure from those involving ϕ^\dagger . We compute the cut-containing pieces of the amplitudes using generalized unitarity. The remaining rational parts are obtained by on-shell recursion. Our results for $H\bar{q}q\bar{Q}Q$ agree with previous semi-numerical computations. We also show how to convert existing semi-numerical results for the production of a scalar Higgs boson into analogous results for a pseudoscalar Higgs boson.

KEYWORDS: QCD, Higgs boson, Hadron Colliders, LHC.

Submitted to JHEP

^{*}Research supported by the US Department of Energy under contract DE-AC02-76SF00515.

1. Introduction

The Large Hadron Collider (LHC) at CERN is now beginning operation, and will be the major source of data from the energy frontier for many years to come. The main goal of the LHC experimental program is to discover physics beyond the Standard Model (SM), as well as the mechanism of electroweak symmetry breaking. In the SM, this breaking is due to a single scalar field, the Higgs field [1, 2, 3]. Similar fields exist in most extensions of the SM, such as the Minimal Supersymmetric Standard Model (MSSM).

The discovery and the measurement of the Higgs sector will be a central piece of the experimental effort at the LHC. The production of the Higgs boson is dominated by gluon fusion through a top quark loop, for the whole relevant Higgs mass range [4]. The next-to-leading-order (NLO) corrections to the gluon-fusion production cross section are very large, of the order of 100% [5, 6, 7, 8]. The second most important contribution to the Higgs production cross section comes from the vector boson fusion (VBF) process, which proceeds at tree-level and receives much smaller QCD corrections [9, 10, 11].

Both of these channels participate in the phenomenologically interesting signal of $pp \rightarrow H + 2$ jets. The jets coming from the two processes have different angular distributions: well-separated and forward jets in the VBF case, in contrast to less separated jets and further central jet activity in the gluon fusion case. Thus, the cross-contamination can be reduced by imposing appropriate experimental cuts. A good theoretical understanding is also necessary to reduce the uncertainties coming from the backgrounds and interference effects, and to allow us to perform precision studies of the Higgs sector.

For the gluon-fusion contribution, in order to make the computation more tractable, it is possible to make the approximation of a large top quark mass m_t [12, 13, 5, 6]. This approximation replaces the full one-loop coupling of the Higgs boson to gluons via a top quark loop, by an effective local operator $C(m_t) H G_{\mu\nu} G^{\mu\nu}$; thus it reduces the problem by one loop order. Formally, this approximation requires the Higgs mass to obey $m_H \ll 2m_t \approx 350$ GeV. However, for inclusive Higgs production, the approximation works very well up to quite large Higgs masses, $m_H \approx 2m_t$ or more, if $C(m_t)$ is taken to have the exact m_t dependence from one loop [14]. Here we are interested primarily in processes where the Higgs boson is relatively light, but because of the extra jet activity the partonic center-of-mass energy and final-state invariant masses may be large. It has been shown that the large- m_t approximation is still valid for such configurations, as long as the jet transverse energies are smaller than m_t [15, 16].

Several groups have computed various relevant quantities for the gluon-fusion contribution to $pp \rightarrow H + 2$ jets, at LO, in the large m_t limit [17, 18, 19] and with the exact m_t dependence [20]; and at NLO accuracy in the large m_t limit [21, 22]. The real corrections to this process, involving tree amplitudes for a Higgs plus five partons, were studied in [23]. The interference between gluon fusion and VBF production has been computed, and found to be very small [24, 25]. Our results for the $H\bar{q}q\bar{Q}Q$ amplitudes can also be used to

calculate the one-loop interference between the color-singlet pieces of these two processes. We outline this calculation in section 4.

New methods have been developed for computing one-loop amplitudes for multi-leg processes. Some are based on Feynman diagrams [26, 27, 28, 29, 30, 31, 32, 33, 34, 35, 36] while others exploit generalized unitarity [37, 38, 39, 40, 41, 42, 43] and recursion relations [44]. The methods based on Feynman diagrams have been employed to compute several quantities involving the Higgs boson to next-to-leading-order [45, 46, 47].

In the large m_t approximation, the NLO corrections to the production of a Higgs boson plus various numbers of jets at a hadron collider require one-loop amplitudes in QCD, with one insertion of the effective operator $H G_{\mu\nu} G^{\mu\nu}$. We will refer to these amplitudes as one-loop Higgs plus multi-parton amplitudes. Because these virtual amplitudes contain infrared divergences, they are invariably presented using dimensional regularization (we take $D = 4 - 2\epsilon$), as a Laurent expansion in ϵ through the finite $\mathcal{O}(\epsilon^0)$ terms. The complete set of such amplitudes for three external partons (ggg or $q\bar{q}g$) was provided in ref. [48]. Results for various numbers of legs and helicity configurations have appeared more recently [49, 50, 51, 52]. In particular, the amplitudes with four gluons, all of the same helicity [49], and those with two negative and two positive helicities [51, 52] have now been computed analytically, using techniques very similar to what we will employ here.

The full analytic results for the one-loop Higgs plus four-parton amplitudes, for a complete set of parton helicities, have not yet appeared. However, the analytic expressions for the color- and helicity-summed NLO interference of one-loop and tree amplitudes have been presented for the four-quark case [21], along with numerical results for the two-quark-two-gluon and four-gluon cases. These results have been incorporated into the NLO gluon fusion contributions to $pp \rightarrow H + 2$ jets mentioned earlier [22]. In this paper we present analytic results at the amplitude level for the four-quark case, $H\bar{q}q\bar{Q}Q$. We also give the two-quark-two-gluon amplitudes, with the restriction that the two gluons must have opposite helicity, $H\bar{q}qg^\pm g^\mp$.

In our method, the Higgs field H is rewritten as the sum of a complex field ϕ , and its complex conjugate ϕ^\dagger . This has the advantage that the analytic structure of the two components is much simpler than in the total amplitude. Furthermore, we only need to compute the ϕ -amplitudes because parity relates them to the ϕ^\dagger ones. Our technique for calculating these amplitudes consists of a unitarity-recursive bootstrap approach: by performing appropriate unitarity cuts we obtain all cut-containing terms of the amplitudes (logarithmic, polylogarithmic functions, and associated terms), while the rational terms are computed using on-shell recursion relations. In this process we only use on-shell lower-point amplitudes as input in our calculation. This greatly simplifies our task and allows us to obtain compact analytic answers efficiently.

In slightly more detail, we employ quadruple cuts [53] to determine the coefficients of scalar box integrals in the amplitudes. The only scalar triangle integrals appearing in the amplitudes described here have one or two external massive legs, not three; the

coefficients of such integrals are fixed easily using the amplitudes’ known infrared poles. The coefficients of bubble integrals are computed using the method of spinor integration via residue extraction [54, 55]. As just mentioned, the rational terms are computed using on-shell recursion relations. Certain spurious poles arising in this technique are dealt with using an approach which is a *hybrid* between the cut-completion method [56, 57, 58] and the method of evaluating the spurious pole residue of the cut part [59] which is implemented numerically in BLACKHAT [44].

Our analytic expressions can easily be incorporated into one of the NLO computer programs for computing cross sections. They provide a fast evaluation of the amplitudes and are more stable compared to (semi)numerical approaches. In the computation of Higgs amplitudes with yet one more external parton (five in all), they can serve to check limiting cases, when two partons become collinear, or one gluon becomes soft. In a numerical on-shell recursive approach such as BLACKHAT [44], they could provide a more important role: the four-parton amplitudes could be used as a fast analytic input for some of the terms in the on-shell recursion relations for the five-parton amplitudes.

By performing the appropriate sum over colors and helicities of the interference between tree and one-loop amplitudes, we are able to confirm (numerically) the expression for the virtual part of the NLO cross section for $H\bar{q}q\bar{Q}Q$ presented in ref. [21]. At the same time, because our results are color decomposed, we can project them into a color-singlet channel with respect to the $\bar{q}q$ (and $\bar{Q}Q$) quantum numbers. The color-singlet channel can interfere with the electroweak VBF process [60]. We have verified numerically that this interference, which is one of the two virtual contributions to the full interference, agrees with one [24] of the two recent computations [24, 25] of this (quite small) effect [61].

The color-singlet parts of the one-loop amplitudes may be of use in determining how frequently the gluon-fusion process produces events with large “rapidity gaps” that would survive typical central jet vetoes proposed to select the VBF process. Resummed estimates of the efficacy of such vetoes have been performed recently in ref. [62] for example; however, there may also be important contributions at fixed order in α_s .

The paper is organized as follows: In section 2 we introduce some basic notions that simplify the task of computing the $H\bar{q}q\bar{Q}Q$ and $H\bar{q}qgg$ amplitudes — the $\phi\text{-}\phi^\dagger$ and color decomposition of Higgs amplitudes, and the spinor helicity formalism. In section 3 we outline the basics of the unitarity-recursive method at the core of the calculation. We also apply the technique to specific examples. In section 4 we present the full analytic answers, numerical results, and applications of our expressions. We describe checks that we have used to verify their correctness. In section 5 we present our conclusions and mention possible future directions.

2. Notation

In this section we introduce the basic notation used in the rest of this paper, as well

as some prerequisite notions. In particular, we decompose the Higgs amplitudes into ϕ and ϕ^\dagger components with simpler analytic properties, describe the color decomposition of scattering amplitudes in terms of partial and primitive amplitudes, and recall the spinor-helicity formalism.

2.1 The ϕ - ϕ^\dagger decomposition of Higgs amplitudes

In the amplitudes we study in this paper, all external quarks are taken to be massless, and the Higgs couples to them through gluons. The coupling of the SM Higgs boson to gluons is dominated by an intermediate top quark loop, because the top is much heavier than the other quarks. In the limit of very large top mass, $m_t \rightarrow \infty$, the top quark can be integrated out, giving rise to the following effective interaction [12, 13],

$$\mathcal{L}_H^{\text{int}} = \frac{C}{2} H \text{tr} G_{\mu\nu} G^{\mu\nu}, \quad (2.1)$$

with the coefficient C given by $C = \alpha_s/(6\pi v) = g^2/(24\pi^2 v)$, to leading order in α_s . Here v is the vacuum expectation value of the Higgs field, $v = 246$ GeV. (The value of C is known to $\mathcal{O}(\alpha_s^4)$ [63].) Our convention for the normalization of generators is $\text{tr} T^a T^b = \delta^{ab}$, and $G_{\mu\nu} = \sum_a T^a G_{\mu\nu}^a$, so that $\text{tr} G_{\mu\nu} G^{\mu\nu} = G_{\mu\nu}^a G^{a\mu\nu}$.

Tree-level amplitudes (not counting the top quark loop) for a Higgs boson plus multiple partons were first computed analytically for up to four partons in refs. [17, 18, 19], and up to five partons in ref. [64]. The structure of these amplitudes could be simplified [65] by splitting the effective interaction Lagrangian into two parts, a holomorphic (self-dual) and an anti-holomorphic (anti-self-dual) part. In fact, certain “maximally helicity violating (MHV) rules” that had been developed for QCD tree amplitudes [66] could be applied straightforwardly to Higgs amplitudes after making this split [65, 67]. Specifically, we consider the Higgs boson to be the real part of a complex field ϕ , with

$$\phi = \frac{1}{2}(H + iA). \quad (2.2)$$

The interaction Lagrangian can then be rewritten as

$$\mathcal{L}_{H,A}^{\text{int}} = \frac{C}{2} \left[H \text{tr} G_{\mu\nu} G^{\mu\nu} + iA \text{tr} G_{\mu\nu} {}^* G^{\mu\nu} \right] \quad (2.3)$$

$$= C \left[\phi \text{tr} G_{SD\mu\nu} G_{SD}^{\mu\nu} + \phi^\dagger \text{tr} G_{ASD\mu\nu} G_{ASD}^{\mu\nu} \right], \quad (2.4)$$

where the gluon field strength has been divided into a self-dual (SD) and an anti-self-dual (ASD) component, given by

$$G_{SD}^{\mu\nu} = \frac{1}{2}(G^{\mu\nu} + {}^* G^{\mu\nu}), \quad G_{ASD}^{\mu\nu} = \frac{1}{2}(G^{\mu\nu} - {}^* G^{\mu\nu}), \quad {}^* G^{\mu\nu} \equiv \frac{i}{2} \epsilon^{\mu\nu\rho\sigma} G_{\rho\sigma}. \quad (2.5)$$

From eq. (2.2) and its conjugate we can reconstruct the scalar H and pseudoscalar A fields according to

$$H = \phi + \phi^\dagger, \quad A = \frac{1}{i}(\phi - \phi^\dagger). \quad (2.6)$$

It follows from eq. (2.6) that the scattering amplitude for a scalar Higgs boson plus any number of partons can be obtained, at any loop order l , by the sum of the amplitudes with ϕ and ϕ^\dagger ,

$$\mathcal{A}_n^{(l)}(H, \dots) = \mathcal{A}_n^{(l)}(\phi, \dots) + \mathcal{A}_n^{(l)}(\phi^\dagger, \dots), \quad (2.7)$$

with “...” indicating any arbitrary configuration of partons.

Similarly, the amplitudes for a pseudoscalar A plus partons are given by

$$\mathcal{A}_n^{(l)}(A, \dots) = \frac{1}{i} \left[\mathcal{A}_n^{(l)}(\phi, \dots) - \mathcal{A}_n^{(l)}(\phi^\dagger, \dots) \right], \quad (2.8)$$

recognizing that the constant C is different for the A case [50]. The relation between the ϕ and ϕ^\dagger amplitudes is through parity, or complex conjugation of spinors,

$$\mathcal{A}_n^{(l)}(\phi^\dagger, 1^{h_1}, 2^{h_2}, \dots, n^{h_n}) = (-1)^{n_{\bar{q}q}} \left[\mathcal{A}_n^{(l)}(\phi, 1^{-h_1}, 2^{-h_2}, \dots, n^{-h_n}) \right] \Big|_{\langle ij \rangle \leftrightarrow [ji]}, \quad (2.9)$$

where the spinor products $\langle ij \rangle$ and $[ji]$ are defined in eqs. (2.26) and (2.27), and $n_{\bar{q}q}$ denotes the number of external antiquark-quark pairs [64]. In other words, to generate an amplitude with ϕ^\dagger from an amplitude with ϕ , one reverses the helicities of all quarks and gluons, and replaces all spinors $\langle ij \rangle$ with $[ji]$. Thus, it is possible to reconstruct the H and A helicity amplitudes by computing only their ϕ -components, using parity to get the ϕ^\dagger -components, and then assembling the two ingredients together.

It is important to note that in the separation of any Higgs amplitude into a ϕ and a ϕ^\dagger amplitude, all color and kinematic information (*e.g.*, the momentum of the scalar particle) remains the same in the original and the component amplitudes. What separates is the self-duality properties of the amplitudes, and consequently their analytic structure, resulting in a simplification of the calculation.

2.2 Color decomposition and color sums

An important tool for QCD calculations is the color decomposition of amplitudes [68, 69, 70]. It allows us to write down a color-ordered expression for any amplitude, which is a sum of products of color structures and uncolored functions of the kinematic variables, called partial amplitudes. The color and kinematic information is neatly separated in this way, and one has to compute only the partial amplitudes, which have simpler analytic properties. The partial amplitudes can be expressed in terms of yet simpler building blocks, called primitive amplitudes. Primitive amplitudes are color ordered; that is, they receive contributions only from planar one-loop Feynman diagrams with a fixed cyclic ordering of the external legs. Furthermore, a given primitive amplitude either contains a closed fermion loop (f), or it does not. If it does not, then the primitive amplitude is further characterized by how the external fermion lines are routed as they enter the loop: whether they turn left (L) or right (R) in the case of one fermion line; and according to leading-color (lc) and subleading-color (slc) designations in the case of two separate fermion lines.

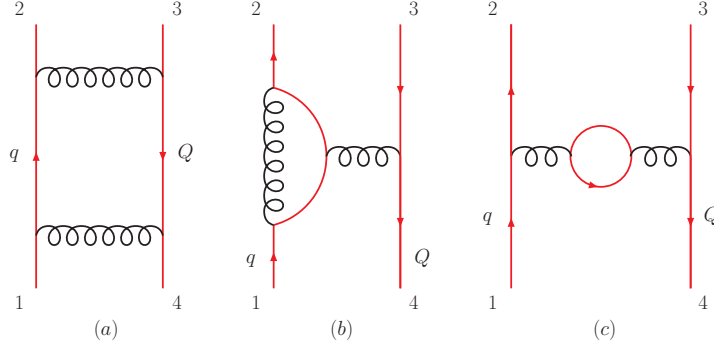


Figure 1: Sample diagrams corresponding to the (a) leading color or “lc”, (b) subleading-color or “slc” and (c) fermion loop or “f” primitive amplitudes. The Higgs field can attach to any gluon line in these diagrams.

Computing the primitive amplitudes will be the focus of this paper. First, we describe the decomposition of the $\phi\bar{q}q\bar{Q}Q$ and $\phi\bar{q}qgg$ amplitudes in terms of partial, and then primitive, amplitudes.

2.2.1 $\phi\bar{q}q\bar{Q}Q$

Because the Higgs boson, and ϕ and ϕ^\dagger fields, are color-neutral, they play no role in the color structure of the amplitude. The color decomposition of the $H\bar{q}q\bar{Q}Q$ or $\phi\bar{q}q\bar{Q}Q$ amplitude is identical to the decomposition of the four-quark $\bar{q}q\bar{Q}Q$ amplitude [71]. There are two independent color structures, corresponding to the two independent ways we can contract the color indices of the quarks. At tree level, the coefficients of the two color structures are simply related,

$$\mathcal{A}_4^{(0)}(\phi, 1_{\bar{q}}, 2_q, 3_{\bar{Q}}, 4_Q) = Cg^2 A_4^{(0)}(\phi, 1_{\bar{q}}, 2_q, 3_{\bar{Q}}, 4_Q) \left[\delta_{i_4}^{\bar{i}_1} \delta_{i_2}^{\bar{i}_3} - \frac{1}{N_c} \delta_{i_2}^{\bar{i}_1} \delta_{i_4}^{\bar{i}_3} \right], \quad (2.10)$$

where the tree helicity amplitudes $A_4^{(0)}(\phi, 1_{\bar{q}}, 2_q, 3_{\bar{Q}}, 4_Q)$ are given in eq. (A.4), and N_c denotes the number of colors, $N_c = 3$ in QCD.

At one loop, the color decomposition is

$$\begin{aligned} \mathcal{A}_4^{(1)}(\phi, 1_{\bar{q}}, 2_q, 3_{\bar{Q}}, 4_Q) = Cg^4 c_\Gamma \left[N_c \delta_{i_4}^{\bar{i}_1} \delta_{i_2}^{\bar{i}_3} A_{4;1}(\phi, 1_{\bar{q}}, 2_q, 3_{\bar{Q}}, 4_Q) \right. \\ \left. + \delta_{i_2}^{\bar{i}_1} \delta_{i_4}^{\bar{i}_3} A_{4;2}(\phi, 1_{\bar{q}}, 2_q, 3_{\bar{Q}}, 4_Q) \right], \end{aligned} \quad (2.11)$$

where we have also extracted a factor from the loop integrals,

$$c_\Gamma \equiv \frac{1}{(4\pi)^{2-\epsilon}} \frac{\Gamma(1+\epsilon)\Gamma^2(1-\epsilon)}{\Gamma(1-2\epsilon)}. \quad (2.12)$$

Formulas (2.10) and (2.11) apply to the case of different quark flavors, $q \neq Q$. The amplitude for identical flavors, $q = Q$, is found from the unequal-flavor formula by subtracting

the same formula with the labels for q and Q exchanged,

$$\mathcal{A}_4^{(l)}(\phi, 1_{\bar{q}}, 2_q, 3_{\bar{q}}, 4_q) = \mathcal{A}_4^{(l)}(\phi, 1_{\bar{q}}, 2_q, 3_{\bar{Q}}, 4_Q) - \mathcal{A}_4^{(l)}(\phi, 1_{\bar{q}}, 4_q, 3_{\bar{Q}}, 2_Q). \quad (2.13)$$

Note that the helicities of q and Q must be the same in order to get a nonvanishing exchange term. Of course if there are two identical quarks in the final state, there is also an identical-particle factor of $\frac{1}{2}$ in the phase-space measure.

The partial amplitudes $A_{4;1}$ and $A_{4;2}$ can in turn be expressed in terms of primitive amplitudes, using the results of refs. [71] for the analogous amplitudes, $e^+e^- \rightarrow \bar{q}q\bar{Q}Q$. Because the e^+e^- pair and the scalar ϕ are both colorless, the color structure is identical to our case. The results could be given in a helicity-independent form; however, we list the two different helicity cases separately, so that we can use relations among the primitive amplitudes in order to minimize the number that appear:

$$\begin{aligned} A_{4;1}(\phi, 1_{\bar{q}}^-, 2_q^+, 3_{\bar{Q}}^+, 4_Q^-) &= A_4^{\text{lc}}(\phi, 1_{\bar{q}}^-, 2_q^+, 3_{\bar{Q}}^+, 4_Q^-) \\ &\quad - \frac{2}{N_c^2} \left[A_4^{\text{lc}}(\phi, 1_{\bar{q}}^-, 2_q^+, 3_{\bar{Q}}^+, 4_Q^-) + A_4^{\text{lc}}(\phi, 1_{\bar{q}}^-, 2_q^+, 4_{\bar{Q}}^-, 3_Q^+) \right] \\ &\quad - \frac{1}{N_c^2} A_4^{\text{slc}}(\phi, 1_{\bar{q}}^-, 2_q^+, 3_{\bar{Q}}^+, 4_Q^-) + \frac{n_f}{N_c} A_4^{\text{f}}(\phi, 1_{\bar{q}}^-, 2_q^+, 3_{\bar{Q}}^+, 4_Q^-), \end{aligned} \quad (2.14)$$

$$\begin{aligned} A_{4;1}(\phi, 1_{\bar{q}}^-, 2_q^+, 3_{\bar{Q}}^-, 4_Q^+) &= A_4^{\text{lc}}(\phi, 1_{\bar{q}}^-, 2_q^+, 3_{\bar{Q}}^-, 4_Q^+) \\ &\quad - \frac{2}{N_c^2} \left[A_4^{\text{lc}}(\phi, 1_{\bar{q}}^-, 2_q^+, 3_{\bar{Q}}^-, 4_Q^+) + A_4^{\text{lc}}(\phi, 1_{\bar{q}}^-, 2_q^+, 4_{\bar{Q}}^+, 3_Q^-) \right] \\ &\quad + \frac{1}{N_c^2} A_4^{\text{slc}}(\phi, 1_{\bar{q}}^-, 2_q^+, 4_{\bar{Q}}^+, 3_Q^-) + \frac{n_f}{N_c} A_4^{\text{f}}(\phi, 1_{\bar{q}}^-, 2_q^+, 3_{\bar{Q}}^-, 4_Q^+), \end{aligned} \quad (2.15)$$

$$\begin{aligned} A_{4;2}(\phi, 1_{\bar{q}}^-, 2_q^+, 3_{\bar{Q}}^+, 4_Q^-) &= A_4^{\text{lc}}(\phi, 1_{\bar{q}}^-, 2_q^+, 4_{\bar{Q}}^-, 3_Q^+) \\ &\quad + \frac{1}{N_c^2} \left[A_4^{\text{lc}}(\phi, 1_{\bar{q}}^-, 2_q^+, 4_{\bar{Q}}^-, 3_Q^+) + A_4^{\text{lc}}(\phi, 1_{\bar{q}}^-, 2_q^+, 3_{\bar{Q}}^+, 4_Q^-) \right] \\ &\quad + \frac{1}{N_c^2} A_4^{\text{slc}}(\phi, 1_{\bar{q}}^-, 2_q^+, 3_{\bar{Q}}^+, 4_Q^-) - \frac{n_f}{N_c} A_4^{\text{f}}(\phi, 1_{\bar{q}}^-, 2_q^+, 3_{\bar{Q}}^+, 4_Q^-), \end{aligned} \quad (2.16)$$

$$\begin{aligned} A_{4;2}(\phi, 1_{\bar{q}}^-, 2_q^+, 3_{\bar{Q}}^-, 4_Q^+) &= A_4^{\text{lc}}(\phi, 1_{\bar{q}}^-, 2_q^+, 3_{\bar{Q}}^-, 4_Q^+) \\ &\quad - \frac{1}{N_c^2} \left[A_4^{\text{lc}}(\phi, 1_{\bar{q}}^-, 2_q^+, 3_{\bar{Q}}^-, 4_Q^+) + A_4^{\text{lc}}(\phi, 1_{\bar{q}}^-, 2_q^+, 4_{\bar{Q}}^+, 3_Q^-) \right] \\ &\quad - \frac{1}{N_c^2} A_4^{\text{slc}}(\phi, 1_{\bar{q}}^-, 2_q^+, 4_{\bar{Q}}^+, 3_Q^-) - \frac{n_f}{N_c} A_4^{\text{f}}(\phi, 1_{\bar{q}}^-, 2_q^+, 3_{\bar{Q}}^-, 4_Q^+). \end{aligned} \quad (2.17)$$

Here A_4^{lc} , A_4^{slc} , and A_4^{f} describe respectively the leading-color, subleading-color and fermion-loop primitive amplitudes. The number of massless quark flavors is denoted by n_f . The quantity $A_4^{\text{lc}}(\phi, 1_{\bar{q}}^-, 2_q^+, 4_{\bar{Q}}^-, 3_Q^+)$ refers to the primitive amplitude $A_4^{\text{lc}}(\phi, 1_{\bar{q}}^-, 2_q^+, 3_{\bar{Q}}^-, 4_Q^+)$ with the labels on legs 3 and 4 exchanged. Sample Feynman diagrams corresponding to these amplitudes are shown in figure 1.

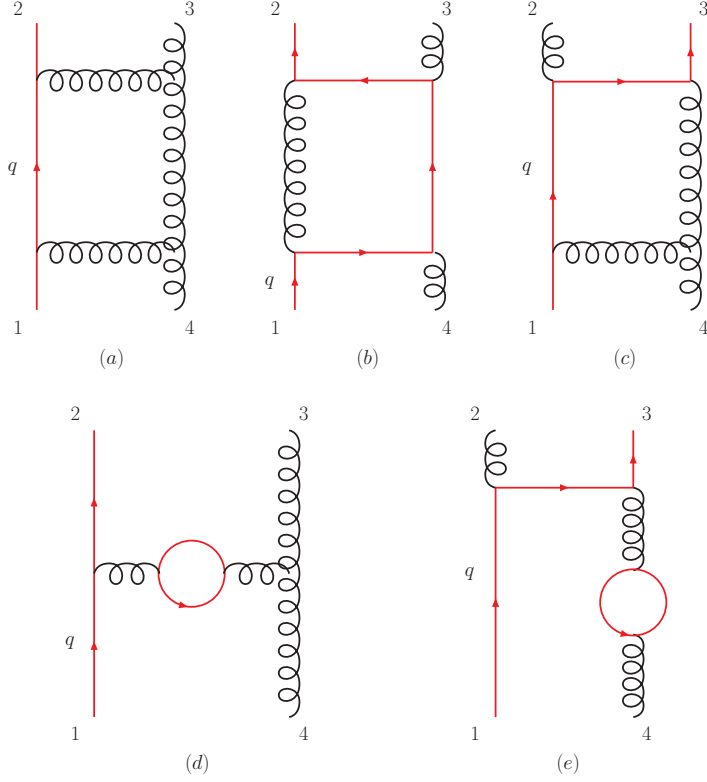


Figure 2: Sample diagrams corresponding to the (a) $\bar{q}qgg$ L , (b) $\bar{q}qgg$ R , (c) $\bar{q}gqg$ L , (d) $\bar{q}qgg$ fermion loop, and (e) $\bar{q}gqg$ fermion loop primitive amplitudes. The Higgs field can attach to any gluon line in these diagrams.

The virtual part of the unpolarized NLO cross section for $H\bar{q}q\bar{Q}Q$ requires the sum over both helicities and colors of the interference of the tree and one-loop amplitudes. The color sum is straightforward to work out from eqs. (2.10) and (2.11),

$$\sum_{\text{colors}} [\mathcal{A}_4^* \mathcal{A}_4]_{\text{NLO}} = 2C^2 c_{\Gamma} g^6 (N_c^2 - 1) N_c \text{Re} \left[\mathcal{A}_4^{(0)*}(H, 1_{\bar{q}}, 2_q, 3_{\bar{Q}}, 4_Q) A_{4;1}(H, 1_{\bar{q}}, 2_q, 3_{\bar{Q}}, 4_Q) \right]. \quad (2.18)$$

The same formula also applies with H replaced by A . The formula for the case of identical quarks $q = Q$ follows from eq. (2.13).

2.2.2 $\phi\bar{q}qgg$

Similarly, the color decomposition for the $\phi\bar{q}qgg$ amplitudes is identical to that for the process $e^+e^- \rightarrow \bar{q}qgg$ [72]. The tree amplitude is given by

$$\mathcal{A}_4^{(0)}(\phi, 1_{\bar{q}}, 2_q, 3, 4) = Cg^2 \sum_{\sigma \in S_2} (T^{a_{\sigma(3)}} T^{a_{\sigma(4)}})_{i_2^{\bar{1}}} A_4^{(0)}(\phi, 1_{\bar{q}}, 2_q, \sigma(3), \sigma(4)), \quad (2.19)$$

where the tree helicity amplitudes $A_4^{(0)}(\phi, 1_{\bar{q}}, 2_q, 3, 4)$ are given in eq. (A.5).

The one-loop amplitude is decomposed as

$$\begin{aligned} \mathcal{A}_4^{(1)}(\phi, 1_{\bar{q}}, 2_q, 3, 4) = Cg^4 c_\Gamma \left[N_c \sum_{\sigma \in S_2} (T^{a_{\sigma(3)}} T^{a_{\sigma(4)}})_{i_2}^{\bar{i}_1} A_{4;1}(\phi, 1_{\bar{q}}, 2_q, \sigma(3), \sigma(4)) \right. \\ \left. + \delta^{a_3 a_4} \delta_{i_2}^{\bar{i}_1} A_{4;3}(\phi, 1_{\bar{q}}, 2_q; 3, 4) \right]. \end{aligned} \quad (2.20)$$

The partial amplitudes $A_{4;1}$ and $A_{4;3}$ are given, in a helicity-independent fashion, by

$$\begin{aligned} A_{4;1}(\phi, 1_{\bar{q}}, 2_q, 3, 4) = A_4^L(\phi, 1_{\bar{q}}, 2_q, 3, 4) - \frac{1}{N_c^2} A_4^R(\phi, 1_{\bar{q}}, 2_q, 3, 4) \\ + \frac{n_f}{N_c} A_4^f(\phi, 1_{\bar{q}}, 2_q, 3, 4), \end{aligned} \quad (2.21)$$

$$\begin{aligned} A_{4;3}(\phi, 1_{\bar{q}}, 2_q; 3, 4) = A_4^L(\phi, 1_{\bar{q}}, 2_q, 3, 4) + A_4^L(\phi, 1_{\bar{q}}, 2_q, 4, 3) + A_4^L(\phi, 1_{\bar{q}}, 3, 2_q, 4) \\ + A_4^L(\phi, 1_{\bar{q}}, 4, 2_q, 3) + A_4^R(\phi, 1_{\bar{q}}, 2_q, 3, 4) + A_4^R(\phi, 1_{\bar{q}}, 2_q, 4, 3). \end{aligned} \quad (2.22)$$

Here we choose to label the leading- and subleading-color primitive amplitudes by “ L ” and “ R ” (corresponding to fermion lines turning left or right upon entering the loop) to be compatible with the notation used in ref. [50]. Again A_4^f denotes a fermion-loop contribution. Sample Feynman diagrams corresponding to these primitive amplitudes are shown in figure 2.

The virtual part of the unpolarized NLO cross section for $H\bar{q}qgg$ requires the sum over both helicities and colors of the interference of the tree and one-loop amplitudes. The color sum can be expressed in the same form as that for $e^+e^- \rightarrow \bar{q}qgg$ [72],

$$\begin{aligned} \sum_{\text{colors}} [\mathcal{A}_4^* \mathcal{A}_4]_{\text{NLO}} = 2C^2 c_\Gamma g^6 (N_c^2 - 1) \text{Re} \left\{ A_4^{(0)*}(H, 1_{\bar{q}}, 2_q, 3, 4) \left[(N_c^2 - 1) A_{4;1}(H, 1_{\bar{q}}, 2_q, 3, 4) \right. \right. \\ \left. \left. - A_{4;1}(H, 1_{\bar{q}}, 2_q, 4, 3) + A_{4;3}(H, 1_{\bar{q}}, 2_q; 3, 4) \right] \right\} \\ + \{3 \leftrightarrow 4\}. \end{aligned} \quad (2.23)$$

The same formula also applies with H replaced by A .

2.3 Spinor helicity formalism

Primitive amplitudes depend only on kinematic variables. They are functions of the external momenta of the Higgs boson, $k_\phi = k_H$, and of the four partons, k_i , $i = 1, \dots, 4$. These momenta are all outgoing, by convention, so momentum conservation and the on-shell conditions read,

$$k_\phi + \sum_{i=1}^4 k_i = 0, \quad (2.24)$$

$$k_\phi^2 = k_H^2 = m_H^2, \quad k_i^2 = 0. \quad (2.25)$$

A very convenient representation of the amplitudes is in terms of spinor inner products, as reviewed *e.g.* in refs. [69, 70]. Let $u_{\pm}(k_i)$ be a massless Weyl spinor of momentum k_i and positive or negative chirality. The corresponding two-component spinors are often denoted λ_i^{α} and $\tilde{\lambda}_i^{\dot{\alpha}}$. The spinor products are defined by

$$\langle i j \rangle = \lambda_i^{\alpha} \lambda_j_{\alpha} = \langle i^{-} | j^{+} \rangle = \bar{u}_{-}(k_i) u_{+}(k_j), \quad (2.26)$$

$$[i j] = \tilde{\lambda}_{i\dot{\alpha}} \tilde{\lambda}_j^{\dot{\alpha}} = \langle i^{+} | j^{-} \rangle = \bar{u}_{+}(k_i) u_{-}(k_j). \quad (2.27)$$

We use the convention $[i j] = \text{sgn}(k_i^0 k_j^0) \langle j i \rangle^{*}$, so that

$$\langle i j \rangle [j i] = 2k_i \cdot k_j \equiv s_{ij}. \quad (2.28)$$

For real momenta, and up to a complex phase, the spinor inner products are square roots of the corresponding kinematic invariant $s_{ij} \equiv (k_i + k_j)^2$.

Three-parton invariant masses are defined by,

$$s_{ijl} \equiv (k_i + k_j + k_l)^2 = \langle i j \rangle [j i] + \langle j l \rangle [l j] + \langle i l \rangle [l i]. \quad (2.29)$$

We also define the spinor strings,

$$\langle a | i | b \rangle = \langle a i \rangle [i b], \quad \langle a | (i + j) | b \rangle = \langle a i \rangle [i b] + \langle a j \rangle [j b]. \quad (2.30)$$

Strings involving the Higgs momentum, such as $\langle a^{-} | k_H | b^{-} \rangle$, could also show up; however, they can be eliminated in favor of strings such as in eq. (2.30) using momentum conservation.

Besides momentum conservation, the other two spinor product identities used to simplify expressions are antisymmetry,

$$\langle j i \rangle = -\langle i j \rangle, \quad [j i] = -[i j], \quad (2.31)$$

and the Schouten identity,

$$\langle a b \rangle \langle c d \rangle = \langle a d \rangle \langle c b \rangle + \langle a c \rangle \langle b d \rangle, \quad (2.32)$$

$$[a b] [c d] = [a d] [c b] + [a c] [b d]. \quad (2.33)$$

Composite spinors can appear in these products as well and they can be handled similarly,

$$\langle a | P_{i\dots j} | b \rangle \langle c d \rangle = \langle a d \rangle \langle c | P_{i\dots j} | b \rangle - \langle a c \rangle \langle d | P_{i\dots j} | b \rangle, \quad (2.34)$$

$$\langle a | P_{i\dots j} | b \rangle [c d] = \langle a | P_{i\dots j} | d \rangle [c b] + \langle a | P_{i\dots j} | c \rangle [b d], \quad (2.35)$$

$$\langle a | P_{i\dots j} | b \rangle \langle c | P_{i\dots j} | d \rangle = \langle a | P_{i\dots j} | d \rangle \langle c | P_{i\dots j} | b \rangle - P_{i\dots j}^2 \langle a c \rangle [b d], \quad (2.36)$$

where $P_{i\dots j}$ denotes an arbitrary momentum sum, $P_{i\dots j}^{\mu} \equiv \sum_{m=i}^j k_m^{\mu}$. The spinor products defined above form the building blocks for the primitive amplitudes and the basis for our calculations in the next sections.

3. Unitarity and recursive bootstrap method

The method we employ in our paper combines the (generalized) unitarity method [73, 74, 72, 53, 54, 55] with on-shell recursion relations [75] operating at one loop [76, 77, 56]. Using general integral reduction formulae [78, 79], any dimensionally-regulated one-loop amplitude $\mathcal{A}_n^{(1)}$ with massless internal lines can be decomposed as,

$$\mathcal{A}_n^{(1)} = C_n + R_n, \quad (3.1)$$

where the *cut part* C_n is a linear combination of scalar integrals [78, 79],

$$C_n = \sum_i d_i \mathcal{I}_4^i + \sum_i c_i \mathcal{I}_3^i + \sum_i b_i \mathcal{I}_2^i, \quad (3.2)$$

and R_n denotes the *rational part*, which contains no branch cuts (in four dimensions). The box integrals \mathcal{I}_4^i , triangle integrals \mathcal{I}_3^i and bubble integrals \mathcal{I}_2^i are well known (see for example refs. [80, 81, 82, 83]). Hence determining C_n is equivalent to computing the coefficients of the respective integrals, d_i , c_i and b_i . These coefficients are found by taking (generalized) four-dimensional unitarity cuts of the amplitude in various channels. The rational part R_n will be calculated by utilizing on-shell recursion relations, which requires only information about lower-point loop amplitudes and tree amplitudes. (For a review of the on-shell approach, see ref. [37].)

In the remainder of this section, we outline the various ingredients in the method, and apply them to specific primitive amplitudes for $\phi\bar{q}q\bar{Q}Q$ and $\phi\bar{q}qgg$. The results for these amplitudes are collected in section 4.

3.1 Generalized unitarity for box coefficients

In this paper, the generalized unitarity method, along with complex spinor integration [53, 54, 55] is employed in a twofold manner for the calculation of box functions and bubble (single log) functions respectively.

In ref. [53] it was shown that using quadruple cuts, it is possible to reduce the task of calculating the coefficient of any box function into that of calculating a product of four tree amplitudes. This method can be applied to box functions with any number of external masses by taking advantage of the generally non-vanishing behavior of the all-massless three-point amplitudes when momenta are complexified. A three-point amplitude with one leg carrying opposite helicity from the other two can have either an MHV or an anti-MHV (sometimes also denoted $\overline{\text{MHV}}$) representation while satisfying energy-momentum conservation. The complex momenta allow for all four loop momenta of a box diagram to become on shell, freezing the cut integral completely and simplifying it into an algebraic product of tree amplitudes.

For example, the coefficient of the box integral in figure 3 is given by

$$d = \frac{1}{\Delta_{\text{LS}} \mathcal{I}_4} \int d^4 \ell_1 \delta^{(+)}(\ell_1^2) \delta^{(+)}(\ell_2^2) \delta^{(+)}(\ell_3^2) \delta^{(+)}(\ell_4^2) A_1^{(0)} A_2^{(0)} A_3^{(0)} A_4^{(0)}, \quad (3.3)$$

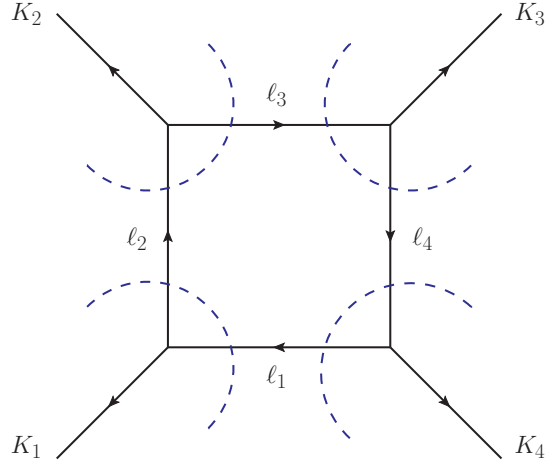


Figure 3: Evaluation of a box function coefficient using quadruple cuts. The four on-shell conditions on the loop momentum reduce the integration to an algebraic product of four tree amplitudes.

where $\ell_2 = \ell_1 - K_1$, $\ell_3 = \ell_1 - K_1 - K_2$, $\ell_4 = \ell_1 + K_4$, and each $A_i^{(0)}$ corresponds to the tree amplitude in the respective corner with massive (or massless) momentum K_i ($i = 1 \dots 4$). The quadruple cut (or leading singularity) of the scalar box integral is given by

$$\Delta_{\text{LS}} \mathcal{I}_4 = \int d^4 \ell_1 \delta^{(+)}(\ell_1^2) \delta^{(+)}(\ell_2^2) \delta^{(+)}(\ell_3^2) \delta^{(+)}(\ell_4^2), \quad (3.4)$$

from which we obtain

$$d = \frac{1}{2} \sum_{\sigma, h} A_1^{(0)}(\ell_1^\sigma) A_2^{(0)}(\ell_1^\sigma) A_3^{(0)}(\ell_1^\sigma) A_4^{(0)}(\ell_1^\sigma), \quad (3.5)$$

where the summation is over the two discrete solutions ℓ_1^σ , $\sigma = 1, 2$, of the loop-momentum localization constraints,

$$\ell_1^2 = \ell_2^2 = \ell_3^2 = \ell_4^2 = 0, \quad (3.6)$$

and over all possible helicities h of internal particles propagating in the loop.

3.1.1 A two-mass box coefficient

Let's consider, for example, the leading-color primitive amplitude $A_4^{\text{lc}}(\phi, 1_{\bar{q}}^-, 2_q^+, 3_Q^+, 4_Q^-)$. One of the box coefficients that needs to be determined for this primitive amplitude is that of the “easy two mass” box integral, with diagonally opposite massive legs having mass m_H^2 and s_{23} . Because all the two-mass boxes have m_H^2 as one of the two masses, we denote this coefficient, using the other mass, as d_{23}^{2me} . This box integral is defined by the clustering of the five external particles into the four legs of the box: $(1)(23)(4)(\phi)$. The associated quadruple cut is shown in figure 4.

The tree amplitude with ϕ and two gluons vanishes unless both helicities are negative [65]. It is easy to see that this fact, plus fermion helicity conservation, forces the

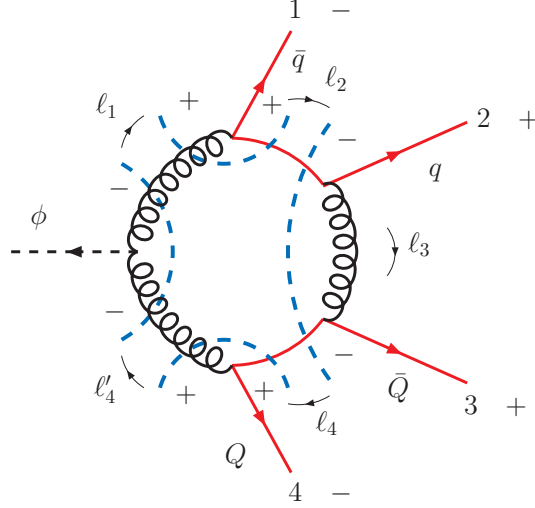


Figure 4: Quadruple cut for the evaluation of the easy-two-mass box coefficient d_{23}^{2me} of $A_4^{\text{lc}}(\phi, 1_{\bar{q}}^-, 2_q^+, 3_{\bar{Q}}^+, 4_Q^-)$.

unique assignment of intermediate helicities shown in figure 4. The three-point vertices containing legs 1 and 4 are only nonvanishing for one of the two solutions to the quadruple cut conditions (3.6). Equation (3.5) then becomes,

$$d_{23}^{2me} = \frac{1}{2} A_2^{(0)}(\phi, \ell_1^-, -\ell_4'^-) A_3^{(0)}(-\ell_1^+, 1_{\bar{q}}^-, \ell_{2q}^+) A_4^{(0)}(-\ell_{2\bar{q}}^-, 2_q^+, 3_{\bar{Q}}^+, \ell_{4Q}^-) A_3^{(0)}(-\ell_{4\bar{Q}}^+, 4_Q^-, \ell_4'^+). \quad (3.7)$$

Using the expressions for the tree amplitudes, we get

$$d_{23}^{2me} = \frac{i^4}{2} \times \left(-\langle \ell_1 (-\ell_4') \rangle^2 \right) \times \frac{[(-\ell_1) \ell_2]^2}{[1 \ell_2]} \times \left(-\frac{[2 3]^2}{[(-\ell_2) 2] [3 \ell_4]} \right) \times \frac{[\ell_4' (-\ell_4)]^2}{[(-\ell_4) 4]}. \quad (3.8)$$

The positive chirality spinors for the three-point vertices containing legs 1 and 4 are proportional,

$$\lambda_{\ell_1} \propto \lambda_{\ell_2} \propto \lambda_1, \quad \lambda_{\ell_4} \propto \lambda_{\ell_4'} \propto \lambda_4. \quad (3.9)$$

Using this fact, along with momentum conservation relations, we can eliminate all explicit loop momenta from eq. (3.8):

$$\begin{aligned} d_{23}^{2me} &= \frac{1}{2} [2 3]^2 \frac{([\ell_2 \ell_1] \langle \ell_1 \ell_4' \rangle [\ell_4' \ell_4])^2}{[1 \ell_2] [\ell_2 2] [3 \ell_4] [\ell_4 4]} \\ &= \frac{1}{2} [2 3]^2 \frac{([\ell_2 1] \langle 1 4 \rangle [4 \ell_4])^2}{[1 \ell_2] [\ell_2 2] [3 \ell_4] [\ell_4 4]} \\ &= \frac{1}{2} \langle 1 4 \rangle^2 [2 3]^2 \frac{[1 \ell_2] \langle \ell_2 4 \rangle \langle 1 \ell_4 \rangle [\ell_4 4]}{[2 \ell_2] \langle \ell_2 4 \rangle \langle 1 \ell_4 \rangle [\ell_4 3]} \\ &= \frac{1}{2} \langle 1 4 \rangle^2 [2 3]^2 \frac{[1 | (2 + 3) | 4 \rangle \langle 1 | (2 + 3) | 4 \rangle}{[2 3] \langle 3 4 \rangle \langle 1 2 \rangle [2 3]} \\ &= \frac{1}{2} \langle 4 | (2 + 3) | 1 \rangle \langle 1 | (2 + 3) | 4 \rangle \frac{\langle 1 4 \rangle^2}{\langle 1 2 \rangle \langle 3 4 \rangle}. \end{aligned} \quad (3.10)$$

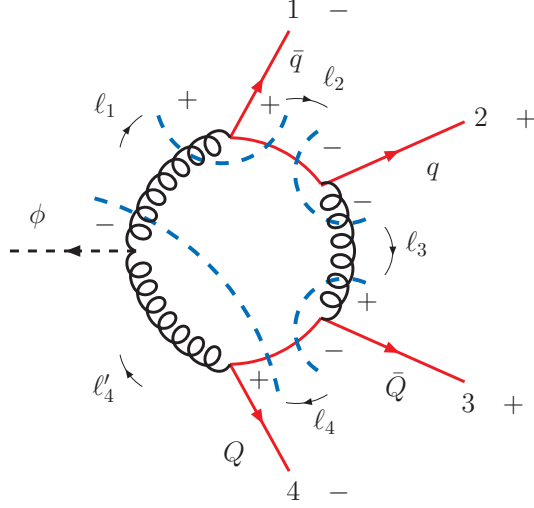


Figure 5: Quadruple cut for the evaluation of the one-mass box coefficient d_{123}^{1m} appearing in $A_4^{\text{lc}}(\phi, 1_{\bar{q}}^-, 2_q^+, 3_{\bar{Q}}^+, 4_Q^-)$.

In section 4 we express the result, not in terms of the scalar box integral \mathcal{I}_4^{2me} , but in terms of the infrared-finite box function $\text{Ls}_{-1}^{2me}(s_{123}, s_{234}; s_{23}, m_H^2)$. These are related by eq. (B.6). After removing a factor of c_{F} associated with eq. (2.11), and using the identity

$$s_{123}s_{234} - s_{23}m_H^2 = \langle 4|(2+3)|1\rangle\langle 1|(2+3)|4\rangle, \quad (3.11)$$

the coefficient of the box function $\text{Ls}_{-1}^{2me}(s_{123}, s_{234}; s_{23}, m_H^2)$ in $A_4^{\text{lc}}(\phi, 1_{\bar{q}}^-, 2_q^+, 3_{\bar{Q}}^+, 4_Q^-)$ is

$$D_{23}^{2me} \equiv \frac{2i}{s_{123}s_{234} - s_{23}m_H^2} d_{23}^{2me} = i \frac{\langle 14 \rangle^2}{\langle 12 \rangle \langle 34 \rangle} = -A_4^{(0)}(\phi, 1_{\bar{q}}^-, 2_q^+, 3_{\bar{Q}}^+, 4_Q^-). \quad (3.12)$$

It is a general feature of every primitive amplitude presented in section 4 that all easy-two-mass box functions have coefficients equal to the negative of the corresponding tree amplitude. We therefore collect all the Ls_{-1}^{2me} functions into “V” functions, which also contain the infrared and ultraviolet poles in ϵ , since the latter have to be proportional to the tree amplitude as well.

3.1.2 Calculation of a one-mass box coefficient

As our second box example, we compute for the same primitive amplitude the coefficient of the one-mass box function $\text{Ls}_{-1}(s_{12}, s_{23}; s_{123})$, associated with the external leg clustering $(1)(2)(3)(4\phi)$. The quadruple cut is depicted in figure 5. We label the box integral coefficient by d_{123}^{1m} . Again the vanishing of a tree amplitude involving ϕ , in this case $A_3^{(0)}(\phi, \ell_1^+, -\ell_{4\bar{Q}}^+, 4_Q^-)$, along with fermion helicity conservation and the vanishing of $A_4^{(0)}(\bar{q}^-, q^+, g^+, g^+)$, forces the unique helicity assignment shown in the figure. The cut

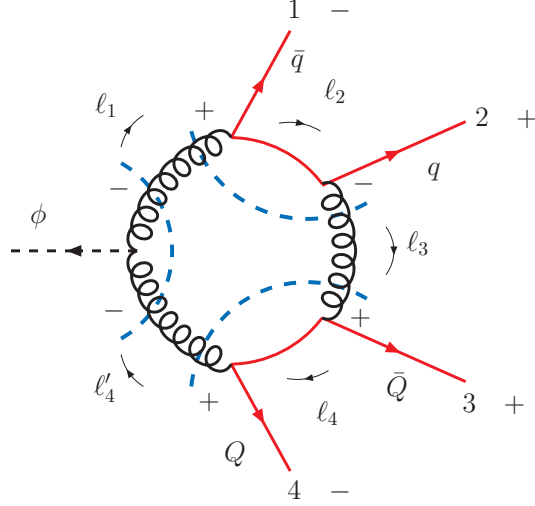


Figure 6: Sample $\phi\bar{q}q\bar{Q}Q$ triple cut, illustrating the vanishing coefficient for a three-mass triangle integral, caused by the tree amplitude in the lower right corner associated with the external invariant s_{34} . Consequently, hard-two-mass box functions are absent from the amplitude as well.

evaluates to

$$\begin{aligned}
d_{123}^{1m} &= \frac{1}{2} A_3^{(0)}(\phi, \ell_1^-, -\ell_{4Q}^+, 4_Q^-) A_3^{(0)}(-\ell_1^+, 1_{\bar{q}}^-, \ell_{2q}^+) A_3^{(0)}(-\ell_{2\bar{q}}^-, 2_q^+, \ell_3^-) A_3^{(0)}(-\ell_3^+, 3_{\bar{Q}}^+, \ell_{4Q}^-) \\
&= \frac{i^4}{2} \times \left(-\frac{\langle \ell_1 4 \rangle^2}{\langle (-\ell_4) 4 \rangle} \right) \times \frac{[(-\ell_1) \ell_2]^2}{[1 \ell_2]} \times \left(-\frac{\langle \ell_3 (-\ell_2) \rangle^2}{\langle (-\ell_2) 2 \rangle} \right) \times \frac{[(-\ell_3) 3]^2}{[3 \ell_4]}. \quad (3.13)
\end{aligned}$$

After some spinor product manipulations similar to eq. (3.10), we have

$$d_{123}^{1m} = \frac{1}{2} s_{12} s_{23} \frac{\langle 14 \rangle^2}{\langle 12 \rangle \langle 34 \rangle}, \quad (3.14)$$

which yields for the coefficient of the function $\text{Ls}_{-1}(s_{12}, s_{23}; s_{123})$,

$$D_{123}^{1m} = \frac{2i}{s_{12} s_{23}} d_{123}^{1m} = i \frac{\langle 14 \rangle^2}{\langle 12 \rangle \langle 34 \rangle} = -A_4^{(0)}(\phi, 1_{\bar{q}}^-, 2_q^+, 3_{\bar{Q}}^+, 4_Q^-). \quad (3.15)$$

The result is again proportional to the tree, up to a sign. This property holds for all the one-mass box coefficients Ls_{-1} in the $\phi\bar{q}q\bar{Q}Q$ primitive amplitudes, apart from the leading-color piece of the $(-+-+)$ helicity configuration. However, in the $\phi\bar{q}qgg$ primitive amplitudes it is typically not true.

3.2 Absence of three-mass triangles

The one-loop ϕ amplitudes that we consider in this paper have the property that the triple cuts associated with three-mass triangle integrals all vanish. This general feature holds because the tree-level four-parton amplitudes in QCD, $A_4^{(0)}(1, 2, 3, 4)$, and those with an additional ϕ boson, $A_4^{(0)}(\phi, 1, 2, 3, 4)$, each require two negative helicities to be nonvanishing.

A nonvanishing product of three such amplitudes, as required for a triple cut, implies six negative helicities. Three of the negative helicities are associated with the three cut lines, so there must be three external negative helicities. However, the one-loop ϕ amplitudes we consider here only have two negative helicities. An example of a vanishing triple cut is shown in figure 6. The same argument implies that all “hard-two-mass” boxes, with two adjacent massive legs, must vanish: For any hard-two-mass box quadruple cut, one can remove the cut between the two adjacent massless legs, relaxing the quadruple cut into a (vanishing) triple cut. Because the $\phi + 4$ parton amplitudes obviously contain no three-mass or four-mass box integrals, only one-mass and easy-two-mass box coefficients have to be computed here.

The amplitudes $\phi g^- g^- g^+ g^+$ [51] and $\phi g^- g^+ g^- g^+$ [52] also contain only one-mass and easy-two-mass boxes, and no three-mass triangles, for the same reason, insufficiently many negative helicities in the triple cuts. Interestingly, the amplitude $\phi g^- g^- g^- g^-$ computed in ref. [49] also contains only one-mass and easy-two-mass boxes, and no three-mass triangles, for the opposite reason, a paucity of positive helicity gluons. On the other hand, the primitive amplitudes for $\phi \bar{q}^- q^+ g^- g^-$ and $\phi g^+ g^- g^- g^-$, which have not yet been computed analytically, will contain three-mass triangles and hard-two-mass boxes.

For the coefficients of two-mass and one-mass triangles, the above triple-cut vanishing argument does not hold. The existence of a massless external leg implies that one of the tree amplitudes can be an $\overline{\text{MHV}}$ three-point amplitude, which contains only one negative helicity, not two. However, the two-mass and one-mass triangle integrals, given in eqs. (B.7) and (B.8), contain single log terms at order $1/\epsilon$. Because of this, their coefficients are completely determined by the known infrared poles of the amplitude, so they do not have to be computed separately. The remainder of the work to compute the cut part of the amplitude involves determining the coefficients of bubble integrals.

3.3 Unitarity and spinor integration for bubbles

In the case of the ordinary two-particle cuts used to determine bubble coefficients, there are not enough constraints to fully localize the cut integral. The cut contains a residual phase-space integral. The method we use in this case was proposed in refs. [54, 55] and consists of writing the cut loop momentum integral as an integral over spinor variables $\ell \equiv |\ell\rangle$ and $\tilde{\ell} \equiv |\ell]$ [66]. The integrand can be transformed into a total derivative in $\tilde{\ell}$, leaving a single integral over ℓ which can be evaluated by residue extraction.

For the cut shown in figure 7, the coefficient of the logarithm will be given by an integral of the form

$$\int d^4\ell_1 \delta^{(+)}(\ell_1^2) \delta^{(+)}(\ell_2^2) A_1^{(0)} A_2^{(0)} = \int_0^\infty dt \, t \int \langle \ell d\ell \rangle [\ell d\ell] \delta(P^2 - t\langle \ell | P | \ell \rangle) f(\ell, \tilde{\ell}), \quad (3.16)$$

where ℓ can be either ℓ_1 or ℓ_2 , whichever is more convenient. The function $f(\ell, \tilde{\ell})$ represents

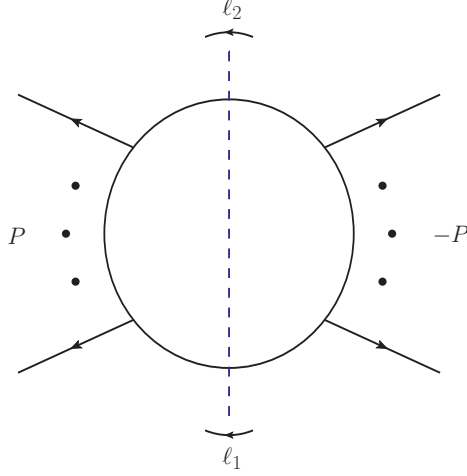


Figure 7: Example of the evaluation of a bubble (single log) function using an ordinary two-particle cut. Integration over the loop momentum is required in this case.

the product of the two tree amplitudes and is in general a sum of terms of the form

$$\frac{\prod_i \langle a_i \ell \rangle \prod_j [b_j \ell] \prod_k \langle \ell | R_k | \ell \rangle}{\prod_i \langle c_i \ell \rangle \prod_j [d_j \ell] \prod_k \langle \ell | Q_k | \ell \rangle}, \quad \text{with } Q_k \neq P, \quad Q_k^2 \neq 0. \quad (3.17)$$

After performing the integration over t and partial fractioning using Schouten identities, we can always bring the remaining integrand into a form where we can take advantage of the identity

$$[\ell \, d\ell] \left(\frac{[\eta \ell]^n}{\langle \ell | P | \ell \rangle^{n+2}} \right) = [d\ell \, \partial_\ell] \left(\frac{1}{n+1} \frac{1}{\langle \ell | P | \eta \rangle} \frac{[\eta \ell]^{n+1}}{\langle \ell | P | \ell \rangle^{n+1}} \right), \quad (3.18)$$

and convert it into a total derivative with respect to $|\ell\rangle$. (In the special case of $n = 0$, the spinor $|\eta\rangle$ appears only on the right-hand side of eq. (3.18); hence it can be chosen arbitrarily.) Then we can evaluate the integral over $|\ell\rangle$ by calculating the residue for each pole. The case of multiple poles was also examined in ref. [55].

In this process one also detects the coefficients of box integrals sharing the same cut. These are the terms that scale like $1/\langle \ell | P | \ell \rangle$ after partial fractioning of the integrand. They can serve as an independent check of the box coefficients determined by the quadruple cuts.

3.3.1 Calculation of a bubble coefficient

As an example, we compute the coefficient of the bubble integral $\mathcal{I}_2(s_{123})$, or equivalently, of the single logarithm $\ln(-s_{123})$, in the primitive amplitude $A_4^{\text{lc}}(\phi, 1_{\bar{q}}^-, 2_q^+, 3_Q^+, 4_{\bar{Q}}^-)$. The

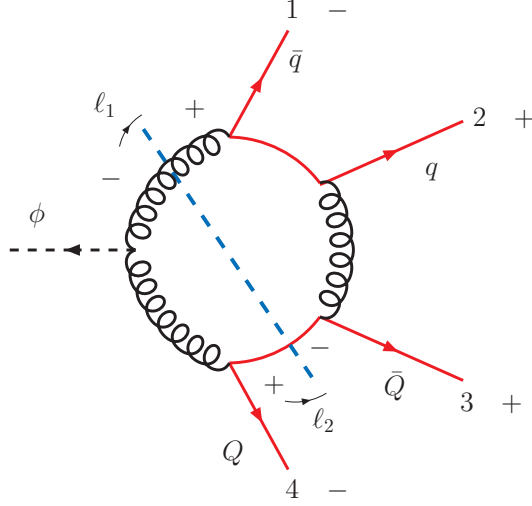


Figure 8: Two-particle cut for the evaluation of the bubble function coefficient b_{123} of $A_4^{\text{lc}}(\phi, 1_{\bar{q}}^-, 2_q^+, 3_{\bar{Q}}^+, 4_Q^-)$.

corresponding two-particle cut is shown in figure 8, and the cut integral is given by

$$\begin{aligned}
& i \int \text{dLIPS} A_3^{(0)}(\phi, \ell_1^-, \ell_2^+, 4_Q^-) \times A_5^{(0)}(-\ell_1^+, 1_{\bar{q}}^-, 2_q^+, 3_{\bar{Q}}^+, -\ell_2^-) \\
&= i^3 \int \text{dLIPS} \left(-\frac{\langle \ell_1 4 \rangle^2}{\langle \ell_2 4 \rangle} \right) \times \frac{\langle 1 (-\ell_2) \rangle^3 \langle 2 3 \rangle}{\langle 1 2 \rangle \langle 2 3 \rangle \langle 3 (-\ell_2) \rangle \langle (-\ell_2) (-\ell_1) \rangle \langle (-\ell_1) 1 \rangle} \\
&= \int \text{dLIPS} \frac{\langle \ell_2 1 \rangle^3 \langle \ell_1 4 \rangle^2}{\langle 1 2 \rangle \langle \ell_2 3 \rangle \langle \ell_2 \ell_1 \rangle \langle \ell_1 1 \rangle \langle \ell_2 4 \rangle}. \tag{3.19}
\end{aligned}$$

Here dLIPS stands for the Lorentz-invariant phase space measure.

By multiplying both the numerator and denominator of the integrand in eq. (3.19) with factors of $[\ell_2 \ell_1]$ we can eliminate one of the loop momenta (in this case we choose to eliminate ℓ_1), leaving us with an expression that depends only on the other loop momentum (in this case, ℓ_2). Furthermore, we rewrite the integral over the Lorentz-invariant phase space as an integral over spinor variables, as in eq. (3.16),

$$\int \text{dLIPS} = \int_0^\infty t dt \int \langle \ell_2 d\ell_2 \rangle [\ell_2 d\ell_2] \delta(P^2 - t \langle \ell_2 | P | \ell_2 \rangle), \tag{3.20}$$

with $P \equiv P_{123} = k_1 + k_2 + k_3$. We also need to track factors of \sqrt{t} from rescaling the ℓ_2 spinors in the integrand. Performing these steps yields

$$- \int_0^\infty t^2 dt \int \langle \ell_2 d\ell_2 \rangle [\ell_2 d\ell_2] \delta(P^2 - t \langle \ell_2 | P | \ell_2 \rangle) \frac{\langle \ell_2 1 \rangle^3 \langle 4 | P | \ell_2 \rangle^2}{\langle 1 2 \rangle \langle \ell_2 3 \rangle P^2 \langle 1 | P | \ell_2 \rangle \langle \ell_2 4 \rangle}. \tag{3.21}$$

We can readily integrate over t , eliminating the δ -function, to get

$$- \int \langle \ell_2 d\ell_2 \rangle [\ell_2 d\ell_2] \frac{P^2 \langle \ell_2 1 \rangle^3 \langle 4 | P | \ell_2 \rangle^2}{\langle \ell_2 | P | \ell_2 \rangle^3 \langle 1 2 \rangle \langle \ell_2 3 \rangle \langle 1 | P | \ell_2 \rangle \langle \ell_2 4 \rangle}. \tag{3.22}$$

The two-particle cut we have considered detects not only bubbles, but also boxes that have cuts in this channel. By using Schouten identities we can rearrange terms so that we separate the bubble contributions from the box contributions,

$$- \int \langle \ell_2 d\ell_2 \rangle [\ell_2 d\ell_2] \left\{ \frac{P^2 \langle \ell_2 1 \rangle \langle 1|P|\ell_2 \rangle \langle \ell_2 4 \rangle}{\langle \ell_2|P|\ell_2 \rangle^3 \langle 1 2 \rangle \langle \ell_2 3 \rangle} - \frac{2P^2 \langle \ell_2 1 \rangle \langle 1 4 \rangle}{\langle \ell_2|P|\ell_2 \rangle^2 \langle 1 2 \rangle \langle \ell_2 3 \rangle} + \frac{P^2 \langle \ell_2 1 \rangle \langle 1 4 \rangle^2}{\langle \ell_2|P|\ell_2 \rangle \langle 1 2 \rangle \langle \ell_2 3 \rangle \langle 1|P|\ell_2 \rangle \langle \ell_2 4 \rangle} \right\}. \quad (3.23)$$

We identify the box contribution as the last term in eq. (3.23), with the $1/\langle \ell_2|P|\ell_2 \rangle$ dependence. Because the box contributions are obtained straightforwardly from the quadruple cuts, we can safely discard them (or use them as an independent check, but we won't do so here). The remaining part will be the coefficient of the bubble $\mathcal{I}_2(s_{123})$, given by

$$b_{123} = - \int \langle \ell_2 d\ell_2 \rangle [\ell_2 d\ell_2] \left\{ \frac{P^2 \langle \ell_2 1 \rangle \langle 1|P|\ell_2 \rangle \langle \ell_2 4 \rangle}{\langle \ell_2|P|\ell_2 \rangle^3 \langle 1 2 \rangle \langle \ell_2 3 \rangle} - \frac{2P^2 \langle \ell_2 1 \rangle \langle 1 4 \rangle}{\langle \ell_2|P|\ell_2 \rangle^2 \langle 1 2 \rangle \langle \ell_2 3 \rangle} \right\}. \quad (3.24)$$

Transforming the integral over $|\ell_2 \rangle$ into a total derivative using the general formula (3.18), with $n = 0, 1$ for the two terms in eq. (3.24), we obtain

$$b_{123} = \int \langle \ell_2 d\ell_2 \rangle [d\ell_2 \partial_{\ell_2}] \left\{ \frac{1}{2} \frac{\langle 1|P|\ell_2 \rangle^2 \langle \ell_2 4 \rangle}{\langle \ell_2|P|\ell_2 \rangle^2 \langle 1 2 \rangle \langle \ell_2 3 \rangle} + \frac{2P^2 \langle \ell_2 1 \rangle \langle 1 4 \rangle [3 \ell_2]}{\langle \ell_2|P|\ell_2 \rangle \langle 1 2 \rangle \langle \ell_2 3 \rangle \langle \ell_2|P|3 \rangle} \right\}. \quad (3.25)$$

In this last step we have chosen the value $|\eta \rangle = |3 \rangle$ for the arbitrary spinor $|\eta \rangle$ appearing in the $n = 0$ term after its transformation into a total derivative.

At this point we are ready to evaluate the integral over $|\ell_2 \rangle$ by computing the residues of the poles of the integrand. We only have simple poles occurring for $|\ell_2 \rangle = |3 \rangle$ in the first term, and for $|\ell_2 \rangle = P|3 \rangle$ in the second term of eq. (3.25). Note that our choice for $|\eta \rangle$ eliminates a pole for $|\ell_2 \rangle = |3 \rangle$ in the second term. After substituting and simplifying, using $\langle 3|P|3 \rangle = s_{123} - s_{12}$, we get for the coefficient of the single log $\ln(-s_{123})$ in $A_4^{\text{lc}}(\phi, 1_{\bar{q}}, 2_q^+, 3_Q^+, 4_Q^-)$,

$$B_{123} = -i b_{123} = -i \left[\frac{1}{2} \frac{\langle 1 2 \rangle [2 3]^2 \langle 3 4 \rangle}{(s_{123} - s_{12})^2} - 2 \frac{[2 3] \langle 1 4 \rangle}{s_{123} - s_{12}} \right], \quad (3.26)$$

which is a rather simple final answer.

The procedure outlined above for the computation of B_{123} is a typical example of the steps that have to be carried out to calculate any bubble function coefficient. It has been automated and implemented in MAPLE and yields a fast analytical evaluation of these cuts.

3.4 On-shell recursion

The (four-dimensional) unitarity technique can give us the cut-containing parts of the amplitudes (terms associated with functions with an imaginary part), but not the parts that

are rational functions of the kinematic variables. However, these terms can be determined from their analytic properties as well, namely their factorization poles. On-shell recursion relations, developed first at tree level [84, 75] and later at one loop [76, 77, 56, 57, 58, 85], exploit the known factorization behavior and have greatly simplified the task of calculating these terms.

At tree level, all amplitudes are rational functions and one can consider [75] a complex shift of any two of the external momenta j and l of an amplitude A_n , given by

$$\tilde{\lambda}_j \rightarrow \tilde{\lambda}_j - z\tilde{\lambda}_l, \quad \lambda_l \rightarrow \lambda_l + z\lambda_j. \quad (3.27)$$

This $[j, l]$ shift preserves momentum conservation as well as the massless conditions for the momenta k_j and k_l , which are now modified as follows,

$$k_j^\mu \rightarrow k_j^\mu - \frac{z}{2}\langle j|\gamma^\mu|l\rangle, \quad k_l^\mu \rightarrow k_l^\mu + \frac{z}{2}\langle j|\gamma^\mu|l\rangle. \quad (3.28)$$

The shifted amplitude $A_n(z)$ is an analytic function of z with only simple poles, which are associated with factorizations of $A_n(z)$ onto lower-point tree amplitudes.

Provided that $A_n(z) \rightarrow 0$ as $z \rightarrow \infty$, the integral of $A_n(z)/z$ over the contour at infinity vanishes. This integral is also given by the sum over the residues at the poles for finite z . Therefore, the unshifted physical amplitude we wish to compute is given by the residue at $z = 0$,

$$A_n = A_n(0) = - \sum_{\text{poles } \alpha} \text{Res}_{z=z_\alpha} \frac{A_n(z)}{z}. \quad (3.29)$$

Each pole z_α in eq. (3.29) is associated with a physical factorization channel of the amplitude. Factorization allows the evaluation of the residue, leading to the tree-level on-shell recursion relation [84, 75]

$$A_n = \sum_h \sum_{r,s} A_L^h(z_{rs}) \frac{i}{P_{r\dots s}^2} A_R^{-h}(z_{rs}), \quad (3.30)$$

where $h = \pm 1$ denotes the helicity of the intermediate state carrying momentum $P_{r\dots s}$. The double sum over r and s is over partitions of the external legs into two sets (contiguous with respect to the color-ordering), for which the shifted legs j and l lie on opposite sides of the pole ($j \in L$ and $l \in R$). In the case of ϕ amplitudes, because ϕ is uncolored (and we do not shift the ϕ leg), it can appear on either the L or R side. The tree amplitudes on each side are evaluated at the complex momenta (3.28), shifted by $z = z_{rs}$, where

$$z_{rs} = \frac{P_{r\dots s}^2}{\langle j^- | P_{r\dots s} | l^- \rangle} \quad (3.31)$$

is the solution to the condition $P_{r\dots s}^2(z_{rs}) = 0$.

At the one-loop level the situation is more intricate. Figure 9(a) shows schematically the pole structure of a typical tree amplitude $A_n^{(0)}(z)$. As shown in figure 9(b), the shifted one-loop amplitude $A_n^{(1)}(z)$ can in general have not just simple physical poles, but

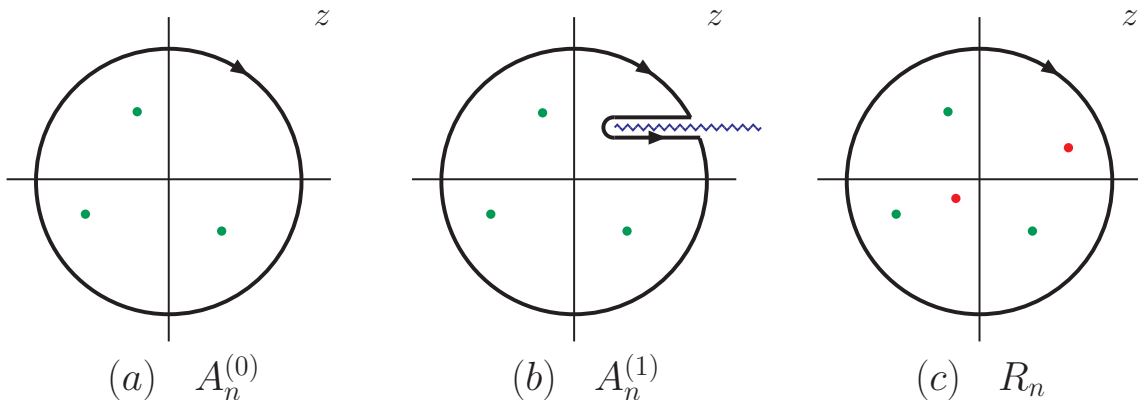


Figure 9: Analytic structure in the z plane of (a) tree amplitudes $A_n^{(0)}(z)$, (b) one-loop amplitudes $A_n^{(1)}(z)$, and (c) the rational part of one-loop amplitudes $R_n(z)$. The contour of integration is shown. The (green) dots in (a) and (b) represent physical poles. The additional (red) dots displayed in (c) represent spurious poles.

also branch cuts in the complex plane, as well as double poles [76]. In addition, it more frequently has non-vanishing behavior at infinity.

Branch cuts would result in the need to evaluate discontinuities along an integration contour, as shown in figure 9(b). To avoid this, one can use the decomposition (3.1) of the one-loop amplitude $A_n^{(1)}$ into a cut part C_n and a rational part R_n , and then work with the shifted rational part $R_n(z)$, instead of analyzing the behavior of the full shifted one-loop amplitude $A_n^{(1)}(z)$. Although $R_n(z)$ is a rational function of z , only containing poles, some of these poles are spurious. The spurious poles are represented by the additional (red) dots in figure 9(c). Unlike the physical poles, the spurious poles are not associated with physical factorization channels. Their contribution to the entire shifted amplitude $A_n^{(1)}(z)$ cancels between the shifted cut part $C_n(z)$ and the shifted rational part $R_n(z)$.

One type of spurious pole arises from the existence of terms such as $(\ln r)/(1-r)^2$ in C_n . Here r is a ratio of two kinematic invariants that differ by a single massless leg. For example, eq. (3.26) displays a factor of $(s_{123} - s_{12})^2$ in the denominator of the coefficient of $\ln(-s_{123})$ in the primitive amplitude $A_4^{\text{lc}}(\phi, 1_q^-, 2_q^+, 3_Q^+, 4_Q^-)$. It corresponds to a term $(\ln r)/(1-r)^2$ with $r = s_{123}/s_{12}$. Under many choices of shift (3.27), r will become a nontrivial function of z . In this case a spurious pole, located at the solution to $r(z) = 1$, will be generated for $C_n(z)$, and a compensating one for $R_n(z)$.

An analytic method for handling the contributions of spurious poles was developed in a number of papers [56, 57, 58, 85]. The method has also been applied to Higgs boson amplitudes [51, 52]. It consists of the following approach: We assume that the cut-containing pieces C_n have been obtained using methods such as those described in the previous subsection. Then, for a general shifted one-loop amplitude we can write

$$A_n^{(1)}(z) = C_n(z) + R_n(z). \quad (3.32)$$

Our goal is to compute the rational terms R_n . We can absorb spurious singularities present in R_n into the cut-containing pieces by rewriting

$$A_n^{(1)}(z) = \widehat{C}_n(z) + \widehat{R}_n(z), \quad (3.33)$$

where the *completed-cut terms* $\widehat{C}_n(z)$ are free of spurious singularities, as are the *remaining rational terms* $\widehat{R}_n(z)$.

To absorb all spurious singularities located at solutions to $r(z) = 1$, we make substitutions in C_n of the form

$$\frac{\ln r}{(1-r)^2} \rightarrow \frac{\ln r + 1 - r}{(1-r)^2} \equiv L_1(r), \quad (3.34)$$

$$\frac{\ln r}{(1-r)^3} \rightarrow \frac{\ln r - (r - 1/r)/2}{(1-r)^3} \equiv L_2(r), \quad (3.35)$$

where r represents the ratio of any two kinematic invariants that differ by a single massless leg. The amount by which the completed-cut terms have changed in this process is given by the *rational completed-cut terms*,

$$\widehat{CR}_n(z) = \widehat{C}_n(z) - C_n(z). \quad (3.36)$$

Consequently,

$$\widehat{R}_n(z) = R_n(z) - \widehat{CR}_n(z). \quad (3.37)$$

One can then consider the contour integral at infinity for $\widehat{R}_n(z)/z$.

Provided that all spurious poles are removed from $\widehat{R}_n(z)$ by the substitutions (3.34) and (3.35), this contour integral leads to an equation analogous to the tree-level recursion relation (3.29), featuring residues only at physical poles,

$$\widehat{R}_n = \widehat{R}_n(0) = - \sum_{\text{poles } \alpha} \text{Res}_{z=z_\alpha} \frac{\widehat{R}_n(z)}{z}. \quad (3.38)$$

These residues can be split into two sets of terms, using eq. (3.37). The first set consists of the *recursive diagrams*, associated with residues of $R_n(z)$; it can be evaluated analogously to the tree-level recursive diagrams (3.30):

$$\begin{aligned} R_n^D &\equiv - \sum_{\text{poles } \alpha} \text{Res}_{z=z_\alpha} \frac{R_n(z)}{z} \\ &= \sum_h \sum_{r,s} \left\{ R(k_r, \dots, \hat{k}_j, \dots, k_s, -\hat{P}_{r\dots s}^{-h}) \frac{i}{P_{r\dots s}^2} A^{(0)}(k_{s+1}, \dots, \hat{k}_l, \dots, k_{r-1}, \hat{P}_{r\dots s}^h) \right. \\ &\quad + A^{(0)}(k_r, \dots, \hat{k}_j, \dots, k_s, -\hat{P}_{r\dots s}^{-h}) \frac{i}{P_{r\dots s}^2} R(k_{s+1}, \dots, \hat{k}_l, \dots, k_{r-1}, \hat{P}_{r\dots s}^h) \\ &\quad \left. + A^{(0)}(k_r, \dots, \hat{k}_j, \dots, k_s, -\hat{P}_{r\dots s}^{-h}) \frac{i R_{\mathcal{F}}(P_{r\dots s}^2)}{P_{r\dots s}^2} A^{(0)}(k_{s+1}, \dots, \hat{k}_l, \dots, k_{r-1}, \hat{P}_{r\dots s}^h) \right\}. \end{aligned} \quad (3.39)$$

The recursive diagrams are computed from the rational parts R of lower-point loop amplitudes, and lower-point tree amplitudes $A^{(0)}$, as well as the rational part of the factorization function $R_{\mathcal{F}}$, which only enters for multi-particle poles [56] (and not for collinear, two-particle channels). Just as at tree level, ϕ can appear on either side of the pole.

The second contribution from the physical poles consists of the overlap terms,

$$O_n = \sum_{\text{poles } \alpha} \text{Res}_{z=z_\alpha} \frac{\widehat{CR}_n(z)}{z}. \quad (3.40)$$

They correct for the difference between $R_n(z)$ and $\widehat{R}_n(z)$ in eq. (3.37). In section 3.4.2 we will describe a modification of this procedure that can be used when the cut-completion described above fails to remove all spurious poles.

Finally, we have to consider the potential contributions to the integral from infinity, because $\widehat{R}_n(z) = A_n^{(1)}(z) - \widehat{C}_n(z)$ may not vanish as $z \rightarrow \infty$. In the case of the $H\bar{q}q\bar{Q}Q$ amplitudes there is always a shift that ensures a vanishing behavior of $\widehat{R}_n(z)$ for large z , but there is no guarantee that this is always the case. In fact, some of the shifts used to compute the $H\bar{q}qgg$ amplitudes have non-vanishing large z behavior. Usually it is straightforward to compute the $z \rightarrow \infty$ limit of $A_n(z)$ and $\widehat{C}_n(z)$, denoted by $\text{Inf}A_n$ and $\text{Inf}\widehat{C}_n$ respectively. In some cases, a pair of shifts is necessary [57] (the original shift plus an auxiliary one), but that was not required for the amplitudes computed here. Putting together all the pieces, the full answer is given by

$$A_n^{1\text{-loop}} = \widehat{C}_n + R_n^D + O_n - \text{Inf}\widehat{C}_n + \text{Inf}A_n. \quad (3.41)$$

3.4.1 Calculation of rational parts for $A_4^{\text{lc}}(\phi, 1_{\bar{q}}^-, 2_q^+, 3_Q^+, 4_Q^-)$

To illustrate the calculation of the rational parts, we consider the primitive amplitude $A_4^{\text{lc}}(\phi, 1_{\bar{q}}^-, 2_q^+, 3_Q^+, 4_Q^-)$. After completing the cut terms to form \widehat{CR}_4 , the first step is to choose a pair of legs $[j, l]$ to shift according to eq. (3.27). Then we compute the recursive diagrams R_4^D and overlap terms O_4 , as well as any contributions from infinity (Inf terms) under this shift.

For the case of $A_4^{\text{lc}}(\phi, 1_{\bar{q}}^-, 2_q^+, 3_Q^+, 4_Q^-)$, the only parts of the cut terms that need completing, to remove spurious singularities, are the single log terms. From the first term in eq. (3.26) we see that the function $L_1(\frac{-s_{123}}{-s_{12}})$, as defined in eq. (3.34), should be introduced to remove the singularity as $s_{123} \rightarrow s_{12}$. Similarly, the coefficient of $\ln(-s_{234})$ (which is related by symmetry to that of $\ln(-s_{123})$) requires the function $L_1(\frac{-s_{234}}{-s_{34}})$. These functions are collected in eq. (4.8). From the rational parts of the L_1 functions we obtain \widehat{CR}_4 ,

$$\widehat{CR}_4 = \frac{i}{2} \frac{\langle 34 \rangle [23]^2}{[12] (s_{12} - s_{123})} + \frac{i}{2} \frac{\langle 12 \rangle [23]^2}{[34] (s_{34} - s_{234})}. \quad (3.42)$$

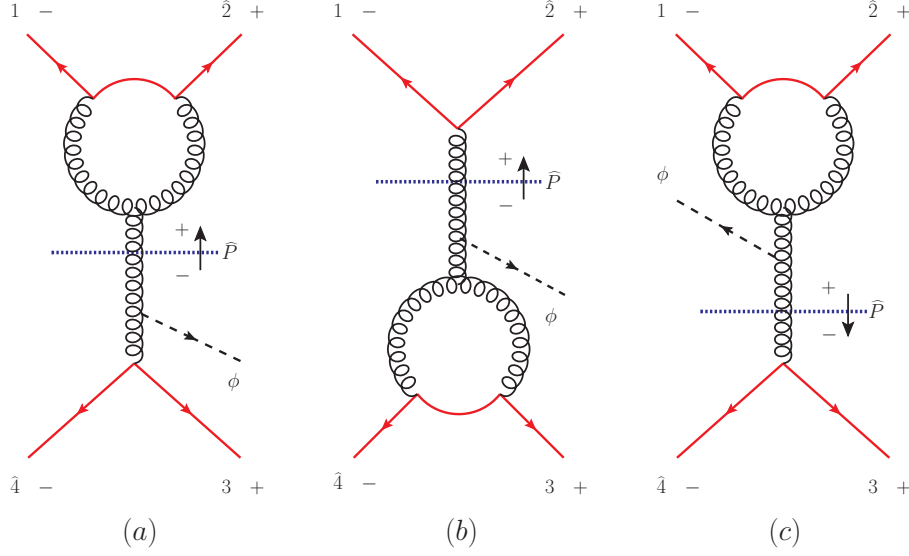


Figure 10: Diagrams needed to evaluate the recursive diagrams R_4^D of $A_4^{\text{lc}}(\phi, 1_{\bar{q}}^-, 2_q^+, 3_Q^+, 4_Q^-)$.

At this point there are no spurious poles left in \widehat{C}_4 , so we can proceed to choose a complex momentum shift (3.27). For $A_4^{\text{lc}}(1_{\bar{q}}^-, 2_q^+, 3_Q^+, 4_Q^-)$ we choose the $[4, 2\rangle$ shift, namely

$$\tilde{\lambda}_4 \rightarrow \tilde{\lambda}_4 - z\tilde{\lambda}_2, \quad \lambda_2 \rightarrow \lambda_2 + z\lambda_4, \quad (3.43)$$

or equivalently,

$$|\widehat{4}\rangle = |4\rangle - z|2\rangle, \quad |\widehat{2}\rangle = |2\rangle + z|4\rangle. \quad (3.44)$$

The contribution from infinity vanishes for this shift, $\text{Inf } A_4 = 0$. This behavior for the full amplitude can be inferred from the corresponding behavior of the known one-loop QCD amplitude found by deleting ϕ , $A_4^{\text{lc}}(1_{\bar{q}}^-, 2_q^+, 3_Q^+, 4_Q^-)$. The rational part of this amplitude is a constant times the tree amplitude [86], and it is easy to see from eq. (A.4) that the tree amplitude vanishes under the $[4, 2\rangle$ shift. Injecting a finite amount of momentum through the field ϕ should not affect the large- z behavior. We confirm this assumption *a posteriori* by checking factorization limits that are independent of the ones used to construct the recursion relation. It is also easy to verify that $\widehat{C}_4(z)$ vanishes at infinity; *i.e.*, $\text{Inf } \widehat{C}_4 = 0$.

Next we look at the recursive diagrams R_4^D . The only diagrams that give non-vanishing contributions are the ones shown in figure 10. We evaluate each of them separately.

Diagram (a) is given by,

$$D_4^{(a)} = R_3(1_{\bar{q}}^-, \widehat{2}_q^+, -\widehat{P}^+) \frac{i}{s_{12}} A_3^{(0)}(\phi, 3_Q^+, \widehat{4}_Q^-, \widehat{P}^-). \quad (3.45)$$

The tree amplitude $A_3^{(0)}(\phi, 3_Q^+, \widehat{4}_Q^-, \widehat{P}^-)$ is a simple MHV ϕ -amplitude. The loop three-point rational part $R_3(1_{\bar{q}}^-, \widehat{2}_q^+, -\widehat{P}^+)$ can be extracted from the rational part of a one-loop splitting amplitude for $g \rightarrow \bar{q}q$. It is equal to the MHV tree amplitude $A_3^{(0)}(1_{\bar{q}}^-, \widehat{2}_q^+, -\widehat{P}^+)$,

multiplied by the ($\mathcal{O}(\epsilon^0)$) rational part of the loop splitting factor $r_S^{[1]}(\pm, \bar{q}^\mp, q^\pm)$ defined in ref. [73],

$$r_S^{[1]}(\pm, \bar{q}^\mp, q^\pm) \Big|_{\text{rat.}} = \frac{83}{18} - \frac{\delta_R}{6}. \quad (3.46)$$

Here δ_R is a regularization-scheme dependent parameter, which fixes the number of helicity states of the gluons running in the loop to $(4 - 2\delta_R\epsilon)$. For the 't Hooft-Veltman scheme [87] $\delta_R = 1$, while in the four-dimensional helicity (FDH) scheme [88, 89] $\delta_R = 0$.

Thus we get for diagram (a),

$$D_4^{(a)} = \left(-i \frac{[2(-\hat{P})]^2}{[12]} \right) \left(\frac{83}{18} - \frac{\delta_R}{6} \right) \frac{i}{s_{12}} \left(-i \frac{\langle \hat{P} 4 \rangle^2}{\langle 34 \rangle} \right). \quad (3.47)$$

To remove the dependence on \hat{P} we use the on-shell condition,

$$\langle 1 \hat{2} \rangle = 0 \quad \Leftrightarrow \quad \langle 12 \rangle + z \langle 14 \rangle = 0 \quad \Leftrightarrow \quad z = -\frac{\langle 12 \rangle}{\langle 14 \rangle}, \quad (3.48)$$

and

$$\hat{P} = |1\rangle\langle 1| + |\hat{2}\rangle\langle \hat{2}| = |1\rangle\langle 1| + |2\rangle\langle 2| + z|2\rangle\langle 4| = P + z|2\rangle\langle 4|, \quad (3.49)$$

plus some simple spinor product algebra, to get

$$D_4^{(a)} = -i \frac{\langle 14 \rangle^2}{\langle 12 \rangle \langle 34 \rangle} \left(\frac{83}{18} - \frac{\delta_R}{6} \right) = A_4^{(0)}(\phi, 1_{\bar{q}}^-, 2_q^+, 3_Q^+, 4_Q^-) \times \left(\frac{83}{18} - \frac{\delta_R}{6} \right). \quad (3.50)$$

For diagram (b) we have the same on-shell condition as for (a). We also need the rational part of the leading-color $\phi \bar{q} q g$ amplitude $A_3^{(1)}(\phi, 1_{\bar{q}}^-, 2_q^+, 3^-)$. This can be extracted from the $H \bar{q} q g$ amplitude [48] and the finite amplitude $A_3^{(1)}(\phi, 1_{\bar{q}}^-, 2_q^+, 3^+)$ [50]. Then a calculation very similar to that for diagram (a) yields

$$\begin{aligned} D_4^{(b)} &= A_3^{(0)}(1_{\bar{q}}^-, \hat{2}_q^+, -\hat{P}^+) \frac{i}{s_{12}} R_3(\phi, 3_Q^+, \hat{4}_Q^-, \hat{P}^-) \\ &= \left(-i \frac{[2(-\hat{P})]^2}{[12]} \right) \frac{i}{s_{12}} \left(-i \frac{\langle \hat{P} 4 \rangle^2}{\langle 34 \rangle} \right) \left(2 + \frac{83}{18} - \frac{\delta_R}{6} \right) \\ &= A_4^{(0)}(\phi, 1_{\bar{q}}^-, 2_q^+, 3_Q^+, 4_Q^-) \times \left(\frac{119}{18} - \frac{\delta_R}{6} \right). \end{aligned} \quad (3.51)$$

For diagram (c), the required one-loop ϕ amplitude is $A_3^{(1)}(\phi, 1_{\bar{q}}^-, 2_q^+, 3^+)$ [50]. The on-shell condition becomes

$$[3\hat{4}] = 0 \quad \Leftrightarrow \quad [34] - z[32] = 0 \quad \Leftrightarrow \quad z = \frac{[34]}{[32]} \quad (3.52)$$

and

$$\hat{P} = |3\rangle\langle 3| + |\hat{4}\rangle\langle \hat{4}| = |3\rangle\langle 3| + |4\rangle\langle 4| - z|2\rangle\langle 4| = P - z|2\rangle\langle 4|. \quad (3.53)$$

The diagram evaluates to

$$\begin{aligned}
D_4^{(c)} &= R_3(\phi, 1_{\bar{q}}^-, 2_q^+, \hat{P}^+) \frac{i}{s_{34}} A_3^{(0)}(3_Q^+, 4_Q^-, -\hat{P}^-) \\
&= \left(-i \frac{[2\hat{P}]^2}{[1\ 2]} \right) \left(-2 - \frac{1}{2} \frac{s_{1\hat{2}}}{s_{2\hat{P}}} \right) \frac{i}{s_{34}} \left(-i \frac{\langle (-\hat{P}) 4 \rangle^2}{\langle 3\ 4 \rangle} \right). \tag{3.54}
\end{aligned}$$

By substituting z with its value given by the on-shell condition for \hat{P} , eq. (3.52), and using the Schouten identity, we find that

$$\begin{aligned}
D_4^{(c)} &= -i \frac{[2\ 3]^2}{[1\ 2][3\ 4]} \left(-2 + \frac{1}{2} \frac{[1\ 2] \langle 1|(2+4)|3 \rangle}{[2\ 3] s_{234}} \right) \\
&= A_4^{(0)}(\phi^\dagger, 1_{\bar{q}}^-, 2_q^+, 3_Q^+, 4_Q^-) \left(-2 + \frac{1}{2} \frac{[1\ 2] \langle 1|(2+4)|3 \rangle}{[2\ 3] s_{234}} \right). \tag{3.55}
\end{aligned}$$

In principle, there could be recursive diagrams associated with the s_{123} and s_{341} channels. However, these diagrams vanish because on one side of the pole is a $\phi\bar{q}q$ amplitude. The amplitude $\mathcal{A}_2(\phi, 1_{\bar{q}}^-, 2_q^+)$ vanishes by angular momentum conservation, while the amplitude $\mathcal{A}_2(\phi, 1_{\bar{q}}^+, 2_q^+)$ vanishes because the quarks are massless and interact only with gluons, via chirality-preserving interactions. Similarly, the s_{23} and s_{41} poles are absent because there is no three-point amplitude containing two different flavor quarks. The sum of the recursive diagrams is

$$R_4^D = D_4^{(a)} + D_4^{(b)} + D_4^{(c)}. \tag{3.56}$$

Next we evaluate the overlap terms O_4 . They are given by

$$O_4 = \sum_{\text{poles } \alpha} \text{Res}_{z=z_\alpha} \frac{\widehat{CR}_4(z)}{z}, \tag{3.57}$$

where the sum is only over the physical poles. In our case, physical poles can arise only when the following intermediate momenta go on shell (the same channels that admit possible recursive diagrams):

$$\hat{P}_{12}^2 = 0 \Leftrightarrow z = -\frac{\langle 1\ 2 \rangle}{\langle 1\ 4 \rangle}, \quad \hat{P}_{23}^2 = 0 \Leftrightarrow z = \frac{\langle 2\ 3 \rangle}{\langle 3\ 4 \rangle}, \tag{3.58}$$

$$\hat{P}_{34}^2 = 0 \Leftrightarrow z = \frac{[3\ 4]}{[3\ 2]}, \quad \hat{P}_{41}^2 = 0 \Leftrightarrow z = \frac{[1\ 4]}{[1\ 2]}, \tag{3.59}$$

$$\hat{P}_{123}^2 = 0 \Leftrightarrow z = -\frac{s_{123}}{\langle 4|(1+3)|2 \rangle}, \quad \hat{P}_{341}^2 = 0 \Leftrightarrow z = \frac{s_{341}}{\langle 4|(1+3)|2 \rangle}. \tag{3.60}$$

However, we note that the s_{23} , s_{41} , s_{123} and s_{341} channels had no recursive diagrams. This does not necessarily imply the absence of an overlap diagram (in principle \widehat{CR}_4 could have a worse behavior than R_4 in a given channel), but it is easy to check that eq. (3.42) has no poles in these channels.

The two remaining cases correspond schematically to diagrams (a) and (b) shown in figure 11. We write

$$O_4 = O_4^{(a)} + O_4^{(b)}, \tag{3.61}$$

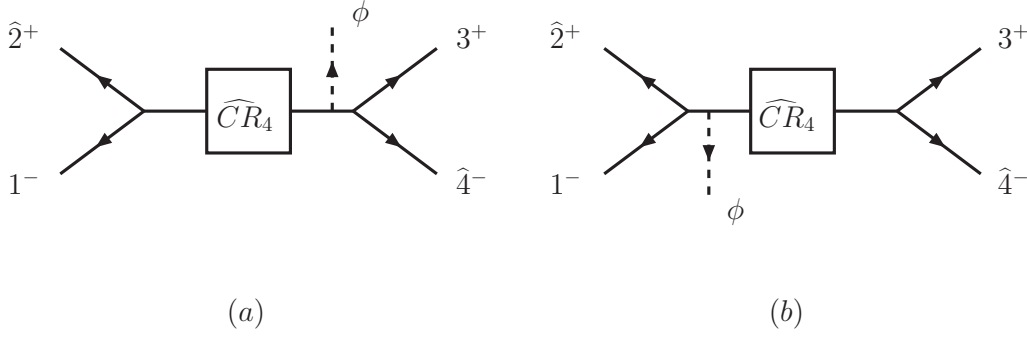


Figure 11: Schematic diagrams corresponding to the overlap terms O_4 of $A_4^{\text{lc}}(\phi, 1_{\bar{q}}^-, 2_q^+, 3_{\bar{Q}}^+, 4_Q^-)$. The diagrams are computed from the residues of $\widehat{CR}_4(z)/z$ at poles in the z plane satisfying (a) $\hat{P}_{12}^2 = 0$ and (b) $\hat{P}_{34}^2 = 0$.

where diagram (a) corresponds to $\hat{P}_{12}^2 = 0$ and diagram (b) to $\hat{P}_{34}^2 = 0$. It is simple to see from the $[4, 2]$ shift of \widehat{CR}_4 in eq. (3.42) that $O_4^{(a)}$ also vanishes, because there is no factor of $\langle 12 \rangle$ in the denominator of \widehat{CR}_4 . Thus the only non-vanishing overlap contribution comes from $O_4^{(b)}$, due to the factor of $[34]$ in the denominator of \widehat{CR}_4 . The residue is easily found to be

$$O_4 = O_4^{(b)} = \frac{i}{2} \frac{\langle 1|(2+4)|3\rangle [23]}{[34] s_{234}}. \quad (3.62)$$

We are finally ready to assemble the remaining rational terms of $A_4^{\text{lc}}(\phi, 1_{\bar{q}}^-, 2_q^+, 3_{\bar{Q}}^+, 4_Q^-)$, given by the sum

$$\widehat{R}_4 = R_4^D + O_4. \quad (3.63)$$

Using eqs. (3.56) and (3.62), we get

$$\widehat{R}_4 = A_4^{(0)}(\phi, 1_{\bar{q}}^-, 2_q^+, 3_{\bar{Q}}^+, 4_Q^-) \times \left(\frac{101}{9} - \frac{\delta_R}{3} \right) - 2 A_4^{(0)}(\phi^\dagger, 1_{\bar{q}}^-, 2_q^+, 3_{\bar{Q}}^+, 4_Q^-), \quad (3.64)$$

which is also recorded in eq. (4.8). Note that the term with the unphysical pole in s_{234} in the recursive diagram $D_4^{(c)}$ cancels against the overlap diagram $O_4^{(b)}$ for the same channel. Such recursive-overlap cancellations are a common feature.

3.4.2 Spurious poles in rational parts

The cut-completion process described in eqs. (3.34) and (3.35) removes certain types of spurious singularities, namely those associated with terms like $(\ln r)/(1-r)^n$ for $n > 1$, where r is a ratio of two momentum invariants that differ by one massless external leg. It ensures that $\widehat{C}_n(z)$, and therefore $\widehat{R}_n(z)$, is free of spurious singularities when $r(z) \rightarrow 1$, where $r(z)$ is the shifted value of r . In refs. [56, 57, 58, 51] it was found that this type of cut completion was sufficient to remove all spurious poles in the z plane for a large class of QCD and ϕ amplitudes. (Note that if a spurious denominator factor is unaffected by the particular shift used, eq. (3.27), then it will not produce a spurious pole in the z plane.)

However, poles of the type $r(z) = 1$ certainly do not exhaust the set of potential spurious poles for a general amplitude. These poles correspond specifically to Gram determinants associated with two-mass triangle integrals. In a general amplitude, there are also poles associated with the Gram determinants of a multitude of scalar box and triangle integrals with varying numbers of external masses. It would be very difficult to construct a cut completion \hat{C}_n that removed all spurious poles.

On the other hand, a completely general alternative method for handling the spurious poles was sketched in ref. [59], and fully implemented numerically in the BLACKHAT program [44]. This method did not use cut completion, but rather the original decomposition $A_n^{(1)} = C_n + R_n$, and instead relied on the fact that the residues of $C_n(z)/z$ and $R_n(z)/z$ cancel at every spurious pole. The contour integral of $R_n(z)/z$ at infinity requires the sum over spurious pole residues of $R_n(z)/z$, but this sum can be evaluated using the shifted cut part $C_n(z)$, as

$$-\sum_{\text{spurious poles } \beta} \text{Res}_{z=z_\beta} \frac{R_n(z)}{z} = \sum_{\text{spurious poles } \beta} \text{Res}_{z=z_\beta} \frac{C_n(z)}{z}. \quad (3.65)$$

Here we simply note that a hybrid approach is also feasible: First one removes the spurious poles that can be easily removed by cut completion, such as eqs. (3.34) and (3.35). This procedure leads to the overlap terms (3.40) in the usual way. Then one considers the contour integral at infinity of the remaining rational terms $\hat{R}_n(z)/z$. One evaluates the sum over residues of $\hat{R}_n(z)/z$, at the spurious poles z_γ that were *not* removed by cut completion, by using the fact that their residues still cancel against those of the completed cut terms, $\hat{C}_n(z)/z$:

$$-\sum_{\text{spurious poles } \gamma} \text{Res}_{z=z_\gamma} \frac{\hat{R}_n(z)}{z} = \sum_{\text{spurious poles } \gamma} \text{Res}_{z=z_\gamma} \frac{\hat{C}_n(z)}{z}, \quad (3.66)$$

where $\{\gamma\}$ is a subset of $\{\beta\}$.

Note that $\hat{C}_n(z)$ in eq. (3.66) includes rational terms as well as cut terms; whereas $C_n(z)$ in eq. (3.65) is a pure cut function, which nevertheless can have rational-function spurious-pole residues after Taylor expansion around the pole. In fact, it is only the rational-function part of the residue of $\hat{C}_n(z)/z$ that we require; the terms containing logarithms, polylogarithms and π^2 factors are guaranteed to cancel, because the residue of the rational function $\hat{R}_n(z)/z$ can have no such terms.

In our calculation of the $\phi\bar{q}qgg$ amplitudes, after removing the $r(z) = 1$ spurious poles, we found that certain spurious poles still remained, due to denominator factors in integral coefficients of the form $\langle ij \rangle$ or $[ij]$, where i and j are color *non-adjacent* legs. If i and j are color-adjacent, then $\langle ij \rangle$ and $[ij]$ denominator factors represent physical singularities, corresponding (for real momenta) to the region where k_i and k_j become collinear, $s_{ij} \rightarrow 0$. However, physical collinear poles for color-ordered primitive amplitudes only occur when i and j are color-adjacent; in the non-adjacent case, the $\langle ij \rangle$ and $[ij]$ factors generate spurious singularities. They are associated with the “easy two mass” box integral in which

the two diagonally opposite massless momenta are k_i and k_j , whose Gram determinant contains a factor of $s_{ij} = \langle i j \rangle [j i]$. The factors $\langle i j \rangle$ and $[i j]$ can also be seen in the denominators of the solutions for the loop momenta in the quadruple cut for the easy-two-mass box kinematics (see *e.g.* eq. (2.7) of ref. [44]). The same factors also persist in the limiting case of a one-mass box.

Factors of $\langle i j \rangle$ or $[i j]$ do appear in the denominators of coefficients of scalar integrals in the QCD and ϕ MHV n -gluon amplitudes with non-adjacent negative-helicity gluons labeled i and j , whose rational parts were computed using on-shell recursion relations [58, 52]. However, in these cases the $[i, j]$ shift was used, which leaves both $\langle i j \rangle$ and $[i j]$ unshifted, and therefore produces no spurious pole in this channel.

In this work we encountered spurious poles associated with $\langle i j \rangle$ factors in several $\phi \bar{q} q g g$ amplitudes. Here we illustrate how to use the method described above for the specific example of the leading-color primitive amplitude $A_4^L(\phi, 1_{\bar{q}}^-, 2_q^+, 3^+, 4^-)$. Using the methods of sections 3.1–3.3, we have calculated the cut-containing parts of $A_4^L(\phi, 1_{\bar{q}}^-, 2_q^+, 3^+, 4^-)$, and obtained the completed-cut terms \hat{C}_4 , which can be read off eq. (4.19) by ignoring the purely rational terms in the last few lines. To compute the rational part of this amplitude we chose to use a $[4, 1]$ shift. Inspecting \hat{C}_4 , we see that several terms contain the spurious denominator factor $\langle 1 3 \rangle$, which will potentially lead to a spurious pole under the $[4, 1]$ shift. These terms are,

$$i \frac{\langle 1 4 \rangle^3}{\langle 1 2 \rangle \langle 3 4 \rangle \langle 1 3 \rangle} \left[\text{Ls}_{-1}(s_{12}, s_{23}; s_{123}) + \text{Ls}_{-1}(s_{34}, s_{41}; s_{341}) \right] \\ - \frac{i}{3} \frac{\langle 1 2 \rangle^2 [2 3]^3 \langle 3 4 \rangle^2}{\langle 1 3 \rangle} \frac{\text{L}_2\left(\frac{-s_{123}}{-s_{12}}\right)}{s_{12}^3} + \frac{i}{2} \frac{\langle 1 2 \rangle \langle 3 4 \rangle [2 3]^2 \langle 1 4 \rangle}{\langle 1 3 \rangle} \frac{\text{L}_1\left(\frac{-s_{123}}{-s_{12}}\right)}{s_{12}^2}. \quad (3.67)$$

The spurious pole satisfies $0 = \langle \hat{1} 3 \rangle = \langle 1 3 \rangle + z \langle 4 3 \rangle$, or $z = \langle 1 3 \rangle / \langle 3 4 \rangle \equiv z_{\text{sp}}$.

Using eq. (3.66), we need to compute

$$\text{Res}_{z=z_{\text{sp}}} \frac{\hat{C}_4(z)}{z}. \quad (3.68)$$

Now the Ls_{-1} functions in eq. (3.67) actually vanish as $z \rightarrow z_{\text{sp}}$. This is because the relevant scalar box integral in $D = 6$ dimensions, which is nonsingular as $s_{13} \rightarrow 0$, can be written as

$$\mathcal{I}_4^{D=6}(s_{12}, s_{23}; s_{123}) = -i c_{\Gamma} \frac{\text{Ls}_{-1}(s_{12}, s_{23}; s_{123})}{s_{13}}, \quad (3.69)$$

and similarly for the other Ls_{-1} function. Because $\mathcal{I}_4^{D=6}$ is smooth in this limit, the Ls_{-1} functions must contain a factor of $s_{13} = \langle 1 3 \rangle [3 1]$ in the limit $s_{13} \rightarrow 0$. Thus the terms containing the Ls_{-1} functions in eq. (3.67) do not contribute to the residue.

After expanding the remaining logarithms and rational terms in eq. (3.67) around $z = z_{\text{sp}}$, we find that the logarithmic part of the residue cancels, as expected. Keeping the

rational part of the residue, and simplifying, we get

$$\text{Res}_{z=z_{\text{sp}}} \frac{\widehat{C}_4(z)}{z} = -\frac{i}{6} \frac{\langle 34 \rangle \langle 14 \rangle^2 [23]}{\langle 23 \rangle \langle 13 \rangle \langle 4|(1+3)|2]} + i \frac{2 \langle 14 \rangle [23] \langle 34 \rangle}{3 [12] \langle 23 \rangle \langle 13 \rangle}. \quad (3.70)$$

This term has to be added to the recursive diagrams, overlap terms and $\widehat{C}R_4$ to complete the full rational terms of $A_4^L(\phi, 1_{\bar{q}}^-, 2_q^+, 3^+, 4^-)$. The full rational terms, as well as the full amplitude, are now free of spurious singularities as $\langle 13 \rangle \rightarrow 0$.

The procedure outlined above can be performed in a systematic way for any amplitude, since the locations of the possible spurious poles under a chosen shift are known *a priori*, or they can be inferred simply by inspecting the completed-cut terms, \widehat{C}_n . Whenever, after absorbing spurious singularities according to eqs. (3.34) and (3.35), we are left with residual spurious poles, we can always compute their contribution to the remaining rational terms by evaluating the corresponding residues of $\widehat{C}_n(z)/z$ instead.

4. The one-loop $H\bar{q}q\bar{Q}Q$ and $H\bar{q}qgg$ amplitudes

In this section we present our main results for the one-loop $H\bar{q}q\bar{Q}Q$ and $H\bar{q}qg^\pm g^\mp$ amplitudes. First we outline how to obtain all primitive ϕ -amplitudes, using only a minimum set of them. Then we give the full analytic expressions for these amplitudes, followed by numerical results at a specific kinematic point. We then show how to obtain the color- and helicity-summed cross section for a pseudoscalar Higgs plus two quarks and two gluons, using our results and those of ref. [21]. As another application, we show how to compute part of the virtual one-loop color-singlet interference term between the gluon-fusion and VBF Higgs production mechanisms. Finally, we mention the various consistency checks we used to verify the correctness of our expressions.

4.1 Preliminaries

We obtain the one-loop corrections to $\mathcal{A}_4(H, 1_{\bar{q}}, 2_q, 3_{\bar{Q}}, 4_Q)$ and $\mathcal{A}_4(H, 1_{\bar{q}}, 2_q, 3, 4)$ by computing color-ordered primitive ϕ -amplitudes in a helicity basis, following our discussion in section 2.2. Once we have the complete set of ϕ -amplitudes, the ϕ^\dagger -amplitudes are obtained by parity, eq. (2.9).

Consider first $\mathcal{A}_4(\phi, 1_{\bar{q}}, 2_q, 3_{\bar{Q}}, 4_Q)$. Because the quarks are massless, chirality is preserved along a quark line. By convention, all external legs are outgoing, so the helicities of any quark-antiquark pair have to be opposite. Thus we need only consider the four helicity configurations $\mathcal{A}_4(\phi, 1_{\bar{q}}^{-\lambda}, 2_q^\lambda, 3_{\bar{Q}}^{-\Lambda}, 4_Q^\Lambda)$, where $\lambda, \Lambda = \pm$ are the helicities of the q and Q quarks, respectively.

Suppose the anti-quark \bar{q} (leg 1) has positive helicity. We can obtain these cases from the cases where it has negative helicity by using charge conjugation, which reverses both

quark lines ($q \leftrightarrow \bar{q}$ and $Q \leftrightarrow \bar{Q}$):

$$\mathcal{A}_4(\phi, 1_{\bar{q}}^+, 2_q^-, 3_{\bar{Q}}^-, 4_Q^+) = \mathcal{A}_4(\phi, 2_{\bar{q}}^-, 1_q^+, 4_{\bar{Q}}^+, 3_Q^-), \quad (4.1)$$

$$\mathcal{A}_4(\phi, 1_{\bar{q}}^+, 2_q^-, 3_{\bar{Q}}^+, 4_Q^-) = \mathcal{A}_4(\phi, 2_{\bar{q}}^-, 1_q^+, 4_{\bar{Q}}^-, 3_Q^+). \quad (4.2)$$

Now taking the anti-quark \bar{q} to have negative helicity, we see that there are two independent helicity configurations that we need to compute,

$$\mathcal{A}_4(\phi, 1_{\bar{q}}^-, 2_q^+, 3_{\bar{Q}}^+, 4_Q^-) \quad \text{and} \quad \mathcal{A}_4(\phi, 1_{\bar{q}}^-, 2_q^+, 3_{\bar{Q}}^-, 4_Q^+). \quad (4.3)$$

Here \mathcal{A}_4 is shorthand for the three types of primitive amplitude in this case (lc, slc, and f).

Recall from eq. (2.9) that parity gives the ϕ^\dagger -amplitudes in terms of the ϕ -amplitudes,

$$\mathcal{A}_4(\phi^\dagger, 1_{\bar{q}}^\lambda, 2_q^{-\lambda}, 3_{\bar{Q}}^\Lambda, 4_Q^{-\Lambda}) = \left[\mathcal{A}_4(\phi, 1_{\bar{q}}^{-\lambda}, 2_q^\lambda, 3_{\bar{Q}}^{-\Lambda}, 4_Q^\Lambda) \right] \Big|_{\langle i j \rangle \leftrightarrow [j i]}, \quad (4.4)$$

where the operation $\langle i j \rangle \leftrightarrow [j i]$ conjugates spinors but does not reverse the sign of absorptive parts of loop integrals.

For the $H\bar{q}qgg$ amplitude, there are two cases to consider, depending on whether the helicities of the two gluons are the same or opposite. In the case that they are the same, say both positive, we have, using the decomposition (2.7) and parity,

$$\mathcal{A}_4(H, 1_{\bar{q}}^-, 2_q^+, 3^+, 4^+) = \mathcal{A}_4(\phi, 1_{\bar{q}}^-, 2_q^+, 3^+, 4^+) - \left[\mathcal{A}_4(\phi, 1_{\bar{q}}^+, 2_q^-, 3^-, 4^-) \right] \Big|_{\langle i j \rangle \leftrightarrow [j i]}. \quad (4.5)$$

The amplitude $\mathcal{A}_4(\phi, 1_{\bar{q}}^-, 2_q^+, 3^+, 4^+)$ vanishes at tree level. For this reason, the one-loop amplitude is quite simple [50] and is given below in eqs. (4.16), (4.17) and (4.18). However, the amplitude $\mathcal{A}_4(\phi, 1_{\bar{q}}^+, 2_q^-, 3^-, 4^-)$ is next-to-maximally-helicity violating (NMHV), and at one-loop it is considerably more complex. (For example, the coefficients of the three-mass triangle integrals are nonzero for this amplitude.) We will leave its analytic computation for future work.

Instead we turn to the case of opposite-helicity gluons, which can be decomposed as

$$\mathcal{A}_4(H, 1_{\bar{q}}^-, 2_q^+, 3^\pm, 4^\mp) = \mathcal{A}_4(\phi, 1_{\bar{q}}^-, 2_q^+, 3^\pm, 4^\mp) - \left[\mathcal{A}_4(\phi, 1_{\bar{q}}^+, 2_q^-, 3^\mp, 4^\pm) \right] \Big|_{\langle i j \rangle \leftrightarrow [j i]}. \quad (4.6)$$

In this case the ϕ amplitudes are both MHV, and of a similar complexity as the $\phi\bar{q}q\bar{Q}Q$ amplitudes. Again, using charge conjugation we can exchange the roles of anti-quark and quark, so as to obtain the remaining ϕ -amplitude helicity configurations, in which the anti-quark \bar{q} has positive helicity,

$$\mathcal{A}_4(1_{\bar{q}}^+, 2_q^-, 3^\pm, 4^\mp) = \mathcal{A}_4(2_{\bar{q}}^-, 1_q^+, 4^\mp, 3^\pm). \quad (4.7)$$

Using the color decompositions in section 2.2, the problem is reduced to computing the primitive amplitudes A_4^{lc} , A_4^{slc} and A_4^{f} for two four-quark helicity configurations, $1_{\bar{q}}^- 2_q^+ 3_{\bar{Q}}^\pm 4_Q^\mp$, and A_4^L , A_4^R and A_4^{f} for two two-quark-two-gluon helicity configurations, and two color orderings, namely $1_{\bar{q}}^- 2_q^+ 3^\pm 4^\mp$ and $1_{\bar{q}}^- 3^\pm 2_q^+ 4^\mp$.

4.2 Full results

In section 3 we showed in specific examples how to compute various ingredients necessary to obtain the full $A_4^{\text{lc}}(\phi, 1_{\bar{q}}^-, 2_q^+, 3_{\bar{Q}}^+, 4_Q^-)$ and $A_4^L(\phi, 1_{\bar{q}}^-, 2_q^+, 3^+, 4^-)$ amplitudes. We used the same techniques for the quadruple cuts and ordinary two-particle cuts in all channels, and for all other color components and independent helicity configurations, in order to arrive at the full results for the ϕ -amplitudes.

It is worth noting that the computation of the $\phi\bar{q}q\bar{Q}Q$ primitive amplitudes in both helicity configurations was significantly simpler than that of the $\phi\bar{q}qgg$ amplitudes. The expressions were more compact at each stage (due in part to the higher symmetry of these amplitudes). In addition, we had no remaining spurious poles for the shifts we chose to perform. Specifically, we used a $[4, 2\rangle$ shift for all the $A_4(\phi, 1_{\bar{q}}^-, 2_q^+, 3_{\bar{Q}}^+, 4_Q^-)$ primitive amplitudes, and encountered no contributions from $z \rightarrow \infty$ (*i.e.*, $\hat{C}_4(z)$ as well as $A_4^{(1)}(z)$ vanish in this limit). We used a $[1, 3\rangle$ shift for $A_4^{\text{lc}}(\phi, 1_{\bar{q}}^-, 2_q^+, 3_{\bar{Q}}^-, 4_Q^+)$. Here there was a contribution from $z \rightarrow \infty$, from \hat{C}_4 . We used a symmetry to obtain the slc and f components of this helicity configuration from the previous one.

The $\phi\bar{q}qgg$ amplitudes were more intricate. For $A_4(\phi, 1_{\bar{q}}^-, 2_q^+, 3^+, 4^-)$, we used the $[4, 1\rangle$ shift, and we had to compute residues of spurious poles in the L , R and fermion loop (f) amplitudes, although there were no contributions from $z \rightarrow \infty$. For $A_4(\phi, 1_{\bar{q}}^-, 2_q^+, 3^-, 4^+)$, we used the $[3, 2\rangle$ shift. There were not only spurious pole residues in the L and R components, but also a contribution from $z \rightarrow \infty$ (from \hat{C}_4) in the L component. We cross-checked our results for the L and R components of $A_4(\phi, 1_{\bar{q}}^-, 2_q^+, 3^-, 4^+)$ using the $[2, 4\rangle$ shift.

Finally, for the $\phi\bar{q}qgg$ L amplitudes, we used a $[4, 1\rangle$ shift for $A_4^L(\phi, 1_{\bar{q}}^-, 2^+, 3_q^+, 4^-)$, and a $[2, 1\rangle$ shift for $A_4^L(\phi, 1_{\bar{q}}^-, 2^-, 3_q^+, 4^+)$. There were neither spurious pole contributions, nor contributions from $z \rightarrow \infty$. The full results, after assembly and simplification, are presented below.

4.2.1 $\phi\bar{q}q\bar{Q}Q$

For the $\phi\bar{q}q\bar{Q}Q$ $(-++-)$ configuration we have

$$\begin{aligned}
& -iA_4^{\text{lc}}(\phi, 1_{\bar{q}}^-, 2_q^+, 3_{\bar{Q}}^+, 4_Q^-) = -iA_4^{(0)}(\phi, 1_{\bar{q}}^-, 2_q^+, 3_{\bar{Q}}^+, 4_Q^-) \times V^{\text{lc}} \\
& -\frac{1}{2} \langle 12 \rangle \langle 34 \rangle [23]^2 \left[\frac{L_1\left(\frac{-s_{123}}{-s_{12}}\right)}{s_{12}^2} + \frac{L_1\left(\frac{-s_{234}}{-s_{34}}\right)}{s_{34}^2} \right] - 2 \langle 14 \rangle [23] \left[\frac{L_0\left(\frac{-s_{123}}{-s_{12}}\right)}{s_{12}} + \frac{L_0\left(\frac{-s_{234}}{-s_{34}}\right)}{s_{34}} \right] \\
& + 2i A_4^{(0)}(\phi^\dagger, 1_{\bar{q}}^-, 2_q^+, 3_{\bar{Q}}^+, 4_Q^-), \tag{4.8}
\end{aligned}$$

with

$$\begin{aligned}
V^{\text{lc}} = & -\frac{1}{\epsilon^2} \left[\left(\frac{\mu^2}{-s_{23}} \right)^\epsilon + \left(\frac{\mu^2}{-s_{41}} \right)^\epsilon \right] + \frac{13}{6\epsilon} \left[\left(\frac{\mu^2}{-s_{12}} \right)^\epsilon + \left(\frac{\mu^2}{-s_{34}} \right)^\epsilon \right] \\
& - \text{Ls}_{-1}^{2\text{me}}(s_{123}, s_{234}; s_{23}, m_H^2) - \text{Ls}_{-1}^{2\text{me}}(s_{341}, s_{412}; s_{41}, m_H^2) \\
& - \text{Ls}_{-1}(s_{23}, s_{34}; s_{234}) - \text{Ls}_{-1}(s_{34}, s_{41}; s_{341}) \\
& - \text{Ls}_{-1}(s_{41}, s_{12}; s_{412}) - \text{Ls}_{-1}(s_{12}, s_{23}; s_{123}) + \frac{101}{9} - \frac{\delta_R}{3}, \tag{4.9}
\end{aligned}$$

$$\begin{aligned}
-iA_4^{\text{slc}}(\phi, 1_{\bar{q}}^-, 2_q^+, 3_Q^+, 4_Q^-) = & -iA_4^{(0)}(\phi, 1_{\bar{q}}^-, 2_q^+, 3_Q^+, 4_Q^-) \times V^{\text{slc}} \\
& + \frac{1}{2} \langle 12 \rangle \langle 34 \rangle [23]^2 \left[\frac{\text{L}_1\left(\frac{-s_{123}}{-s_{12}}\right)}{s_{12}^2} + \frac{\text{L}_1\left(\frac{-s_{234}}{-s_{34}}\right)}{s_{34}^2} \right] - \langle 14 \rangle [23] \left[\frac{\text{L}_0\left(\frac{-s_{123}}{-s_{12}}\right)}{s_{12}} + \frac{\text{L}_0\left(\frac{-s_{234}}{-s_{34}}\right)}{s_{34}} \right], \tag{4.10}
\end{aligned}$$

with

$$\begin{aligned}
V^{\text{slc}} = & -\frac{1}{\epsilon^2} \left[\left(\frac{\mu^2}{-s_{12}} \right)^\epsilon + \left(\frac{\mu^2}{-s_{34}} \right)^\epsilon \right] - \frac{3}{2\epsilon} \left[\left(\frac{\mu^2}{-s_{12}} \right)^\epsilon + \left(\frac{\mu^2}{-s_{34}} \right)^\epsilon \right] \\
& - \text{Ls}_{-1}^{2\text{me}}(s_{412}, s_{123}; s_{12}, m_H^2) - \text{Ls}_{-1}^{2\text{me}}(s_{234}, s_{341}; s_{34}, m_H^2) - 7 - \delta_R, \tag{4.11}
\end{aligned}$$

and

$$A_4^{\text{f}}(\phi, 1_{\bar{q}}^-, 2_q^+, 3_Q^+, 4_Q^-) = A_4^{(0)}(\phi, 1_{\bar{q}}^-, 2_q^+, 3_Q^+, 4_Q^-) \left\{ -\frac{2}{3\epsilon} \left[\left(\frac{\mu^2}{-s_{12}} \right)^\epsilon + \left(\frac{\mu^2}{-s_{34}} \right)^\epsilon \right] - \frac{20}{9} \right\}. \tag{4.12}$$

For the $\phi\bar{q}q\bar{Q}Q$ ($-++-$) case, we find

$$\begin{aligned}
-iA_4^{\text{lc}}(\phi, 1_{\bar{q}}^-, 2_q^+, 3_{\bar{Q}}^-, 4_Q^+) = & -iA_4^{(0)}(\phi, 1_{\bar{q}}^-, 2_q^+, 3_{\bar{Q}}^-, 4_Q^+) \\
& \times \left\{ V^{\text{lc}} + \left[1 - \left(\frac{\langle 14 \rangle \langle 23 \rangle}{\langle 13 \rangle \langle 24 \rangle} \right)^2 \right] \left[\text{Ls}_{-1}(s_{23}, s_{34}; s_{234}) + \text{Ls}_{-1}(s_{41}, s_{12}; s_{412}) \right] \right\} \\
& - \frac{1}{2} \frac{\langle 12 \rangle \langle 34 \rangle}{\langle 24 \rangle^2} \left[s_{41}^2 \frac{\text{L}_1\left(\frac{-s_{412}}{-s_{12}}\right)}{s_{12}^2} + s_{23}^2 \frac{\text{L}_1\left(\frac{-s_{234}}{-s_{34}}\right)}{s_{34}^2} - \ln\left(\frac{-s_{412}}{-s_{12}}\right) - \ln\left(\frac{-s_{234}}{-s_{34}}\right) \right] \\
& + 2 \frac{[24]}{\langle 24 \rangle} \left\{ \frac{\langle 23 \rangle}{[14]} \left[s_{24} \frac{\text{L}_0\left(\frac{-s_{412}}{-s_{12}}\right)}{s_{12}} + \ln\left(\frac{-s_{412}}{-s_{12}}\right) \right] + \frac{\langle 14 \rangle}{[23]} \left[s_{24} \frac{\text{L}_0\left(\frac{-s_{234}}{-s_{34}}\right)}{s_{34}} + \ln\left(\frac{-s_{234}}{-s_{34}}\right) \right] \right\} \\
& + \frac{\langle 14 \rangle \langle 23 \rangle [24]}{\langle 24 \rangle} \left[\frac{\text{L}_0\left(\frac{-s_{412}}{-s_{41}}\right)}{s_{41}} + \frac{\text{L}_0\left(\frac{-s_{234}}{-s_{23}}\right)}{s_{23}} \right] \\
& - \frac{1}{2} \frac{1}{\langle 24 \rangle^2} \left[\frac{\langle 34 \rangle (s_{24} - s_{41})}{[12]} + \frac{\langle 12 \rangle (s_{24} - s_{23})}{[34]} \right] + 2i A_4^{(0)}(\phi^\dagger, 1_{\bar{q}}^-, 2_q^+, 3_{\bar{Q}}^-, 4_Q^+). \tag{4.13}
\end{aligned}$$

The slc and f primitive amplitudes for the $\phi\bar{q}q\bar{Q}Q$ ($-++-$) are simply related to those for ($-++-$), because two of the external legs can be exchanged at the cost of a minus sign,

$$A_4^{\text{slc}}(\phi, 1_{\bar{q}}^-, 2_q^+, 3_{\bar{Q}}^-, 4_Q^+) = -A_4^{\text{slc}}(\phi, 1_{\bar{q}}^-, 2_q^+, 4_Q^+, 3_{\bar{Q}}^-), \quad (4.14)$$

$$A_4^{\text{f}}(\phi, 1_{\bar{q}}^-, 2_q^+, 3_{\bar{Q}}^-, 4_Q^+) = -A_4^{\text{f}}(\phi, 1_{\bar{q}}^-, 2_q^+, 4_Q^+, 3_{\bar{Q}}^-). \quad (4.15)$$

These relations were used already in constructing the partial amplitudes (2.14)–(2.17).

The result for any color or helicity component of $\mathcal{A}_4^{(1)}(H, 1_{\bar{q}}, 2_q, 3_{\bar{Q}}, 4_Q)$ can be readily obtained using eqs. (4.1)–(4.4).

4.2.2 $\phi\bar{q}qgg$

The results for the infrared- and ultraviolet-finite helicity amplitude $\phi\bar{q}qgg$ ($-+++$) can be extracted from ref. [50]. We give them here for completeness:

$$\begin{aligned} -iA_4^L(\phi, 1_{\bar{q}}^-, 2_q^+, 3^+, 4^+) &= \frac{1}{2} \frac{\langle 12 \rangle \langle 1|(3+4)|2 \rangle}{\langle 23 \rangle \langle 34 \rangle \langle 41 \rangle} + \frac{1}{2} \frac{\langle 13 \rangle [34]}{\langle 23 \rangle \langle 34 \rangle} \\ &+ 2 \frac{\langle 1|(3+4)|2 \rangle^2}{\langle 34 \rangle \langle 41 \rangle \langle 3|(1+4)|2 \rangle} - 2 \frac{\langle 1|(2+3)|4 \rangle^2 \langle 2|(1+3)|4 \rangle}{\langle 12 \rangle \langle 23 \rangle s_{123} \langle 3|(1+2)|4 \rangle} \\ &- 2 \frac{[24]^3 m_H^4}{[12] s_{412} \langle 3|(1+2)|4 \rangle \langle 3|(1+4)|2 \rangle} - \frac{1}{3} \frac{\langle 13 \rangle [34] \langle 41 \rangle}{\langle 12 \rangle \langle 34 \rangle^2}, \end{aligned} \quad (4.16)$$

$$-iA_4^R(\phi, 1_{\bar{q}}^-, 2_q^+, 3^+, 4^+) = -\frac{1}{2} \left[\frac{\langle 1|(2+3)|4 \rangle}{\langle 23 \rangle \langle 34 \rangle} + \frac{\langle 12 \rangle [23] \langle 31 \rangle}{\langle 23 \rangle \langle 34 \rangle \langle 41 \rangle} \right], \quad (4.17)$$

$$-iA_4^{\text{f}}(\phi, 1_{\bar{q}}^-, 2_q^+, 3^+, 4^+) = \frac{1}{3} \frac{\langle 13 \rangle [34] \langle 41 \rangle}{\langle 12 \rangle \langle 34 \rangle^2}. \quad (4.18)$$

For $\phi\bar{q}qgg$ ($-++-$) we obtain,

$$\begin{aligned}
& -iA_4^L(\phi, 1_{\bar{q}}^-, 2_q^+, 3^+, 4^-) = -iA_4^{(0)}(\phi, 1_{\bar{q}}^-, 2_q^+, 3^+, 4^-) \\
& \quad \times \left[V_1^L - \text{LS}_{-1}(s_{23}, s_{34}; s_{234}) - \text{LS}_{-1}(s_{41}, s_{12}; s_{412}) \right] \\
& + \frac{\langle 14 \rangle^3}{\langle 12 \rangle \langle 34 \rangle \langle 13 \rangle} \left[\text{LS}_{-1}(s_{12}, s_{23}; s_{123}) + \text{LS}_{-1}(s_{34}, s_{41}; s_{341}) \right] \\
& + \left[\frac{4}{3} \frac{\langle 13 \rangle^2 \langle 4|(1+2)|3\rangle^3}{\langle 12 \rangle \langle 34 \rangle} - \langle 12 \rangle [23]^2 \langle 34 \rangle \langle 4|(1+2)|3\rangle - \frac{1}{3} \frac{\langle 12 \rangle^2 [23]^3 \langle 34 \rangle^2}{\langle 13 \rangle} \right] \frac{\text{L}_2\left(\frac{-s_{123}}{-s_{12}}\right)}{s_{12}^3} \\
& + \left[\frac{1}{2} \frac{\langle 13 \rangle^2 \langle 24 \rangle \langle 4|(1+2)|3\rangle^2}{\langle 12 \rangle \langle 23 \rangle \langle 34 \rangle} + \frac{\langle 13 \rangle \langle 14 \rangle \langle 4|(1+2)|3\rangle^2}{\langle 12 \rangle \langle 34 \rangle} + \frac{1}{2} \frac{\langle 12 \rangle \langle 34 \rangle [23]^2 \langle 14 \rangle}{\langle 13 \rangle} \right] \frac{\text{L}_1\left(\frac{-s_{123}}{-s_{12}}\right)}{s_{12}^2} \\
& - \frac{1}{2} \frac{\langle 12 \rangle \langle 34 \rangle \langle 24 \rangle [23]^2}{\langle 23 \rangle} \frac{\text{L}_1\left(\frac{-s_{234}}{-s_{34}}\right)}{s_{34}^2} + \frac{\langle 14 \rangle^2 \langle 4|(1+2)|3\rangle}{\langle 12 \rangle \langle 34 \rangle} \frac{\text{L}_0\left(\frac{-s_{123}}{-s_{12}}\right)}{s_{12}} \\
& - 2 \frac{\langle 14 \rangle \langle 24 \rangle [23]}{\langle 23 \rangle} \left[\frac{\text{L}_0\left(\frac{-s_{123}}{-s_{12}}\right)}{s_{12}} + \frac{\text{L}_0\left(\frac{-s_{234}}{-s_{34}}\right)}{s_{34}} \right] \\
& - \frac{5}{6} \left[-2iA_4^{(0)}(\phi, 1_{\bar{q}}^-, 2_q^+, 3^+, 4^-) + \frac{\langle 14 \rangle^3}{\langle 12 \rangle \langle 34 \rangle \langle 13 \rangle} \right] \ln\left(\frac{-s_{123}}{-s_{12}}\right) \\
& + \frac{5}{6} \frac{\langle 14 \rangle^2 \langle 4|(1+2)|3\rangle}{s_{12} \langle 12 \rangle \langle 34 \rangle} - \frac{1}{6} \frac{\langle 14 \rangle^2 [23] \langle 34 \rangle}{\langle 23 \rangle \langle 13 \rangle \langle 4|(1+3)|2\rangle} + \frac{2}{3} \frac{\langle 14 \rangle [23] \langle 34 \rangle}{[12] \langle 23 \rangle \langle 13 \rangle} \\
& - \frac{2}{3} \frac{\langle 14 \rangle \langle 24 \rangle \langle 4|(1+3)|2\rangle}{s_{12} \langle 23 \rangle \langle 34 \rangle} + \frac{1}{3} \frac{[23] \langle 4|(1+3)|2\rangle \langle 4|(2+3)|1\rangle}{s_{123} [12]^2 \langle 23 \rangle} \\
& - \frac{1}{6} \frac{\langle 4|(2+3)|1\rangle (\langle 4|1|2\rangle + 2\langle 4|3|2\rangle) (2\langle 4|1|2\rangle + \langle 4|3|2\rangle)^2}{s_{123} [12]^2 \langle 23 \rangle \langle 34 \rangle \langle 4|(1+3)|2\rangle} + \frac{1}{2} \frac{[23] \langle 2|(1+4)|3\rangle}{[14] \langle 23 \rangle [34]} \\
& + \frac{1}{2} \frac{\langle 4|(1+3)|2\rangle \langle 4|(1+2)|3\rangle}{s_{123} \langle 23 \rangle [12]} - \frac{1}{2} \frac{\langle 14 \rangle^2 [13]}{s_{12} \langle 23 \rangle} + 2iA_4^{(0)}(\phi^\dagger, 1_{\bar{q}}^-, 2_q^+, 3^+, 4^-), \tag{4.19}
\end{aligned}$$

with

$$\begin{aligned}
V_1^L = & -\frac{1}{\epsilon^2} \left[\left(\frac{\mu^2}{-s_{23}} \right)^\epsilon + \left(\frac{\mu^2}{-s_{34}} \right)^\epsilon + \left(\frac{\mu^2}{-s_{41}} \right)^\epsilon \right] + \frac{13}{6\epsilon} \left(\frac{\mu^2}{-s_{12}} \right)^\epsilon + \frac{119}{18} - \frac{\delta_R}{6} \\
& - \text{LS}_{-1}^{2\text{me}}(s_{123}, s_{234}; s_{23}, m_H^2) - \text{LS}_{-1}^{2\text{me}}(s_{341}, s_{412}; s_{41}, m_H^2) \\
& - \text{LS}_{-1}^{2\text{me}}(s_{412}, s_{123}; s_{12}, m_H^2), \tag{4.20}
\end{aligned}$$

$$\begin{aligned}
-iA_4^R(\phi, 1_{\bar{q}}^-, 2_q^+, 3^+, 4^-) &= -iA_4^{(0)}(\phi, 1_{\bar{q}}^-, 2_q^+, 3^+, 4^-) \times V^R \\
&+ \frac{\langle 14 \rangle^2}{\langle 23 \rangle \langle 13 \rangle} \left[\text{Ls}_{-1}(s_{12}, s_{23}; s_{123}) + \text{Ls}_{-1}(s_{34}, s_{41}; s_{341}) \right] \\
&- \frac{1}{2} \frac{\langle 12 \rangle^2 [23]^2 \langle 34 \rangle^2}{\langle 23 \rangle \langle 13 \rangle} \frac{\text{L}_1\left(\frac{-s_{123}}{-s_{12}}\right)}{s_{12}^2} + \frac{1}{2} \frac{\langle 24 \rangle^3 \langle 1|(3+4)|2 \rangle^2}{\langle 12 \rangle \langle 23 \rangle \langle 34 \rangle} \frac{\text{L}_1\left(\frac{-s_{234}}{-s_{34}}\right)}{s_{34}^2} \\
&- 2 \frac{\langle 12 \rangle \langle 34 \rangle \langle 14 \rangle [23]}{\langle 23 \rangle \langle 13 \rangle} \frac{\text{L}_0\left(\frac{-s_{123}}{-s_{12}}\right)}{s_{12}} - 2 \frac{\langle 14 \rangle \langle 24 \rangle [23]}{\langle 23 \rangle} \frac{\text{L}_0\left(\frac{-s_{234}}{-s_{34}}\right)}{s_{34}} \\
&- \frac{3}{2} \frac{\langle 14 \rangle^2}{\langle 23 \rangle \langle 13 \rangle} \ln\left(\frac{-s_{123}}{-s_{12}}\right) - \frac{i}{2} A_4^{(0)}(\phi, 1_{\bar{q}}^-, 2_q^+, 3^+, 4^-) \ln\left(\frac{-s_{234}}{-s_{34}}\right) \\
&+ \frac{1}{2} \left[\frac{\langle 14 \rangle [23] \langle 34 \rangle}{[12] \langle 23 \rangle \langle 13 \rangle} + \frac{[23] [13] \langle 2|(1+4)|3 \rangle}{[34] [14] \langle 2|(3+4)|1 \rangle} - \frac{\langle 4|(1+3)|2 \rangle \langle 4|(1+2)|3 \rangle}{s_{123} \langle 23 \rangle [12]} \right. \\
&\quad \left. + \frac{\langle 14 \rangle^2 \langle 24 \rangle^2 (s_{21} + s_{23} + s_{24})}{\langle 12 \rangle \langle 23 \rangle \langle 34 \rangle^2 \langle 2|(1+4)|3 \rangle} - \frac{s_{341}^2 [23] \langle 24 \rangle^3}{s_{34} \langle 23 \rangle \langle 34 \rangle \langle 2|(1+4)|3 \rangle \langle 2|(3+4)|1 \rangle} \right], \tag{4.21}
\end{aligned}$$

with

$$V^R = -\frac{1}{\epsilon^2} \left(\frac{\mu^2}{-s_{12}} \right)^\epsilon - \frac{3}{2\epsilon} \left(\frac{\mu^2}{-s_{12}} \right)^\epsilon - \frac{7}{2} - \frac{\delta_R}{2} - \text{Ls}_{-1}^{2\text{me}}(s_{234}, s_{341}; s_{34}, m_H^2), \tag{4.22}$$

and

$$\begin{aligned}
-iA_4^f(\phi, 1_{\bar{q}}^-, 2_q^+, 3^+, 4^-) &= -iA_4^{(0)}(\phi, 1_{\bar{q}}^-, 2_q^+, 3^+, 4^-) \times \left[-\frac{2}{3\epsilon} \left(\frac{\mu^2}{-s_{12}} \right)^\epsilon - \frac{10}{9} \right] \\
&+ \frac{1}{3} \left[\frac{\langle 12 \rangle^2 [23]^3 \langle 34 \rangle^2}{\langle 13 \rangle} - \frac{\langle 4|(1+2)|3 \rangle^3 \langle 13 \rangle^2}{\langle 12 \rangle \langle 34 \rangle} \right] \frac{\text{L}_2\left(\frac{-s_{123}}{-s_{12}}\right)}{s_{12}^3} \\
&- \frac{1}{3} \left[\frac{\langle 14 \rangle^2}{\langle 23 \rangle \langle 13 \rangle} + \frac{\langle 14 \rangle^2 \langle 24 \rangle}{\langle 12 \rangle \langle 23 \rangle \langle 34 \rangle} \right] \ln\left(\frac{-s_{123}}{-s_{12}}\right) - \frac{1}{2} \frac{\langle 14 \rangle^2 [23]}{s_{12} \langle 13 \rangle} \\
&+ \frac{1}{6} \frac{\langle 14 \rangle (\langle 4|1|2 \rangle \langle 4|(1+3)|2 \rangle - \langle 4|3|2 \rangle^2)}{[12] \langle 34 \rangle \langle 13 \rangle s_{123}} + \frac{1}{6} \frac{\langle 14 \rangle^3 s_{123}}{s_{12} \langle 12 \rangle \langle 34 \rangle \langle 13 \rangle}. \tag{4.23}
\end{aligned}$$

For the $\phi\bar{q}qgg$ ($-++$) case,

$$\begin{aligned}
& -iA_4^L(\phi, 1_{\bar{q}}^-, 2_q^+, 3^-, 4^+) = -iA_4^{(0)}(\phi, 1_{\bar{q}}^-, 2_q^+, 3^-, 4^+) \\
& \quad \times \left[V_1^L - \frac{13}{6} \ln\left(\frac{-s_{412}}{-s_{12}}\right) - \text{Ls}_{-1}(s_{34}, s_{41}; s_{341}) - \text{Ls}_{-1}(s_{12}, s_{23}; s_{123}) \right] \\
& + \frac{\langle 14 \rangle^2 \langle 23 \rangle^3}{\langle 12 \rangle \langle 34 \rangle \langle 24 \rangle^3} \left[\text{Ls}_{-1}(s_{23}, s_{34}; s_{234}) + \text{Ls}_{-1}(s_{41}, s_{12}; s_{412}) \right] \\
& + \frac{2 \langle 12 \rangle^2 \langle 34 \rangle^2 [24]^3}{3 \langle 14 \rangle s_{12}^3} \text{L}_2\left(\frac{-s_{412}}{-s_{12}}\right) - \frac{1 \langle 12 \rangle \langle 23 \rangle \langle 34 \rangle [24]^2}{2 \langle 24 \rangle s_{34}^2} \text{L}_1\left(\frac{-s_{234}}{-s_{34}}\right) \\
& + \left[\frac{1 \langle 14 \rangle \langle 3|(1+2)|4|^2}{2 \langle 24 \rangle} - \frac{1 \langle 13 \rangle \langle 14 \rangle \langle 3|(1+2)|4|^2}{3 \langle 12 \rangle \langle 34 \rangle} - \frac{2 \langle 13 \rangle \langle 12 \rangle \langle 34 \rangle [24]^2}{3 \langle 14 \rangle} \right] \frac{\text{L}_1\left(\frac{-s_{412}}{-s_{12}}\right)}{s_{12}^2} \\
& - \left[\frac{\langle 12 \rangle [24] \langle 3|(1+4)|2|^2}{\langle 14 \rangle [12]} + \frac{1 \langle 14 \rangle \langle 23 \rangle^2 [24]^2}{2 \langle 24 \rangle} \right] \frac{\text{L}_1\left(\frac{-s_{412}}{-s_{41}}\right)}{s_{41}^2} \\
& - \left[\frac{[24] \langle 34 \rangle \langle 1|(2+3)|4|^2}{\langle 14 \rangle [34]} + \frac{1 \langle 14 \rangle \langle 23 \rangle^2 [24]^2}{2 \langle 24 \rangle} \right] \frac{\text{L}_1\left(\frac{-s_{234}}{-s_{23}}\right)}{s_{23}^2} \\
& + \left[3 \frac{\langle 13 \rangle^2 \langle 3|(1+2)|4|}{\langle 12 \rangle \langle 34 \rangle} + 2 \frac{\langle 13 \rangle \langle 3|(1+2)|4|^2}{\langle 12 \rangle \langle 34 \rangle [14]} + \frac{1 \langle 13 \rangle^2 [24]}{3 \langle 14 \rangle} - \frac{\langle 3|(1+2)|4|^2}{[14] \langle 24 \rangle} \right] \frac{\text{L}_0\left(\frac{-s_{412}}{-s_{12}}\right)}{s_{12}} \\
& + 3 \frac{\langle 23 \rangle \langle 13 \rangle [24]}{\langle 24 \rangle} \left[\frac{\text{L}_0\left(\frac{-s_{234}}{-s_{23}}\right)}{s_{23}} + \frac{\text{L}_0\left(\frac{-s_{412}}{-s_{41}}\right)}{s_{41}} \right] \\
& + \frac{\langle 23 \rangle [24] (\langle 12 \rangle \langle 34 \rangle + 2 \langle 14 \rangle \langle 23 \rangle)}{\langle 24 \rangle^2} \frac{\text{L}_0\left(\frac{-s_{234}}{-s_{34}}\right)}{s_{34}} \\
& - \left[\frac{1 \langle 13 \rangle^3}{3 \langle 12 \rangle \langle 34 \rangle \langle 14 \rangle} + \frac{1 \langle 23 \rangle \langle 13 \rangle^2}{2 \langle 12 \rangle \langle 24 \rangle \langle 34 \rangle} + \frac{\langle 23 \rangle^2 [24]}{\langle 24 \rangle^2 [14]} + 2 \frac{\langle 23 \rangle^3 \langle 14 \rangle [24]}{\langle 24 \rangle^2 \langle 34 \rangle \langle 12 \rangle [14]} \right] \ln\left(\frac{-s_{412}}{-s_{12}}\right) \\
& + \frac{\langle 12 \rangle^2 \langle 34 \rangle [24]}{\langle 24 \rangle^2 \langle 14 \rangle [34]} \ln\left(\frac{-s_{234}}{-s_{23}}\right) + \frac{\langle 34 \rangle^2 \langle 12 \rangle [24]}{\langle 24 \rangle^2 \langle 14 \rangle [12]} \ln\left(\frac{-s_{412}}{-s_{41}}\right) \\
& - \frac{5 \langle 13 \rangle^2 [24]}{6 s_{12} \langle 14 \rangle} - \frac{1 \langle 13 \rangle^2 \langle 3|(1+2)|4|}{3 s_{12} \langle 12 \rangle \langle 34 \rangle} - \frac{1 \langle 13 \rangle [24] (2 \langle 34|2 \rangle + \langle 3|1|2 \rangle)}{3 s_{412} \langle 14 \rangle [12]} \\
& + \frac{1}{2} \left[\frac{[24] \langle 3|(1+2)|4| \langle 3|(2+4)|1|}{s_{412} [14] [12] \langle 24 \rangle} - \frac{\langle 13 \rangle^2 [14]}{s_{12} \langle 24 \rangle} - \frac{\langle 13 \rangle [24] \langle 34 \rangle}{\langle 14 \rangle [12] \langle 24 \rangle} + \frac{\langle 12 \rangle [24]^2}{[23] [34] \langle 24 \rangle} \right] \\
& + \frac{\langle 13 \rangle [24] \langle 1|(2+3)|4|}{s_{23} \langle 14 \rangle [34]} - \frac{\langle 13 \rangle [24] \langle 3|(1+4)|2|}{s_{41} \langle 14 \rangle [12]} - \frac{[24]^2 \langle 34 \rangle \langle 23 \rangle}{s_{41} \langle 24 \rangle [12]} \\
& + 2i A_4^{(0)}(\phi^\dagger, 1_{\bar{q}}^-, 2_q^+, 3^-, 4^+), \tag{4.24}
\end{aligned}$$

$$\begin{aligned}
-iA_4^R(\phi, 1_{\bar{q}}^-, 2_q^+, 3^-, 4^+) &= -iA_4^{(0)}(\phi, 1_{\bar{q}}^-, 2_q^+, 3^-, 4^+) \times V^R \\
&+ \frac{\langle 12 \rangle^2 \langle 34 \rangle^2}{\langle 14 \rangle \langle 24 \rangle^3} \left[\text{Ls}_{-1}(s_{23}, s_{34}; s_{234}) + \text{Ls}_{-1}(s_{41}, s_{12}; s_{412}) \right] \\
&- \frac{1}{2} \frac{\langle 12 \rangle^2 \langle 34 \rangle^2 [24]^2}{\langle 14 \rangle \langle 24 \rangle} \frac{\text{L}_1\left(\frac{-s_{412}}{-s_{12}}\right)}{s_{12}^2} + \frac{[24] \langle 34 \rangle \langle 1|(2+3)|4|^2}{\langle 14 \rangle [34]} \frac{\text{L}_1\left(\frac{-s_{234}}{-s_{23}}\right)}{s_{23}^2} \\
&- \left[\frac{\langle 12 \rangle \langle 34 \rangle [24]^3}{[23]} + \frac{1}{2} \frac{\langle 23 \rangle^3 \langle 1|(3+4)|2|^2}{\langle 12 \rangle \langle 34 \rangle \langle 24 \rangle} \right] \frac{\text{L}_1\left(\frac{-s_{234}}{-s_{34}}\right)}{s_{34}^2} \\
&- \frac{1}{2} \frac{\langle 14 \rangle \langle 23 \rangle^2 [24]^2}{\langle 24 \rangle} \left[\frac{\text{L}_1\left(\frac{-s_{412}}{-s_{41}}\right)}{s_{41}^2} - \frac{\text{L}_1\left(\frac{-s_{234}}{-s_{23}}\right)}{s_{23}^2} \right] - \frac{\langle 12 \rangle^2 \langle 34 \rangle^2 [24]}{\langle 14 \rangle \langle 24 \rangle^2} \frac{\text{L}_0\left(\frac{-s_{412}}{-s_{12}}\right)}{s_{12}} \\
&+ \frac{\langle 23 \rangle [24] (2 \langle 12 \rangle \langle 34 \rangle + \langle 14 \rangle \langle 23 \rangle)}{\langle 24 \rangle^2} \frac{\text{L}_0\left(\frac{-s_{412}}{-s_{41}}\right)}{s_{41}} - \frac{\langle 12 \rangle^2 \langle 34 \rangle [24]}{\langle 24 \rangle^2 \langle 14 \rangle [34]} \ln\left(\frac{-s_{234}}{-s_{23}}\right) \\
&+ \left[\frac{\langle 34 \rangle \langle 12 \rangle [24]}{\langle 24 \rangle^2 [23]} + \frac{1}{2} \frac{\langle 23 \rangle \langle 13 \rangle^2}{\langle 12 \rangle \langle 24 \rangle \langle 34 \rangle} \right] \ln\left(\frac{-s_{234}}{-s_{34}}\right) - \frac{1}{2} \frac{[24] \langle 3|(1+2)|4 \rangle \langle 3|(1+4)|2 \rangle}{s_{41} s_{412} [12]} \\
&- \frac{1}{2} \frac{[24]^2 \langle 34 \rangle \langle 23 \rangle}{s_{41} \langle 24 \rangle [12]} - \frac{1}{2} \frac{\langle 13 \rangle \langle 23 \rangle^2 \langle 1|(3+4)|2 \rangle}{s_{34} \langle 34 \rangle \langle 12 \rangle \langle 24 \rangle} + \frac{1}{2} \frac{\langle 23 \rangle [24] \langle 1|(3+4)|2 \rangle (s_{23} + s_{34})}{s_{34} s_{234} [23] \langle 24 \rangle} \\
&+ \frac{1}{2} \frac{[24]^2 \langle 1|(2+3)|4 \rangle}{s_{234} [23] [34]} - \frac{\langle 12 \rangle [24] \langle 34 \rangle \langle 1|(2+3)|4 \rangle}{s_{23} \langle 14 \rangle [34] \langle 24 \rangle} + \frac{\langle 13 \rangle [24]}{[23] \langle 24 \rangle}, \tag{4.25}
\end{aligned}$$

and

$$\begin{aligned}
-iA_4^f(\phi, 1_{\bar{q}}^-, 2_q^+, 3^-, 4^+) &= -iA_4^{(0)}(\phi, 1_{\bar{q}}^-, 2_q^+, 3^-, 4^+) \times \left[-\frac{2}{3\epsilon} \left(\frac{\mu^2}{-s_{12}} \right)^\epsilon - \frac{10}{9} \right] \\
&- \frac{1}{3} \left[\frac{\langle 14 \rangle^2 \langle 3|(1+2)|4|^3}{\langle 12 \rangle \langle 34 \rangle} + \frac{\langle 12 \rangle^2 [24]^3 \langle 34 \rangle^2}{\langle 14 \rangle} \right] \frac{\text{L}_2\left(\frac{-s_{412}}{-s_{12}}\right)}{s_{12}^3} \\
&- \frac{i}{3} A_4^{(0)}(\phi, 1_{\bar{q}}^-, 2_q^+, 3^-, 4^+) \ln\left(\frac{-s_{412}}{-s_{12}}\right) + \frac{1}{2} \frac{\langle 13 \rangle^2 [24]}{s_{12} \langle 14 \rangle} \\
&+ \frac{1}{6} \frac{\langle 13 \rangle (\langle 3|1|2 \rangle \langle 3|(1+4)|2 \rangle - \langle 3|4|2 \rangle^2)}{[12] \langle 34 \rangle \langle 14 \rangle s_{412}} + \frac{1}{6} \frac{\langle 13 \rangle^3 s_{412}}{s_{12} \langle 12 \rangle \langle 34 \rangle \langle 14 \rangle}. \tag{4.26}
\end{aligned}$$

4.2.3 $\phi \bar{q} g q g$

For $\phi \bar{q} g q g$, we have the “reflection” relation $A_4^R(1_{\bar{q}}, 3, 2_q, 4) = A_4^L(1_{\bar{q}}, 4, 2_q, 3)$, so we do not need to quote A_4^R separately.

Again we take the results for the infrared- and ultraviolet-finite helicity amplitude

$\phi\bar{q}gqg$ ($-+++$) from ref. [50]:

$$-iA_4^L(\phi, 1_{\bar{q}}^-, 2^+, 3_q^+, 4^+) = \frac{1}{2} \left[\frac{\langle 13 \rangle \langle 1|(3+4)|2 \rangle}{\langle 23 \rangle \langle 34 \rangle \langle 41 \rangle} + \frac{\langle 13 \rangle^2 [34]}{\langle 12 \rangle \langle 23 \rangle \langle 34 \rangle} \right] - 2 \frac{\langle 1|(2+3)|4 \rangle^2}{\langle 12 \rangle \langle 23 \rangle s_{123}}, \quad (4.27)$$

$$A_4^f(\phi, 1_{\bar{q}}^-, 2^+, 3_q^+, 4^+) = 0. \quad (4.28)$$

The results for $\phi\bar{q}gqg$ ($-++-$) are given by

$$\begin{aligned} -iA_4^L(\phi, 1_{\bar{q}}^-, 2^+, 3_q^+, 4^-) &= -iA_4^{(0)}(\phi, 1_{\bar{q}}^-, 2^+, 3_q^+, 4^-) \\ &\times \left\{ V_2^L - \text{Ls}_{-1}(s_{41}, s_{12}; s_{412}) - \text{Ls}_{-1}(s_{23}, s_{34}; s_{234}) \right\} \\ &+ \frac{1}{2} \frac{\langle 13 \rangle^2 \langle 4|(1+2)|3 \rangle^2}{\langle 12 \rangle \langle 23 \rangle} \frac{\text{L}_1\left(\frac{-s_{123}}{-s_{12}}\right)}{s_{12}^2} - \frac{1}{2} \frac{\langle 12 \rangle \langle 34 \rangle^2 [23]^2}{\langle 23 \rangle} \frac{\text{L}_1\left(\frac{-s_{234}}{-s_{34}}\right)}{s_{34}^2} \\ &- 2 \frac{\langle 14 \rangle [23] \langle 34 \rangle}{\langle 23 \rangle} \left[\frac{\text{L}_0\left(\frac{-s_{123}}{-s_{12}}\right)}{s_{12}} + \frac{\text{L}_0\left(\frac{-s_{234}}{-s_{34}}\right)}{s_{34}} \right] \\ &- \frac{i}{2} A_4^{(0)}(\phi, 1_{\bar{q}}^-, 2^+, 3_q^+, 4^-) \ln\left(\frac{-s_{123}}{-s_{12}}\right) - \frac{1}{2} \frac{s_{341} [23] [13]}{[34] [14] \langle 2|(3+4)|1 \rangle} - \frac{1}{2} \frac{\langle 4|(1+3)|2 \rangle^2}{s_{123} [12] \langle 23 \rangle} \\ &- \frac{\langle 14 \rangle [23] \langle 34 \rangle}{s_{12} \langle 23 \rangle} + \frac{1}{2} \frac{\langle 14 \rangle^2 (s_{13} + s_{23})}{s_{12} \langle 12 \rangle \langle 23 \rangle} - \frac{1}{2} \frac{[23] \langle 34 \rangle \langle 2|(1+4)|3 \rangle}{\langle 23 \rangle [34] \langle 2|(3+4)|1 \rangle}, \end{aligned} \quad (4.29)$$

with

$$\begin{aligned} V_2^L &= -\frac{1}{\epsilon^2} \left[\left(\frac{\mu^2}{-s_{34}} \right)^\epsilon + \left(\frac{\mu^2}{-s_{41}} \right)^\epsilon \right] + \frac{13}{6\epsilon} \left(\frac{\mu^2}{-s_{123}} \right)^\epsilon + \frac{119}{18} - \frac{\delta_R}{6} \\ &- \text{Ls}_{-1}^{2\text{me}}(s_{412}, s_{123}; s_{12}, m_H^2) - \text{Ls}_{-1}^{2\text{me}}(s_{123}, s_{234}; s_{23}, m_H^2), \end{aligned} \quad (4.30)$$

and

$$A_4^f(\phi, 1_{\bar{q}}^-, 2^+, 3_q^+, 4^-) = A_4^{(0)}(\phi, 1_{\bar{q}}^-, 2^+, 3_q^+, 4^-) \left[-\frac{2}{3\epsilon} \left(\frac{\mu^2}{-s_{123}} \right)^\epsilon - \frac{10}{9} \right]. \quad (4.31)$$

The results for $\phi\bar{q}gqg$ ($--++$) are

$$\begin{aligned}
-iA_4^L(\phi, 1_{\bar{q}}^-, 2^-, 3_q^+, 4^+) &= -iA_4^{(0)}(\phi, 1_{\bar{q}}^-, 2^-, 3_q^+, 4^+) \\
&\times \left\{ V_3^L - \text{Ls}_{-1}(s_{34}, s_{41}; s_{341}) - \text{Ls}_{-1}(s_{12}, s_{23}; s_{123}) \right\} \\
&- \frac{1}{2} \frac{\langle 24 \rangle^2 \langle 1|(2+3)|4]^2}{\langle 34 \rangle \langle 14 \rangle} \frac{\text{L}_1\left(\frac{-s_{234}}{-s_{23}}\right)}{s_{23}^2} + \frac{1}{2} \frac{\langle 23 \rangle^2 [34]^2 \langle 14 \rangle}{\langle 34 \rangle} \frac{\text{L}_1\left(\frac{-s_{341}}{-s_{41}}\right)}{s_{41}^2} \\
&+ 2 \frac{\langle 12 \rangle \langle 23 \rangle [34]}{\langle 34 \rangle} \left[\frac{\text{L}_0\left(\frac{-s_{234}}{-s_{23}}\right)}{s_{23}} + \frac{\text{L}_0\left(\frac{-s_{341}}{-s_{41}}\right)}{s_{41}} \right] - \frac{i}{2} A_4^{(0)}(\phi, 1_{\bar{q}}^-, 2^-, 3_q^+, 4^+) \ln\left(\frac{-s_{234}}{-s_{23}}\right) \\
&- \frac{1}{2} \frac{\langle 2|(1+3)|4]^2}{s_{341} [14] \langle 34 \rangle} + \frac{1}{2} \frac{s_{123} [13] [34]}{[12] [23] \langle 4|(2+3)|1]} - \frac{1}{2} \frac{\langle 12 \rangle^2 \langle 24 \rangle (s_{14} + s_{24} + s_{34})}{\langle 14 \rangle \langle 23 \rangle \langle 34 \rangle \langle 4|(1+2)|3]} \\
&- \frac{1}{2} \frac{s_{123}^2 \langle 24 \rangle^2 [34]}{s_{23} \langle 34 \rangle \langle 4|(2+3)|1] \langle 4|(1+2)|3]} + 2i A_4^{(0)}(\phi^\dagger, 1_{\bar{q}}^-, 2^-, 3_q^+, 4^+), \tag{4.32}
\end{aligned}$$

with

$$\begin{aligned}
V_3^L &= -\frac{1}{\epsilon^2} \left[\left(\frac{\mu^2}{-s_{34}} \right)^\epsilon + \left(\frac{\mu^2}{-s_{41}} \right)^\epsilon \right] - \frac{3}{2\epsilon} \left(\frac{\mu^2}{-s_{341}} \right)^\epsilon - \frac{7}{2} - \frac{\delta_R}{2} \\
&- \text{Ls}_{-1}^{2\text{me}}(s_{412}, s_{123}; s_{12}, m_H^2) - \text{Ls}_{-1}^{2\text{me}}(s_{123}, s_{234}; s_{23}, m_H^2), \tag{4.33}
\end{aligned}$$

and

$$A_4^f(\phi, 1_{\bar{q}}^-, 2^-, 3_q^+, 4^+) = 0. \tag{4.34}$$

Using eqs. (2.9) and (4.7), one can obtain any color or helicity component of the $\mathcal{A}_4^{(1)}(H, 1_{\bar{q}}, 2_q, 3^\pm, 4^\mp)$ amplitudes.

4.3 Numerical results

In order to facilitate comparisons with future work, we present here numerical values, at a single phase-space point, for the bare, unrenormalized primitive amplitudes computed in the paper. We choose the same kinematic point as in ref. [21], the configuration $H \rightarrow \bar{q}_1 q_2 \bar{Q}_3 Q_4$ in which the Higgs (or ϕ) and parton four-momenta take the values

$$\begin{aligned}
k_\phi &= (-1.0000000000, 0.0000000000, 0.0000000000, 0.0000000000), \\
k_1 &= (0.30674037867, -0.17738694693, -0.01664472021, -0.24969277974), \\
k_2 &= (0.34445032281, 0.14635282800, -0.10707762397, 0.29285022975), \\
k_3 &= (0.22091667641, 0.08911915938, 0.19733901856, 0.04380941793), \\
k_4 &= (0.12789262211, -0.05808504045, -0.07361667438, -0.08696686795). \tag{4.35}
\end{aligned}$$

We substitute $\mu = m_H = 1$, and use the 't Hooft-Veltman scheme [87], in which $\delta_R = 1$ (in accord with ref. [21]). Discussions of the conversion between different dimensional regularization schemes can be found in refs. [86, 89, 21]. The dependence on δ_R in our

$\phi\bar{q}q\bar{Q}Q$	ϵ^{-2}	ϵ^{-1}	ϵ^0
$(-++-)$ lc	+0.10641628412 $-0.04813723405 i$	+0.25970964611 $+0.28524492960 i$	+1.94930173285 $+0.66145729341 i$
$(-++-)$ slc	+0.10641628412 $-0.04813723405 i$	+0.47949272770 $+0.18582640802 i$	+0.82337543420 $+0.78352094637 i$
$(-++-)$ f	0	+0.07094418941 $-0.03209148937 i$	+0.33148585003 $+0.11853569045 i$
$(-+-+)$ lc	-1.88930338066 $-0.26775736353 i$	-1.08479447284 $-6.20837676158 i$	+8.36061276059 $-4.87467657230 i$
$(-+-+)$ slc	-1.88930338066 $-0.26775736353 i$	-4.98679990840 $-6.76137989415 i$	-4.95070751222 $-19.34119382028 i$
$(-+-+)$ f	0	-1.25953558711 $-0.17850490902 i$	-3.53445587012 $-4.53733741427 i$

Table 1: Numerical values of $\phi\bar{q}q\bar{Q}Q$ primitive amplitudes at kinematic point (4.35).

$\phi\bar{q}qgg$	ϵ^{-2}	ϵ^{-1}	ϵ^0
$(-++-)$ L	-0.06141673303 $-0.16247914884 i$	+0.37791957375 $-0.54354042568 i$	-0.34558862143 $-12.10809400189 i$
$(-++-)$ R	-0.02047224434 $-0.05415971628 i$	+0.12098146140 $-0.19438585924 i$	+0.89774344141 $+5.07992303199 i$
$(-++-)$ f	0	-0.01364816290 $-0.03610647752 i$	+0.08454550896 $-0.11688473115 i$
$(-+-+)$ L	-4.75526937444 $+10.54678423393 i$	-43.39451947571 $+7.81850845690 i$	-67.30255141380 $-40.68074759818 i$
$(-+-+)$ R	-1.58508979148 $+3.51559474465 i$	-14.85133091493 $+3.46337394880 i$	-33.50442466808 $+5.37244309382 i$
$(-+-+)$ f	0	-1.05672652765 $+2.34372982976 i$	-9.74999749954 $+1.83728897650 i$

Table 2: Numerical values of $\phi\bar{q}qgg$ primitive amplitudes at kinematic point (4.35).

formulae agrees with the shift in $H\bar{q}q\bar{Q}Q$ and $H\bar{q}qgg$ amplitudes between HV and FDH regularization schemes that is quoted in ref. [21].

In tables 1, 2 and 3 we present numerical values for the unrenormalized primitive amplitudes computed in the paper. Note that the overall phases are convention-dependent. Phase-independent quantities can be constructed by dividing by the corresponding tree amplitude. The tree amplitude is identified as $-1/2$ of the ϵ^{-2} slc entry in table 1, the negative of the ϵ^{-2} R entry in table 2, and $-1/2$ of the ϵ^{-2} L entry in table 3.

In table 4 we give the numerical value of the virtual correction to the color- and helicity-summed cross section for the $H\bar{q}q\bar{Q}Q$ process, according to eq. (2.18) but omitting an overall factor of $2C^2c_\Gamma g^6(N_c^2 - 1)N_c$. The result is constructed from the one-loop

$\phi\bar{q}gqg$	ϵ^{-2}	ϵ^{-1}	ϵ^0
$(-+-) L$	-0.07267563934 $-0.06793690983 i$	$+0.04895177312$ $-0.38207096287 i$	-1.94503280260 $-4.71626523954 i$
$(-+-) f$	0	-0.02422521311 $-0.02264563661 i$	$+0.02361126144$ $-0.12053858081 i$
$(--+) L$	$+23.05418438416$ $+0.47135348735 i$	$+92.96105880288$ $+74.35776389434 i$	$+154.70151920223$ $+298.96823152311 i$
$(--+) f$	0	0	0

Table 3: Numerical values of $\phi\bar{q}gqg$ primitive amplitudes at kinematic point (4.35).

$H\bar{q}q\bar{Q}Q$ cross section	ϵ^{-2}	ϵ^{-1}	ϵ^0
1	-12.9162958212	-13.1670303819	47.5186460764
$1/N_c^2$	12.9162958212	75.7028593906	172.3194296444
n_f/N_c	0	-8.6108638808	-27.9973052106

Table 4: Numerical value of the one-loop correction to the $H\bar{q}q\bar{Q}Q$ cross section at kinematic point (4.35), omitting an overall factor of $2C^2c_\Gamma g^6(N_c^2 - 1)N_c$ from eq. (2.18).

amplitudes given in this paper and the tree amplitudes (A.4). The dependence on the number of colors N_c and massless quark flavors n_f is shown explicitly. If one substitutes $N_c = 3$ and $n_f = 5$, adds the contributions, and multiplies by $1/4 \times (N_c^2 - 1)N_c$, then the result agrees with that for process A in table I of ref. [21]. (The factor of $1/4$ arises because a factor of $A^2 \equiv (2C)^2$ is extracted instead of C^2 in ref. [21].)

To convert the bare, unrenormalized amplitudes presented here to renormalized ones in an $\overline{\text{MS}}$ -type subtraction scheme, one should subtract the quantity

$$4g^2 \frac{c_\Gamma}{2\epsilon} \left[\frac{11}{3}N_c - \frac{2}{3}n_f \right] \mathcal{A}_4^{(0)} \quad (4.36)$$

from the corresponding one-loop amplitude $\mathcal{A}_4^{(1)}$ in eq. (2.11) or (2.20). After this subtraction, the rational parts of the $1/\epsilon$ poles are purely infrared, and take the form of a sum over contributions from each external parton,

$$\frac{g^2}{(4\pi)^2} 4 \left[-\frac{3}{4} \left(N_c - \frac{1}{N_c} \right) \right] \frac{\mathcal{A}_4^{(0)}}{\epsilon} \quad \text{for } \phi\bar{q}q\bar{Q}Q, \quad (4.37)$$

$$\frac{g^2}{(4\pi)^2} 2 \left[-\frac{3}{4} \left(N_c - \frac{1}{N_c} \right) - \frac{1}{2} \left(\frac{11}{3}N_c - \frac{2}{3}n_f \right) \right] \frac{\mathcal{A}_4^{(0)}}{\epsilon} \quad \text{for } \phi\bar{q}qgg, \quad (4.38)$$

in accordance with the general form of infrared singularities of one-loop amplitudes [90].

A final contribution that needs to be included is the one-loop correction to the Hgg effective operator of eq. (2.1), which shifts its coefficient from C to $C \times [1 + 11\alpha_s/(4\pi)]$ [63]. At the level of the NLO virtual cross section, this effect can be taken into account by an

addition to eqs. (2.11) and (2.20) of the form

$$11 \frac{g^2}{(4\pi)^2} \mathcal{A}_4^{(0)}. \quad (4.39)$$

4.4 Pseudoscalar Higgs amplitudes and cross section for $A\bar{q}qgg$

As a byproduct of our calculation of the ϕ -amplitudes, we can obtain the respective amplitudes where the scalar Higgs boson H has been replaced by a pseudoscalar Higgs boson, A . Pseudoscalar Higgs bosons are present in many extensions of the SM, such as the MSSM. Here we assume that we are in a kinematic regime where the production of the A boson plus jets can also be treated in the large m_t limit. As mentioned earlier, the overall constant C is different for the A case [50]. Otherwise, the only difference between the two computations is that instead of taking the *sum* of the ϕ - and ϕ^\dagger - components, the pseudoscalar amplitudes are given by their *difference* divided by i , according to eq. (2.8).

Furthermore, we can combine our results with those of Ellis, Giele and Zanderighi (EGZ) [21], to obtain the color- and helicity-summed cross section for $A\bar{q}qgg$. EGZ used a semi-numerical method to compute the color- and helicity-summed cross section for $H\bar{q}qgg$, which we may write schematically as,

$$\sigma_{\text{EGZ}} = \sum_{\lambda} \left[\mathcal{A}_H^{(0)*}(\lambda) \mathcal{A}_H^{(1)}(\lambda) + \mathcal{A}_H^{(0)}(\lambda) \mathcal{A}_H^{(1)*}(\lambda) \right] = 2 \text{Re} \left\{ \sum_{\lambda} \left[\mathcal{A}_H^{(0)*}(\lambda) \mathcal{A}_H^{(1)}(\lambda) \right] \right\}. \quad (4.40)$$

Here by $\mathcal{A}_H(\lambda)$ we denote a $H\bar{q}qgg$ amplitude in a helicity configuration λ , and the sum is over all possible helicity configurations. In every summation in this subsection there is also an implicit sum over colors which is given by eq. (2.23), but for simplicity we do not write it out here. The helicity sum includes the two independent MHV configurations $(-++-)$ and $(-+-+)$ analyzed in this paper, and their conjugate ones (obtained by parity). Moreover, they include configurations $(-+--)$, $(-+++)$ and their conjugates. These last configurations require NMHV ϕ amplitudes, which we did not compute here, and which would be needed to provide a full analytic description of the one-loop $H\bar{q}qgg$ and $A\bar{q}qgg$ helicity amplitudes. However, we will see that because the contribution of the latter configurations to the $H\bar{q}qgg$ cross section is encoded in σ_{EGZ} , it is possible to use this result instead for the purpose of computing the $A\bar{q}qgg$ cross section.

Note that we can rewrite eq. (4.40) as

$$\sigma_{\text{EGZ}} = 4 \text{Re} \left\{ \sum_{\lambda'} \left[A_H^{(0)*}(\lambda') A_H^{(1)}(\lambda') \right] \right\}, \quad (4.41)$$

with λ' now labelling each of the four helicity configurations with fixed helicities for the antiquark-quark pair, $\bar{q}^- q^+$, namely $(-+\pm\pm)$. Also, from eq. (4.41) we see that σ_{EGZ} contains the NMHV $H\bar{q}qgg$ amplitudes in the quantity

$$\sigma_{\text{EGZ}}^{\text{NMHV}} \equiv 4 \text{Re} \left\{ A_H^{(0)*}(\lambda_-) A_H^{(1)}(\lambda_-) + A_H^{(0)*}(\lambda_+) A_H^{(1)}(\lambda_+) \right\} \subset \sigma_{\text{EGZ}}, \quad (4.42)$$

with $\lambda_- \equiv (-+--)$ and $\lambda_+ \equiv (-+++)$. We can extract $\sigma_{\text{EGZ}}^{\text{NMHV}}$ from eq. (4.41), knowing the $H\bar{q}qgg$ MHV amplitudes inferred from our formulæ (4.16)–(4.34). Hence we will consider $\sigma_{\text{EGZ}}^{\text{NMHV}}$ known from now on, and we will use it in order to compute the color- and helicity-summed cross section for $A\bar{q}qgg$, σ_A . Similarly to eqs. (4.40) and (4.41), σ_A is given by

$$\sigma_A = 2 \text{Re} \left\{ \sum_{\lambda} \left[A_A^{(0)*}(\lambda) A_A^{(1)}(\lambda) \right] \right\} = 4 \text{Re} \left\{ \sum_{\lambda'} \left[A_A^{(0)*}(\lambda') A_A^{(1)}(\lambda') \right] \right\}, \quad (4.43)$$

with $A_A(\lambda)$ denoting the pseudoscalar $A\bar{q}qgg$ amplitudes.

Because σ_A is expressed as a sum over λ' , we focus on the four configurations $(-+-+)$, $(-++-)$ and $(-+--)$, $(-+++)$. We can straightforwardly compute the terms coming from the first two (MHV) configurations using our results from section 4.2 and eq. (2.8), as mentioned in the beginning of this section. For the last two (NMHV) configurations, we need to compute the quantity

$$\sigma_A^{\text{NMHV}} \equiv 4 \text{Re} \left\{ A_A^{(0)*}(\lambda_-) A_A^{(1)}(\lambda_-) + A_A^{(0)*}(\lambda_+) A_A^{(1)}(\lambda_+) \right\}. \quad (4.44)$$

Let's look at each amplitude in this expression separately. The tree amplitudes are simple, because $A_A^{(0)} = (A_{\phi}^{(0)} - A_{\phi^\dagger}^{(0)})/i$, and $A_{\phi^\dagger}^{(0)}(\lambda_-) = A_{\phi}^{(0)}(\lambda_+) = 0$. Therefore, from eqs. (2.7) and (2.8), we have

$$A_A^{(0)}(\lambda_-) = \frac{1}{i} A_{\phi}^{(0)}(\lambda_-) = \frac{1}{i} A_H^{(0)}(\lambda_-), \quad (4.45)$$

$$A_A^{(0)}(\lambda_+) = -\frac{1}{i} A_{\phi^\dagger}^{(0)}(\lambda_+) = -\frac{1}{i} A_H^{(0)}(\lambda_+). \quad (4.46)$$

We choose to express the one-loop amplitudes $A_A^{(1)}(\lambda_-)$ and $A_A^{(1)}(\lambda_+)$ using eqs. (2.7) and (2.8) in the following way

$$A_A^{(1)}(\lambda_-) = \frac{1}{i} \left[A_{\phi}^{(1)}(\lambda_-) - A_{\phi^\dagger}^{(1)}(\lambda_-) \right] = \frac{1}{i} \left[A_H^{(1)}(\lambda_-) - 2A_{\phi^\dagger}^{(1)}(\lambda_-) \right], \quad (4.47)$$

$$A_A^{(1)}(\lambda_+) = \frac{1}{i} \left[A_{\phi}^{(1)}(\lambda_+) - A_{\phi^\dagger}^{(1)}(\lambda_+) \right] = \frac{1}{i} \left[-A_H^{(1)}(\lambda_+) + 2A_{\phi}^{(1)}(\lambda_+) \right]. \quad (4.48)$$

Substituting eqs. (4.45)–(4.48) into (4.44) we find that

$$\begin{aligned} \sigma_A^{\text{NMHV}} &= 4 \text{Re} \left\{ \left(\frac{1}{i} A_H^{(0)}(\lambda_-) \right)^* \frac{1}{i} \left[A_H^{(1)}(\lambda_-) - 2A_{\phi^\dagger}^{(1)}(\lambda_-) \right] \right. \\ &\quad \left. + \left(-\frac{1}{i} A_H^{(0)}(\lambda_+) \right)^* \frac{1}{i} \left[-A_H^{(1)}(\lambda_+) + 2A_{\phi}^{(1)}(\lambda_+) \right] \right\} \\ &= 4 \text{Re} \left\{ A_H^{(0)*}(\lambda_-) A_H^{(1)}(\lambda_-) + A_H^{(0)*}(\lambda_+) A_H^{(1)}(\lambda_+) \right\} \\ &\quad - 8 \text{Re} \left\{ A_H^{(0)*}(\lambda_-) A_{\phi^\dagger}^{(1)}(\lambda_-) + A_H^{(0)*}(\lambda_+) A_{\phi}^{(1)}(\lambda_+) \right\} \\ &= \sigma_{\text{EGZ}}^{\text{NMHV}} - 8 \text{Re} \left\{ A_{\phi}^{(0)*}(\lambda_-) A_{\phi^\dagger}^{(1)}(\lambda_-) + A_{\phi^\dagger}^{(0)*}(\lambda_+) A_{\phi}^{(1)}(\lambda_+) \right\}. \end{aligned} \quad (4.49)$$

We notice that the first term in eq. (4.49) is given by eq. (4.42), and the second term contains only tree and finite one-loop helicity amplitudes with ϕ and ϕ^\dagger . The required NMHV tree amplitudes (see *e.g.* refs. [18, 64, 67]) are given in eqs. (A.6), (A.7), (A.9) and (A.10). The finite one-loop amplitudes are given in eqs. (4.16)–(4.18) and (4.27)–(4.28). Therefore, we know all the ingredients necessary to obtain the full color- and helicity-summed cross section for $A\bar{q}qgg$, albeit only semi-numerically. Our results of section 4.2 can be used to convert σ_{EGZ} into σ_A .

4.5 Interference with VBF production

Our amplitudes for $H\bar{q}q\bar{Q}Q$ can be used to calculate analytically part of the interference between the $qQ \rightarrow HqQ$ gluon fusion process and the tree-level vector boson fusion processes. Both these processes have the same initial and final states. However, at tree level one has a color-octet exchange and the other a color-singlet exchange. So there is no interference at tree level. (For identical quarks, the exchange term does produce an interference, but it is extremely small [60].) At one loop, however, the color-singlet part of the one-loop correction to the gluon-fusion $H\bar{q}q\bar{Q}Q$ amplitude can interfere with the tree-level VBF amplitude, and we will provide an analytic formula for this contribution. This is only part of the virtual correction; the other part comes from the interference between the tree-level gluon fusion and one-loop VBF $H\bar{q}q\bar{Q}Q$ amplitudes. In addition, there is a real correction. The sum of all three terms has been computed numerically in refs. [24, 25] and it is quite small.

We obtain the color-singlet part of $H\bar{q}q\bar{Q}Q$ from the corresponding ϕ -amplitude, $A_{4;s}(\phi, 1_{\bar{q}}, 2_q, 3_{\bar{Q}}, 4_Q)$, using eq. (2.7). From the color decomposition (2.11), contracted with $\delta_{i_2}^{\bar{i}_1}$, we see that the color-singlet part is given by

$$A_{4;s}(\phi, 1_{\bar{q}}, 2_q, 3_{\bar{Q}}, 4_Q) = A_{4;1}(\phi, 1_{\bar{q}}, 2_q, 3_{\bar{Q}}, 4_Q) + A_{4;2}(\phi, 1_{\bar{q}}, 2_q, 3_{\bar{Q}}, 4_Q). \quad (4.50)$$

Using eqs. (2.14)–(2.17) we get

$$A_{4;s}(\phi, 1_{\bar{q}}^-, 2_q^+, 3_{\bar{Q}}^+, 4_Q^-) = \frac{N_c^2 - 1}{N_c^2} \left[A_4^{\text{lc}}(\phi, 1_{\bar{q}}^-, 2_q^+, 3_{\bar{Q}}^+, 4_Q^-) + A_4^{\text{lc}}(\phi, 1_{\bar{q}}^-, 2_q^+, 4_Q^-, 3_{\bar{Q}}^+) \right], \quad (4.51)$$

$$A_{4;s}(\phi, 1_{\bar{q}}^-, 2_q^+, 3_{\bar{Q}}^-, 4_Q^+) = \frac{N_c^2 - 1}{N_c^2} \left[A_4^{\text{lc}}(\phi, 1_{\bar{q}}^-, 2_q^+, 3_{\bar{Q}}^-, 4_Q^+) + A_4^{\text{lc}}(\phi, 1_{\bar{q}}^-, 2_q^+, 4_Q^+, 3_{\bar{Q}}^-) \right], \quad (4.52)$$

in terms of the leading-color primitive amplitude $A_4^{\text{lc}}(\phi, 1_{\bar{q}}, 2_q, 3_{\bar{Q}}, 4_Q)$. The relevant tree-level $H\bar{q}q\bar{Q}Q$ VBF amplitudes involve only ZZ fusion, not WW or WZ ; they are given by

$$A_{4;\text{VBF}}^{(0)}(H, 1_{\bar{q}}^-, 2_q^+, 3_{\bar{Q}}^+, 4_Q^-) = 2i \frac{m_Z^2}{v} \frac{\langle 14 \rangle [23]}{(s_{12} - m_Z^2)(s_{34} - m_Z^2)}, \quad (4.53)$$

$$A_{4;\text{VBF}}^{(0)}(H, 1_{\bar{q}}^-, 2_q^+, 3_{\bar{Q}}^-, 4_Q^+) = A_{4;\text{VBF}}^{(0)}(H, 1_{\bar{q}}^-, 2_q^+, 4_Q^+, 3_{\bar{Q}}^-), \quad (4.54)$$

with v the vacuum expectation value of the Higgs field. Finally, the color-singlet virtual interference between the two processes is

$$2\alpha_s^2 N_c^2 \text{Re} \left[A_{4;\text{VBF}}^{(0)*}(H, 1_{\bar{q}}, 2_q, 3_{\bar{Q}}, 4_Q) A_{4;s}(H, 1_{\bar{q}}, 2_q, 3_{\bar{Q}}, 4_Q) \right]. \quad (4.55)$$

Equation (4.55) is to be understood with an implicit summation over all allowed polarization states of the external quarks. We implemented eq. (4.55) numerically at a few phase-space points and obtained agreement [61] with this part of the full interference computed in ref. [24]. We did not perform such a comparison against ref. [25].

4.6 Consistency checks

It is important to verify that the methods and the results presented in this paper yield the correct answers for the $H\bar{q}q\bar{Q}Q$ and $H\bar{q}qgg$ amplitudes. We have used three types of independent and non-trivial checks on our expressions. They are based on collinear limits that the amplitudes should satisfy, symmetries under which they should remain invariant, and numerical comparisons with previously computed expressions. For $H\bar{q}qgg$ only the first two types of checks were possible, whereas for $H\bar{q}q\bar{Q}Q$ all of them were performed, providing an even more solid check. We have found that our amplitudes agree with all the checks, and we outline the process further in the remainder of this section.

4.6.1 Collinear behavior

A powerful handle on the correctness of the amplitudes is their collinear behavior. When two neighboring external legs become collinear, an n -point amplitude has to correctly factorize onto an $(n-1)$ -point amplitude, multiplied by the corresponding splitting amplitude for the two collinear legs. In the case of one-loop amplitudes, the factorization is onto a sum of possible factorizations with the loop belonging either to the splitting amplitude, or to the remaining $(n-1)$ -point amplitude [73]. There is also a sum over the helicity h of the intermediate state P carrying momentum $k_P^2 \approx 0$. For the $\phi\bar{q}q\bar{Q}Q$ amplitudes, in the limit that momenta k_1 and k_2 become collinear the factorization is onto a $\phi\bar{Q}Qg$ amplitude,

$$A_4^{(1)}(\phi, 1_{\bar{q}}, 2_q, 3_{\bar{Q}}, 4_Q) \xrightarrow{1\parallel 2} \sum_{h=\pm} \left[A_3^{(1)}(\phi, 3_{\bar{Q}}, 4_Q, P^h) \times \text{Split}_{-h}^{(0)}(1_{\bar{q}}, 2_q; z) \right. \\ \left. + A_3^{(0)}(\phi, 3_{\bar{Q}}, 4_Q, P^h) \times \text{Split}_{-h}^{(1)}(1_{\bar{q}}, 2_q; z) \right], \quad (4.56)$$

with $k_P = k_1 + k_2$, $k_1 \approx zk_P$, and $k_2 \approx (1-z)k_P$. The splitting amplitudes depend on the longitudinal momentum fraction z , which is the momentum fraction carried by leg 1, a real variable with $0 < z < 1$. (It is unrelated to the complex variable z used for the shifts performed in the previous sections.) Replacing ϕ with H in eq. (4.56), we get the collinear behavior of the Higgs amplitudes, while the $3 \parallel 4$ collinear limit can be obtained by exchanging q and Q . The $1 \parallel 2$ and $3 \parallel 4$ limits are the only collinear

limits of $A_4^{(1)}(\phi, 1_{\bar{q}}, 2_q, 3_{\bar{Q}}, 4_Q)$ that exhibit universal singular behavior; there is no splitting amplitude for quarks of different flavor.

The extension of eq. (4.56) to the $\phi\bar{q}gg$ amplitudes is straightforward. In this case, however, there are additional factorization channels, including channels where a gluon becomes collinear with an adjacent quark or gluon. For example, for the $2 \parallel 3$ and $3 \parallel 4$ collinear limits we have

$$A_4^{(1)}(\phi, 1_{\bar{q}}, 2_q, 3, 4) \xrightarrow{2 \parallel 3} \sum_{h=\pm} \left[A_3^{(1)}(\phi, 1_{\bar{q}}, P_q^h, 4) \times \text{Split}_{-h}^{(0)}(2_q, 3; z) + A_3^{(0)}(\phi, 1_{\bar{q}}, P_q^h, 4) \times \text{Split}_{-h}^{(1)}(2_q, 3; z) \right], \quad (4.57)$$

$$A_4^{(1)}(\phi, 1_{\bar{q}}, 2_q, 3, 4) \xrightarrow{3 \parallel 4} \sum_{h=\pm} \left[A_3^{(1)}(\phi, 1_{\bar{q}}, 2_q, P^h) \times \text{Split}_{-h}^{(0)}(3, 4; z) + A_3^{(0)}(\phi, 1_{\bar{q}}, 2_q, P^h) \times \text{Split}_{-h}^{(1)}(3, 4; z) \right], \quad (4.58)$$

and similarly for the $H\bar{q}gg$ amplitudes. Eqs. (4.56)–(4.58) apply separately to the primitive amplitude components lc, slc, L , R and f, after extracting the respective pieces of the one-loop three-parton amplitudes [50] and splitting amplitudes [73].

We have checked that our expressions factorize correctly according to eqs. (4.56)–(4.58) and their analogues, for all possible non-trivial (singular) collinear limits.

4.6.2 Symmetries

The one-loop amplitudes we computed in this paper are MHV four-point amplitudes, with an equal number of positive- and negative-helicity external legs. As a consequence, they have to satisfy certain non-trivial symmetries, that become manifest only after assembling together all the pieces into a full answer.

The symmetries of the four-quark $H\bar{q}q\bar{Q}Q$ primitive amplitudes can be summarized in the following form:

- reflection or quark-exchange symmetry

$$A_4^{(1)}(H, 1_{\bar{q}}^-, 2_q^+, 3_{\bar{Q}}^+, 4_Q^-) = A_4^{(1)}(H, 4_{\bar{q}}^-, 3_q^+, 2_{\bar{Q}}^+, 1_Q^-), \quad (4.59)$$

$$A_4^{(1)}(H, 1_{\bar{q}}^-, 2_q^+, 3_{\bar{Q}}^-, 4_Q^+) = A_4^{(1)}(H, 3_{\bar{q}}^-, 4_q^+, 1_{\bar{Q}}^-, 2_Q^+), \quad (4.60)$$

- parity conjugation symmetry

$$A_4^{(1)}(H, 1_{\bar{q}}^-, 2_q^+, 3_{\bar{Q}}^+, 4_Q^-) = A_4^{(1)}(H, 2_{\bar{q}}^-, 1_q^+, 4_{\bar{Q}}^+, 3_Q^-) \Big|_{\langle i j \rangle \leftrightarrow [j i]}, \quad (4.61)$$

$$A_4^{(1)}(H, 1_{\bar{q}}^-, 2_q^+, 3_{\bar{Q}}^-, 4_Q^+) = A_4^{(1)}(H, 2_{\bar{q}}^-, 1_q^+, 4_{\bar{Q}}^-, 3_Q^+) \Big|_{\langle i j \rangle \leftrightarrow [j i]}. \quad (4.62)$$

The reflection symmetry properties (4.59)–(4.60) are satisfied by the component ϕ and ϕ^\dagger amplitudes as well, whereas the conjugation symmetry (4.61)–(4.62) only holds for the H amplitudes.

For the two-quark-two-gluon $H\bar{q}qgg$ and $H\bar{q}ggq$ primitive MHV amplitudes, although there is no reflection symmetry, the following parity conjugation symmetries hold:

- $H\bar{q}qgg$ conjugation symmetry

$$A_4^{(1)}(H, 1_{\bar{q}}^-, 2_q^+, 3^+, 4^-) = -A_4^{(1)}(H, 2_{\bar{q}}^-, 1_q^+, 4^+, 3^-) \Big|_{\langle ij \rangle \leftrightarrow [j i]}, \quad (4.63)$$

$$A_4^{(1)}(H, 1_{\bar{q}}^-, 2_q^+, 3^-, 4^+) = -A_4^{(1)}(H, 2_{\bar{q}}^-, 1_q^+, 4^-, 3^+) \Big|_{\langle ij \rangle \leftrightarrow [j i]}, \quad (4.64)$$

- $H\bar{q}ggq$ conjugation symmetry

$$A_4^{(1)}(H, 1_{\bar{q}}^-, 2^+, 3_q^+, 4^-) = -A_4^{(1)}(H, 3_{\bar{q}}^-, 4^+, 1_q^+, 2^-) \Big|_{\langle ij \rangle \leftrightarrow [j i]}, \quad (4.65)$$

$$A_4^{(1)}(H, 1_{\bar{q}}^-, 2^-, 3_q^+, 4^+) = -A_4^{(1)}(H, 3_{\bar{q}}^-, 4^-, 1_q^+, 2^+) \Big|_{\langle ij \rangle \leftrightarrow [j i]}. \quad (4.66)$$

The fact that the symmetries (4.59)–(4.66) have to be respected provides a non-trivial check on the amplitudes. Since our computation is done by obtaining separate, in general non-symmetric, pieces of the amplitude (*e.g.*, the coefficient of a single log in a particular channel), it is only after putting them all together that the symmetry becomes manifest. Therefore, it is the combination of many non-symmetric ingredients that gives rise to a symmetric final answer. An error that spoils the symmetry can be detected by this check. We have checked that our amplitudes obey all the required symmetries.

4.6.3 Numerical comparison

Ref. [21] computed the virtual cross section for the $H \rightarrow q\bar{q}Q\bar{Q}$ process to next-to-leading order accuracy (one-loop diagrams, not counting the top quark loop vertex) using a semi-numerical approach. They also obtained analytic expressions for the aforementioned cross section summed over colors and helicities.

Using our color- and helicity-decomposed ϕ -amplitudes presented in our paper, we have constructed the same quantity and have compared with their analytical results numerically. The result at the phase-space point (4.35) was given in table 4, but we have also found agreement with their analytical formulae for all the randomly-generated phase-space points that we examined.

5. Conclusions

In this paper we have presented analytic results for the one-loop amplitudes for a Higgs plus four quarks, and for a Higgs plus two quarks and two opposite-helicity gluons. We have

obtained the cut-containing and rational pieces of the answer separately, using unitarity for the former and on-shell recursion for the latter. We have also shown in specific examples how to compute the various ingredients, and presented a way to deal with spurious poles without fully eliminating them from the completed-cut terms. Our expressions are relatively compact and in agreement with various consistency checks as well as previous results. We believe that they will provide a useful input for faster numerical programs computing NLO cross sections relevant for the LHC, and will be an important ingredient for future higher-point calculations. Together with the NMHV $H\bar{q}qgg$ case, and the remaining helicity amplitudes for $Hgggg$ (beyond those already been computed [49, 51, 52]) they provide the one-loop corrections to Higgs plus four partons, and can be used to compute the gluon fusion contribution to the $H + 2$ jets final state at the LHC, as well as its interference with the vector boson fusion channel. Further NLO studies will be important for understanding SM backgrounds, and enhancing the potential for the discovery of new physics in the upcoming experiments at the LHC.

Acknowledgments

The figures in this paper were made with JAXODRAW [91], based on AXODRAW [92]. We are grateful to Jeppe Andersen, Jeffrey Forshaw, Nigel Glover and Jennifer Smillie for useful discussions, and to John Campbell and Keith Ellis for pointing out two typographical errors in the first version of this article. Y.S. would like to thank Marvin Weinstein for assistance with MAPLE.

A. Tree amplitudes

In this appendix, we record various tree amplitudes entering the main computations and results.

As mentioned in section 3.4.1, the $\phi\bar{q}q$ and $\phi^\dagger\bar{q}q$ amplitudes for massless quarks vanish by fermion chirality conservation and angular momentum conservation. The ϕgg and $\phi^\dagger gg$ tree amplitudes are given by

$$\begin{aligned}
A_2^{(0)}(\phi, 1^+, 2^+) &= A_2^{(0)}(\phi, 1^\pm, 2^\mp) = 0, \\
A_2^{(0)}(\phi, 1^-, 2^-) &= -i \langle 1\,2 \rangle^2, \\
A_2^{(0)}(\phi^\dagger, 1^-, 2^-) &= A_2^{(0)}(\phi^\dagger, 1^\pm, 2^\mp) = 0, \\
A_2^{(0)}(\phi^\dagger, 1^+, 2^+) &= -i [1\,2]^2.
\end{aligned}
\tag{A.1}$$

The $\phi\bar{q}qg$ and $\phi^\dagger\bar{q}qg$ amplitudes are

$$\begin{aligned}
A_3^{(0)}(\phi, 1_{\bar{q}}^-, 2_q^+, 3^+) &= 0, \\
A_3^{(0)}(\phi, 1_{\bar{q}}^-, 2_q^+, 3^-) &= -i \frac{\langle 13 \rangle^2}{\langle 12 \rangle}, \\
A_3^{(0)}(\phi^\dagger, 1_{\bar{q}}^-, 2_q^+, 3^-) &= 0, \\
A_3^{(0)}(\phi^\dagger, 1_{\bar{q}}^-, 2_q^+, 3^+) &= -i \frac{[23]^2}{[12]},
\end{aligned} \tag{A.2}$$

while the ϕggg amplitudes are

$$\begin{aligned}
A_3^{(0)}(\phi, 1^+, 2^+, 3^+) &= A_3^{(0)}(\phi, 1^-, 2^+, 3^+) = 0, \\
A_3^{(0)}(\phi, 1^-, 2^-, 3^+) &= i \frac{\langle 12 \rangle^3}{\langle 23 \rangle \langle 31 \rangle}, \\
A_3^{(0)}(\phi, 1^-, 2^-, 3^-) &= -i \frac{(m_H^2)^2}{[12][23][31]}, \\
A_3^{(0)}(\phi^\dagger, 1^-, 2^-, 3^-) &= A_3^{(0)}(\phi, 1^+, 2^-, 3^-) = 0, \\
A_3^{(0)}(\phi^\dagger, 1^+, 2^+, 3^-) &= -i \frac{[12]^3}{[23][31]}, \\
A_3^{(0)}(\phi^\dagger, 1^+, 2^+, 3^+) &= i \frac{(m_H^2)^2}{\langle 12 \rangle \langle 23 \rangle \langle 31 \rangle}.
\end{aligned} \tag{A.3}$$

The $\phi\bar{q}q\bar{Q}Q$ and $\phi^\dagger\bar{q}q\bar{Q}Q$ tree amplitudes are given by

$$\begin{aligned}
A_4^{(0)}(\phi, 1_{\bar{q}}^-, 2_q^+, 3_{\bar{Q}}^+, 4_Q^-) &= -i \frac{\langle 14 \rangle^2}{\langle 12 \rangle \langle 34 \rangle}, \\
A_4^{(0)}(\phi, 1_{\bar{q}}^-, 2_q^+, 3_{\bar{Q}}^-, 4_Q^+) &= -A_4^{(0)}(\phi, 1_{\bar{q}}^-, 2_q^+, 4_Q^+, 3_{\bar{Q}}^-), \\
A_4^{(0)}(\phi^\dagger, 1_{\bar{q}}^-, 2_q^+, 3_{\bar{Q}}^+, 4_Q^-) &= -i \frac{[23]^2}{[12][34]}, \\
A_4^{(0)}(\phi^\dagger, 1_{\bar{q}}^-, 2_q^+, 3_{\bar{Q}}^-, 4_Q^+) &= -A_4^{(0)}(\phi^\dagger, 1_{\bar{q}}^-, 2_q^+, 4_Q^+, 3_{\bar{Q}}^-).
\end{aligned} \tag{A.4}$$

For the case of $\phi\bar{q}qgg$ and $\phi^\dagger\bar{q}qgg$ we have

$$\begin{aligned}
A_4^{(0)}(\phi, 1_{\bar{q}}^-, 2_q^+, 3^+, 4^+) &= 0, \\
A_4^{(0)}(\phi, 1_{\bar{q}}^-, 2_q^+, 3^+, 4^-) &= -i \frac{\langle 14 \rangle^2 \langle 24 \rangle}{\langle 12 \rangle \langle 23 \rangle \langle 34 \rangle}, \\
A_4^{(0)}(\phi, 1_{\bar{q}}^-, 2_q^+, 3^-, 4^+) &= i \frac{\langle 13 \rangle^3}{\langle 12 \rangle \langle 34 \rangle \langle 41 \rangle}, \\
A_4^{(0)}(\phi^\dagger, 1_{\bar{q}}^-, 2_q^+, 3^-, 4^-) &= 0, \\
A_4^{(0)}(\phi^\dagger, 1_{\bar{q}}^-, 2_q^+, 3^+, 4^-) &= -i \frac{[23]^2 [13]}{[12][34][41]}, \\
A_4^{(0)}(\phi^\dagger, 1_{\bar{q}}^-, 2_q^+, 3^-, 4^+) &= i \frac{[24]^3}{[12][23][34]},
\end{aligned} \tag{A.5}$$

and for the NMHV cases,

$$A_4^{(0)}(\phi, 1_{\bar{q}}^-, 2_q^+, 3^-, 4^-) = -i \frac{\langle 3|(1+4)|2\rangle^2 \langle 41\rangle}{[24] s_{412}} \left[\frac{1}{s_{12}} + \frac{1}{s_{41}} \right] \\ - i \frac{\langle 4|(1+3)|2\rangle^2 \langle 13\rangle}{[23] s_{12} s_{123}} + i \frac{\langle 1|(3+4)|2\rangle^2}{\langle 12\rangle [24] [23] [34]}, \quad (\text{A.6})$$

$$A_4^{(0)}(\phi^\dagger, 1_{\bar{q}}^-, 2_q^+, 3^+, 4^+) = -i \frac{\langle 1|(2+3)|4\rangle^2 [23]}{\langle 13\rangle s_{123}} \left[\frac{1}{s_{12}} + \frac{1}{s_{23}} \right] \\ + i \frac{\langle 1|(2+4)|3\rangle^2 [24]}{\langle 14\rangle s_{12} s_{412}} - i \frac{\langle 1|(3+4)|2\rangle^2}{[12] \langle 13\rangle \langle 14\rangle \langle 34\rangle}. \quad (\text{A.7})$$

The amplitudes for $\phi \bar{q} g q g$ and $\phi^\dagger \bar{q} g q g$ are,

$$A_4^{(0)}(\phi, 1_{\bar{q}}^-, 2^+, 3_q^+, 4^-) = -i \frac{\langle 14\rangle^2}{\langle 12\rangle \langle 23\rangle}, \\ A_4^{(0)}(\phi, 1_{\bar{q}}^-, 2^-, 3_q^+, 4^+) = -i \frac{\langle 12\rangle^2}{\langle 34\rangle \langle 41\rangle}, \quad (\text{A.8}) \\ A_4^{(0)}(\phi^\dagger, 1_{\bar{q}}^-, 2^+, 3_q^+, 4^-) = i \frac{[23]^2}{[34] [41]}, \\ A_4^{(0)}(\phi^\dagger, 1_{\bar{q}}^-, 2^-, 3_q^+, 4^+) = i \frac{[34]^2}{[12] [23]},$$

and for the NMHV cases,

$$A_4^{(0)}(\phi, 1_{\bar{q}}^-, 2^-, 3_q^+, 4^-) = -i \frac{\langle 4|(1+2)|3\rangle^2}{[12] [23] s_{123}} - i \frac{\langle 2|(1+4)|3\rangle^2}{[34] [41] s_{341}}, \quad (\text{A.9})$$

$$A_4^{(0)}(\phi^\dagger, 1_{\bar{q}}^-, 2^+, 3_q^+, 4^+) = i \frac{\langle 1|(2+3)|4\rangle^2}{\langle 12\rangle \langle 23\rangle s_{123}} + i \frac{\langle 1|(3+4)|2\rangle^2}{\langle 34\rangle \langle 41\rangle s_{341}}. \quad (\text{A.10})$$

Our $\phi \bar{q} q g g$ and $\phi \bar{q} q g g$ tree amplitudes, after dividing by i , agree with the ones (implicit) in refs. [18, 19, 67]. For the $\phi^\dagger \bar{q} q g g$ and $\phi^\dagger \bar{q} q g g$ tree amplitudes, after dividing by i , our amplitudes agree with the ones in refs. [18, 19], but have the opposite sign from those in ref. [67]. (The relative sign between ϕ and ϕ^\dagger amplitudes matters in reconstructing the H amplitudes.) Our $\phi \bar{q} q g \dots g$ and $\phi^\dagger \bar{q} q g \dots g$ tree amplitudes are uniformly opposite in sign to ref. [64].

B. L_i and L_{s-1} functions and scalar integrals

The definitions for the L_0 , L_1 , L_2 and L_{s-1} , L_{s-1}^{2me} functions used in the formulæ presented above are

$$L_0(r) = \frac{\ln r}{1-r}, \quad L_1(r) = \frac{\ln r + 1-r}{(1-r)^2}, \quad L_2(r) = \frac{\ln r - (r-1/r)/2}{(1-r)^3}, \quad (\text{B.1})$$

$$\text{Ls}_{-1}(s, t; m^2) = \text{Li}_2\left(1 - \frac{s}{m^2}\right) + \text{Li}_2\left(1 - \frac{t}{m^2}\right) + \ln\left(\frac{-s}{-m^2}\right) \ln\left(\frac{-t}{-m^2}\right) - \frac{\pi^2}{6}, \quad (\text{B.2})$$

$$\begin{aligned} \text{Ls}_{-1}^{2\text{me}}(s, t; m_1^2, m_3^2) = & -\text{Li}_2\left(1 - \frac{m_1^2}{s}\right) - \text{Li}_2\left(1 - \frac{m_1^2}{t}\right) - \text{Li}_2\left(1 - \frac{m_3^2}{s}\right) \\ & - \text{Li}_2\left(1 - \frac{m_3^2}{t}\right) + \text{Li}_2\left(1 - \frac{m_1^2 m_3^2}{st}\right) - \frac{1}{2} \ln^2\left(\frac{-s}{-t}\right), \end{aligned} \quad (\text{B.3})$$

with

$$\text{Li}_2(x) = -\int_0^x dz \frac{\ln(1-z)}{z}. \quad (\text{B.4})$$

The one-mass and easy two-mass box integrals are related to the Ls_{-1} functions by,

$$\begin{aligned} \mathcal{I}_4^{1\text{m}}(s, t; m^2) = & \frac{-2i c_\Gamma}{st} \left\{ -\frac{1}{\epsilon^2} \left[\left(\frac{\mu^2}{-s}\right)^\epsilon + \left(\frac{\mu^2}{-t}\right)^\epsilon - \left(\frac{\mu^2}{-m^2}\right)^\epsilon \right] \right. \\ & \left. - \text{Ls}_{-1}(s, t; m^2) \right\}, \end{aligned} \quad (\text{B.5})$$

$$\begin{aligned} \mathcal{I}_4^{2\text{me}}(s, t; m_1^2, m_3^2) = & \frac{-2i c_\Gamma}{st - m_1^2 m_3^2} \left\{ -\frac{1}{\epsilon^2} \left[\left(\frac{\mu^2}{-s}\right)^\epsilon + \left(\frac{\mu^2}{-t}\right)^\epsilon - \left(\frac{\mu^2}{-m_1^2}\right)^\epsilon - \left(\frac{\mu^2}{-m_3^2}\right)^\epsilon \right] \right. \\ & \left. - \text{Ls}_{-1}^{2\text{me}}(s, t; m_1^2, m_3^2) \right\}. \end{aligned} \quad (\text{B.6})$$

The one-mass and two-mass triangle integrals are related to each other,

$$\mathcal{I}_3^{1\text{m}}(s) = \frac{-i c_\Gamma}{\epsilon^2} \frac{1}{(-s)} \left(\frac{\mu^2}{-s}\right)^\epsilon, \quad (\text{B.7})$$

$$\mathcal{I}_3^{2\text{m}}(s_1, s_2) = \frac{-i c_\Gamma}{\epsilon^2} \frac{1}{(-s_1) - (-s_2)} \left[\left(\frac{\mu^2}{-s_1}\right)^\epsilon - \left(\frac{\mu^2}{-s_2}\right)^\epsilon \right], \quad (\text{B.8})$$

and contain terms of the form $\ln(-s_i)/\epsilon$; hence their coefficients are dictated by the known infrared poles of the amplitude.

The bubble integral is given by,

$$\mathcal{I}_2(s) = \frac{i c_\Gamma}{\epsilon(1-2\epsilon)} \left(\frac{\mu^2}{-s}\right)^\epsilon, \quad (\text{B.9})$$

and contains a single logarithm, $\ln(-s)$, at order ϵ^0 .

References

- [1] P. W. Higgs, Phys. Rev. **145**, 1156 (1966).
- [2] F. Englert and R. Brout, Phys. Rev. Lett. **13**, 321 (1964).
- [3] G. S. Guralnik, C. R. Hagen and T. W. B. Kibble, Phys. Rev. Lett. **13**, 585 (1964).
- [4] H. M. Georgi, S. L. Glashow, M. E. Machacek and D. V. Nanopoulos, Phys. Rev. Lett. **40**, 692 (1978).

- [5] A. Djouadi, M. Spira and P. M. Zerwas, Phys. Lett. B **264**, 440 (1991).
- [6] S. Dawson, Nucl. Phys. B **359**, 283 (1991).
- [7] D. Graudenz, M. Spira and P. M. Zerwas, Phys. Rev. Lett. **70**, 1372 (1993).
- [8] M. Spira, A. Djouadi, D. Graudenz and P. M. Zerwas, Nucl. Phys. B **453**, 17 (1995) [hep-ph/9504378].
- [9] T. Figy, C. Oleari and D. Zeppenfeld, Phys. Rev. D **68**, 073005 (2003) [hep-ph/0306109].
- [10] T. Figy and D. Zeppenfeld, Phys. Lett. B **591**, 297 (2004) [hep-ph/0403297].
- [11] E. L. Berger and J. Campbell, Phys. Rev. D **70**, 073011 (2004) [hep-ph/0403194].
- [12] F. Wilczek, Phys. Rev. Lett. **39**, 1304 (1977).
- [13] M. A. Shifman, A. I. Vainshtein and V. I. Zakharov, Phys. Lett. B **78**, 443 (1978).
- [14] M. Krämer, E. Laenen and M. Spira, Nucl. Phys. B **511**, 523 (1998) [hep-ph/9611272].
- [15] F. Hautmann, Phys. Lett. B **535**, 159 (2002) [hep-ph/0203140].
- [16] V. Del Duca, W. Kilgore, C. Oleari, C. R. Schmidt and D. Zeppenfeld, Phys. Rev. D **67**, 073003 (2003) [hep-ph/0301013].
- [17] S. Dawson and R. P. Kauffman, Phys. Rev. Lett. **68**, 2273 (1992).
- [18] R. P. Kauffman, S. V. Desai and D. Risal, Phys. Rev. D **55**, 4005 (1997) [Erratum-ibid. D **58**, 119901 (1998)] [hep-ph/9610541].
- [19] R. P. Kauffman and S. V. Desai, Phys. Rev. D **59**, 057504 (1999) [hep-ph/9808286].
- [20] V. Del Duca, W. Kilgore, C. Oleari, C. Schmidt and D. Zeppenfeld, Phys. Rev. Lett. **87**, 122001 (2001) [hep-ph/0105129]; Nucl. Phys. B **616**, 367 (2001) [hep-ph/0108030].
- [21] R. K. Ellis, W. T. Giele and G. Zanderighi, Phys. Rev. D **72**, 054018 (2005) [Erratum-ibid. D **74**, 079902 (2006)] [hep-ph/0506196].
- [22] J. M. Campbell, R. K. Ellis and G. Zanderighi, JHEP **0610**, 028 (2006) [hep-ph/0608194].
- [23] V. Del Duca, A. Frizzo and F. Maltoni, JHEP **0405**, 064 (2004) [hep-ph/0404013].
- [24] J. R. Andersen, T. Binoth, G. Heinrich and J. M. Smillie, JHEP **0802**, 057 (2008) [0709.3513 [hep-ph]].
- [25] A. Bredenstein, K. Hagiwara and B. Jäger, Phys. Rev. D **77**, 073004 (2008) [0801.4231 [hep-ph]].
- [26] C. Anastasiou and A. Lazopoulos, JHEP **0407**, 046 (2004) [hep-ph/0404258].
- [27] C. Anastasiou and A. Daleo, JHEP **0610**, 031 (2006) [hep-ph/0511176].
- [28] C. Anastasiou, S. Beerli and A. Daleo, JHEP **0705**, 071 (2007) [hep-ph/0703282].
- [29] R. K. Ellis, W. T. Giele and G. Zanderighi, Phys. Rev. D **73**, 014027 (2006) [hep-ph/0508308].
- [30] A. Denner and S. Dittmaier, Nucl. Phys. B **734**, 62 (2006) [hep-ph/0509141].
- [31] G. Ossola, C. G. Papadopoulos and R. Pittau, Nucl. Phys. B **763**, 147 (2007) [hep-ph/0609007].
- [32] G. Ossola, C. G. Papadopoulos and R. Pittau, JHEP **0803**, 042 (2008) [0711.3596 [hep-ph]].

- [33] G. Ossola, C. G. Papadopoulos and R. Pittau, JHEP **0805**, 004 (2008) [0802.1876 [hep-ph]].
- [34] P. Mastrolia, G. Ossola, C. G. Papadopoulos and R. Pittau, JHEP **0806**, 030 (2008) [0803.3964 [hep-ph]].
- [35] P. Draggiotis, M. V. Garzelli, C. G. Papadopoulos and R. Pittau, JHEP **0904**, 072 (2009) [0903.0356 [hep-ph]].
- [36] A. van Hameren, C. G. Papadopoulos and R. Pittau, 0903.4665 [hep-ph].
- [37] Z. Bern, L. J. Dixon and D. A. Kosower, Annals Phys. **322**, 1587 (2007) [0704.2798 [hep-ph]].
- [38] C. Anastasiou, R. Britto, B. Feng, Z. Kunszt and P. Mastrolia, Phys. Lett. B **645**, 213 (2007) [hep-ph/0609191].
- [39] C. Anastasiou, R. Britto, B. Feng, Z. Kunszt and P. Mastrolia, JHEP **0703**, 111 (2007) [hep-ph/0612277].
- [40] R. K. Ellis, W. T. Giele and Z. Kunszt, JHEP **0803**, 003 (2008) [0708.2398 [hep-ph]].
- [41] W. T. Giele, Z. Kunszt and K. Melnikov, JHEP **0804**, 049 (2008) [0801.2237 [hep-ph]].
- [42] W. T. Giele and G. Zanderighi, JHEP **0806**, 038 (2008) [0805.2152 [hep-ph]].
- [43] R. K. Ellis, W. T. Giele, Z. Kunszt and K. Melnikov, 0806.3467 [hep-ph].
- [44] C. F. Berger *et al.*, Phys. Rev. D **78**, 036003 (2008) [0803.4180 [hep-ph]].
- [45] A. Bredenstein, A. Denner, S. Dittmaier and M. M. Weber, JHEP **0702**, 080 (2007) [hep-ph/0611234].
- [46] M. Ciccolini, A. Denner and S. Dittmaier, Phys. Rev. Lett. **99**, 161803 (2007) [0707.0381 [hep-ph]].
- [47] M. Ciccolini, A. Denner and S. Dittmaier, Phys. Rev. D **77**, 013002 (2008) [0710.4749 [hep-ph]].
- [48] C. R. Schmidt, Phys. Lett. B **413**, 391 (1997) [hep-ph/9707448].
- [49] S. D. Badger and E. W. N. Glover, Nucl. Phys. Proc. Suppl. **160**, 71 (2006) [hep-ph/0607139].
- [50] C. F. Berger, V. Del Duca and L. J. Dixon, Phys. Rev. D **74**, 094021 (2006) [Erratum-ibid. D **76**, 099901 (2007)] [hep-ph/0608180].
- [51] S. D. Badger, E. W. N. Glover and K. Risager, JHEP **0707**, 066 (2007) [0704.3914 [hep-ph]]; Acta Phys. Polon. B **38**, 2273 (2007) [0705.0264 [hep-ph]].
- [52] E. W. N. Glover, P. Mastrolia and C. Williams, JHEP **0808**, 017 (2008) [0804.4149 [hep-ph]].
- [53] R. Britto, F. Cachazo and B. Feng, Nucl. Phys. B **725**, 275 (2005) [hep-th/0412103].
- [54] R. Britto, E. Buchbinder, F. Cachazo and B. Feng, Phys. Rev. D **72**, 065012 (2005) [hep-ph/0503132].
- [55] R. Britto, B. Feng and P. Mastrolia, Phys. Rev. D **73**, 105004 (2006) [hep-ph/0602178].
- [56] Z. Bern, L. J. Dixon and D. A. Kosower, Phys. Rev. D **73**, 065013 (2006) [hep-ph/0507005].
- [57] C. F. Berger, Z. Bern, L. J. Dixon, D. Forde and D. A. Kosower, Phys. Rev. D **74**, 036009 (2006) [hep-ph/0604195].
- [58] C. F. Berger, Z. Bern, L. J. Dixon, D. Forde and D. A. Kosower, Phys. Rev. D **75**, 016006 (2007) [hep-ph/0607014].

- [59] Z. Bern *et al.* [NLO Multileg Working Group], 0803.0494 [hep-ph].
- [60] J. R. Andersen and J. M. Smillie, Phys. Rev. D **75**, 037301 (2007) [hep-ph/0611281].
- [61] J. R. Andersen and J. M. Smillie, private communication.
- [62] J. Forshaw, J. Keates and S. Marzani, JHEP **0907**, 023 (2009) [0905.1350 [hep-ph]].
- [63] K. G. Chetyrkin, B. A. Kniehl and M. Steinhauser, Nucl. Phys. B **510**, 61 (1998) [hep-ph/9708255].
- [64] V. Del Duca, A. Frizzo and F. Maltoni, JHEP **0405**, 064 (2004) [hep-ph/0404013].
- [65] L. J. Dixon, E. W. N. Glover and V. V. Khoze, JHEP **0412**, 015 (2004) [hep-th/0411092].
- [66] F. Cachazo, P. Svrček and E. Witten, JHEP **0409**, 006 (2004) [hep-th/0403047].
- [67] S. D. Badger, E. W. N. Glover and V. V. Khoze, JHEP **0503**, 023 (2005) [hep-th/0412275].
- [68] J. E. Paton and H. M. Chan, Nucl. Phys. B **10**, 516 (1969);
P. Cvitanović, P. G. Lauwers and P. N. Scharbach, Nucl. Phys. B **186**, 165 (1981);
F. A. Berends and W. Giele, Nucl. Phys. B **294**, 700 (1987);
M. L. Mangano, S. J. Parke and Z. Xu, Nucl. Phys. B **298**, 653 (1988);
D. Zeppenfeld, Int. J. Mod. Phys. A **3**, 2175 (1988).
- [69] M. L. Mangano and S. J. Parke, Phys. Rept. **200**, 301 (1991) [hep-th/0509223].
- [70] L. J. Dixon, hep-ph/9601359.
- [71] Z. Bern, L. J. Dixon, D. A. Kosower and S. Weinzierl, Nucl. Phys. B **489** (1997) 3 [hep-ph/9610370].
- [72] Z. Bern, L. J. Dixon and D. A. Kosower, Nucl. Phys. B **513**, 3 (1998) [hep-ph/9708239].
- [73] Z. Bern, L. J. Dixon, D. C. Dunbar and D. A. Kosower, Nucl. Phys. B **425**, 217 (1994) [hep-ph/9403226].
- [74] Z. Bern, L. J. Dixon, D. C. Dunbar and D. A. Kosower, Nucl. Phys. B **435**, 59 (1995) [hep-ph/9409265].
- [75] R. Britto, F. Cachazo, B. Feng and E. Witten, Phys. Rev. Lett. **94**, 181602 (2005) [hep-th/0501052].
- [76] Z. Bern, L. J. Dixon and D. A. Kosower, Phys. Rev. D **71**, 105013 (2005) [hep-th/0501240].
- [77] Z. Bern, L. J. Dixon and D. A. Kosower, Phys. Rev. D **72**, 125003 (2005) [hep-ph/0505055].
- [78] L. M. Brown and R. P. Feynman, Phys. Rev. **85**, 231 (1952);
L. M. Brown, Nuovo Cim. **22**, 178 (1961);
B. Petersson, J. Math. Phys. **6**, 1955 (1965);
G. Källén and J. S. Toll, J. Math. Phys. **6**, 299 (1965);
D. B. Melrose, Nuovo Cim. **40**, 181 (1965);
G. Passarino and M. J. G. Veltman, Nucl. Phys. B **160**, 151 (1979);
W. L. van Neerven and J. A. M. Vermaseren, Phys. Lett. B **137**, 241 (1984).
- [79] Z. Bern, L. J. Dixon and D. A. Kosower, Phys. Lett. B **302**, 299 (1993) [Erratum-ibid. B **318**, 649 (1993)] [hep-ph/9212308].
- [80] Z. Bern, L. J. Dixon and D. A. Kosower, Nucl. Phys. B **412**, 751 (1994) [hep-ph/9306240].
- [81] T. Binoth, J. P. Guillet and G. Heinrich, Nucl. Phys. B **572**, 361 (2000) [hep-ph/9911342].

- [82] G. Duplancić and B. Nizić, Eur. Phys. J. C **35**, 105 (2004) [hep-ph/0303184].
- [83] R. K. Ellis and G. Zanderighi, JHEP **0802**, 002 (2008) [0712.1851 [hep-ph]].
- [84] R. Britto, F. Cachazo and B. Feng, Nucl. Phys. B **715**, 499 (2005) [hep-th/0412308].
- [85] C. F. Berger, Z. Bern, L. J. Dixon, D. Forde and D. A. Kosower, Nucl. Phys. Proc. Suppl. **160**, 261 (2006) [hep-ph/0610089].
- [86] Z. Kunszt, A. Signer and Z. Trócsányi, Nucl. Phys. B **411**, 397 (1994) [hep-ph/9305239].
- [87] G. 't Hooft and M. Veltman, Nucl. Phys. B **44**, 189 (1972).
- [88] Z. Bern and D. A. Kosower, Nucl. Phys. B **379**, 451 (1992).
- [89] S. Catani, M. H. Seymour and Z. Trócsányi, Phys. Rev. D **55**, 6819 (1997) [hep-ph/9610553];
Z. Bern, A. De Freitas, L. J. Dixon and H. L. Wong, Phys. Rev. D **66**, 085002 (2002) [hep-ph/0202271].
- [90] W. T. Giele and E. W. N. Glover, Phys. Rev. D **46**, 1980 (1992);
Z. Kunszt, A. Signer and Z. Trócsányi, Nucl. Phys. B **420**, 550 (1994) [hep-ph/9401294];
S. Catani, Phys. Lett. B **427**, 161 (1998) [hep-ph/9802439].
- [91] D. Binosi and L. Theussl, Comput. Phys. Commun. **161**, 76 (2004) [hep-ph/0309015].
- [92] J. A. M. Vermaseren, Comput. Phys. Commun. **83**, 45 (1994).